

UNIVERSITY OF NAPLES
"FEDERICO II"



SCHOOL OF MATHEMATICS, PHYSICS AND NATURAL SCIENCES

PhD IN CHEMICAL SCIENCES

XXIII CYCLE

2007-2010

COURSE OF SYNTHESIS, STRUCTURE AND REACTIVITY OF ORGANIC
MOLECULES

**Synthesis and reactivity of phenolic systems conjugated with
sulfidrylic compounds**

DR. GIORGIA GRECO

Giorgia Greco

Supervisor

Prof. Alessandra Napolitano

Alessandra Napolitano

PhD Coordinator

Prof. Lucio Previtiera

Lucio Previtiera

Assessor

Prof. Maria Rosaria Iesce

Maria Rosaria Iesce

UNIVERSITA' DEGLI STUDI DI NAPOLI
"FEDERICO II"



FACOLTA' DI SCIENZE MATEMATICHE, FISICHE E NATURALI

DOTTORATO DI RICERCA IN SCIENZE CHIMICHE

XXIII CICLO

2007-2010

INDIRIZZO DI SINTESI, STRUTTURA E REATTIVITA' DI MOLECOLE
ORGANICHE

**Sintesi e reattività di sistemi fenolici coniugati con composti
sulfidrilici**

DOTT.SSA GIORGIA GRECO

Giorgia Greco

Tutore

Prof.ssa Alessandra Napolitano

Alessandra Napolitano

Coordinatore

Prof. Lucio Previtiera

Lucio Previtiera

Relatore

Prof.ssa Maria Rosaria Iesce

Maria Rosaria Iesce

Index

Abstract	5
1. Introduction	7
1.1. Thioconjugated polyphenol metabolites: cysteinyl dopas and pheomelanin pigments	7
1.2. Thioconjugates from dietary polyphenols of plant origin	23
2. Results and discussion	34
2.1. Isomeric cysteinyl dopas provide a (photo)degradable bulk component and a robust structural element in red human hair pheomelanin	34
2.2. A melanin-inspired pro-oxidant system for aerial catechol(amine)-polymerization: implementing a non-enzymatic mimic of the natural casing model	48
2.3. Oxidative chemistry of cysteinyl dopas and properties of related synthetic pheomelanins	57
2.4. Biosynthesis-inspired one-pot access routes to 4-hydroxybenzothiazole aminoacids, red hair-specific markers of UV susceptibility and skin cancer risk	69
2.5. Pheomelanin-related benzothiazole isomers in the urine of patients with diffuse melanosis of melanoma	73
2.6. Mapping structural diversity in red hair pheomelanin: key elusive benzothiazolyldihydroisoquinoline building blocks and their formation pathway uncovered	86
2.7. Reaction of dihydrolipoic acid with juglone and related naphthoquinones: unmasking of a spirocyclic 1,3-dithiane intermediate en route to naphtho[1,4]dithiepin	104
2.8. Synthesis and antioxidant activity of new conjugates of dietary polyphenols of plant origin with dihydrolipoic acid	112
3. Conclusions	126

4. Experimental section	130
4.1. General methods	130
4.2. Isomeric cysteinyl dopas provide a (photo)degradable bulk component and a robust structural element in red human hair pheomelanin	135
4.3. A melanin-inspired pro-oxidant system for aerial catechol(amine)-polymerization: implementing a non-enzymatic mimic of the natural casing model	137
4.4. Oxidative chemistry of cysteinyl dopas and properties of related synthetic pheomelanins	140
4.5. Biologically inspired one-pot access routes to 4-hydroxybenzothiazole aminoacids, red hair-specific markers of UV susceptibility and skin cancer risk	144
4.6. Pheomelanin-related benzothiazole isomers in the urine of patients with diffuse melanosis of melanoma	146
4.7. Mapping structural diversity in red hair pheomelanin: key elusive benzothiazolyldihydroisoquinoline building blocks and their formation pathway uncovered	148
4.8. Reaction of dihydrolipoic acid with juglone and related naphthoquinones: unmasking of a spirocyclic 1,3-dithiane intermediate en route to naphtho[1,4]dithiepin	159
4.9. Synthesis and antioxidant activity of new conjugates of dietary polyphenols of plant origin with dihydrolipoic acid	165
5. References	169
Publication list	182
Acknowledgments	183

Abstract

Conjugates of phenols with biological thiols have recently received increasing interest because of their peculiar properties in most cases enhanced or significantly modified with respect to the parent phenols.

Main focus of the research activity developed in this PhD work was the chemistry of thioalkyl conjugates of catechols, among these cysteinyl dopas, mainly the 5*S* and 2*S* isomers, that are produced by epidermal melanocytes of man and other mammals and are involved in the biosynthesis of pheomelanins, the characteristic pigments of red hair, commonly implicated in the abnormal susceptibility of red haired fair complexioned individuals to sunburn and skin cancer. Overall the results of this work have greatly contributed to the definition of the structure, biosynthesis and functional significance of pheomelanins.

Traditionally pheomelanins have been regarded to arise primarily via the oxidative polymerization of 5-*S*-cysteinyl dopa (5SCD). Yet, it was observed that, in addition to 5SCD, 2-*S*-cysteinyl dopa (2SCD) is an important building block of red human hair pigments. By an improved analytical procedure, allowing simultaneous determination of benzothiazole markers, BTCA and 2-BTCA, originating from oxidative degradation of 5SCD- and 2SCD-derived units respectively, evidence was obtained that the pigment suffers extensive degradation during hair growth affecting mainly the 5SCD-derived components, whereas the 2SCD-derived units remain largely unaffected. Model studies suggested that structural degradation occurs during hair growth probably as a result of oxidative processes related in part to sun exposure.

Detailed studies on the properties of synthetic pheomelanin from 5SCD showed that the pigment is an efficient redox cyler, promoting oxygen-dependent polycatechol(amine) formation and deposition of eumelanin-like antioxidant coatings. Scanning electron microscopy coupled with chemical analysis of the material revealed a eumelanin-like coating completely masking the pheomelanin component. The system provides a new explanation to the origin of the casing architecture of human melanin.

The benzothiazoles BTCA and 2-BTCA turned out to be important and selective markers for pheomelanin quantitation in tissues and identification of red-haired individuals at high risk for skin cancer. A straightforward synthetic procedure for large scale preparation of these compounds was developed which might allow their use for routine population screenings, and for genetic and epidemiologic correlations studies.

The presence of benzothiazole compounds was also investigated in the urine of patients with melanoma with or without diffuse melanosis, a rare condition which may occur in metastasizing melanoma and is associated with a very poor prognosis. The urinary BTCAs were found to be highly associated with melanosis. Moreover, analysis of the pigmented fraction of urine after oxidative degradation provided evidence for the presence of pheomelanins at high levels in patients with melanosis. This finding provided for the first time a direct evidence that benzothiazoles are pheomelanin metabolites, whose formation is associated with advanced stages of melanoma.

Due to the unfavourable chemical and physical properties of pheomelanins, their structure is still mainly unknown. Biomimetic oxidation of the pheomelanin precursor 5SCD led to the isolation of two unprecedented benzothiazolythiazinodihydroisoquinoline dimers. Although the existence of isoquiniline-containing structural motifs in pheomelanins has long been postulated, this study was the first to demonstrate their presence in red hair and to uncover possible precursor compounds and formation mechanism.

As part of studies on thiol-quinone coupling as a viable biomimetic access to novel bioactive compounds for practical applications, the reaction of dihydrolipoic acid (DHLA), a strong endogenous antioxidant, with *p*-napthoquinones was examined, leading to the identification of novel dithiepinines arising from ring expansion of an unstable spirocyclic dithiane. In addition new conjugates of DHLA with naturally occurring polyphenols, such as hydroxytyrosol, caffeic acid and piceatannol, were prepared, which showed higher antioxidant power than the parent catechol, as evidenced by the higher H-donating ability and the tendency to oxidation at physiological pHs.

1. Introduction

1.1. Thioconjugated polyphenol metabolites: cysteinyldopas and pheomelanin pigments

1.1.1. Melanin pigments: classification and origin

The pigments responsible for the carrot to fire-red hues of hair, which are commonly found in Celtic populations, have ever stimulated the curiosity of investigators as representative members of the very limited group of animal pigments. In recent years, interest in these pigments has been renewed by epidemiological and clinical data pointing to the association of a fair complexion and red hair in Caucasians with an abnormal susceptibility to actinic damage and skin cancer.^{1,2} The biogenetic relationship with the other more widely diffused group of epidermal melanin pigments, determining black pigmentation was first recognized in the 1960s by Prota and Nicolaus³ who proposed that red hair pigments might be formed in vivo by some deviation of the normal course of melanogenesis involving cysteine, which would have explained the common origin of dark and red melanins in melanocytes. Once the biogenesis was definitely assessed, the red hair pigments were named *pheomelanins*, to indicate that they represented a lighter variant (*φαιος*: dusky) of the dark melanin pigments, thereafter termed *eumelanins* (*ευ*: good; *μελας*, black).⁴

Spurred in part by the observation that these two types of melanin react differently – eumelanin acts as a photoprotective anti-oxidant while pheomelanin exhibits phototoxic pro-oxidant behavior – there is an increasing research effort to understand the molecular structure of melanins, their organization within intact melanosomes, and how these structures perform biological function(s).⁵

1.1.2. Melanocytes, melanosomes and melanin

Melanin biosynthesis is a complex pathway that appears in highly specialized cells, called melanocytes, responsible of the production of melanosomes, highly organized elliptic membrane-bound organelles in which melanin synthesis takes place.⁶ Melanosomes are transferred *via* dendrites to surrounding keratinocytes, where they play a critical role in photoprotection. The anatomical relationship between keratinocytes and melanocytes is known as “the epidermal melanin unit” and it has been estimated that each melanocyte is in contact with 40 keratinocytes in the basal and suprabasal layers.⁷

Melanosomes are typically divided into four maturation stages (I–IV) determined by their structure and the quantity, quality, and arrangement of the melanin produced (**Fig. 1**).^{8,9} Nascent melanosomes are assembled in the perinuclear region near the Golgi stacks, receiving all enzymatic and structural proteins required for melanogenesis. Stage I melanosomes are spherical vacuoles lacking tyrosinase activity (the main enzyme involved in melanogenesis) and have no internal structural components. At this point, the presence and correct processing of Pmel17, an important melanosomal structural protein, determines the transformation of stage I melanosomes to elongated, fibrillar organelles known as stage II melanosomes;^{9,10} they contain tyrosinase and exhibit minimal deposition of melanin. At this stage melanin synthesis starts and the pigment is uniformly deposited on the internal fibrils, leading to stage III melanosomes. The last developmental stage (IV) is detected in highly pigmented melanocytes; these melanosomes are either elliptical or ellipsoidal. The developmental stages detailed above refer mainly to eu-melanosomes (containing black-brown pigments); however, they are quite in the case of pheo-melanosomes (containing yellow-reddish melanin), the only difference being that the latter remain round and are not fibrillar during maturation.

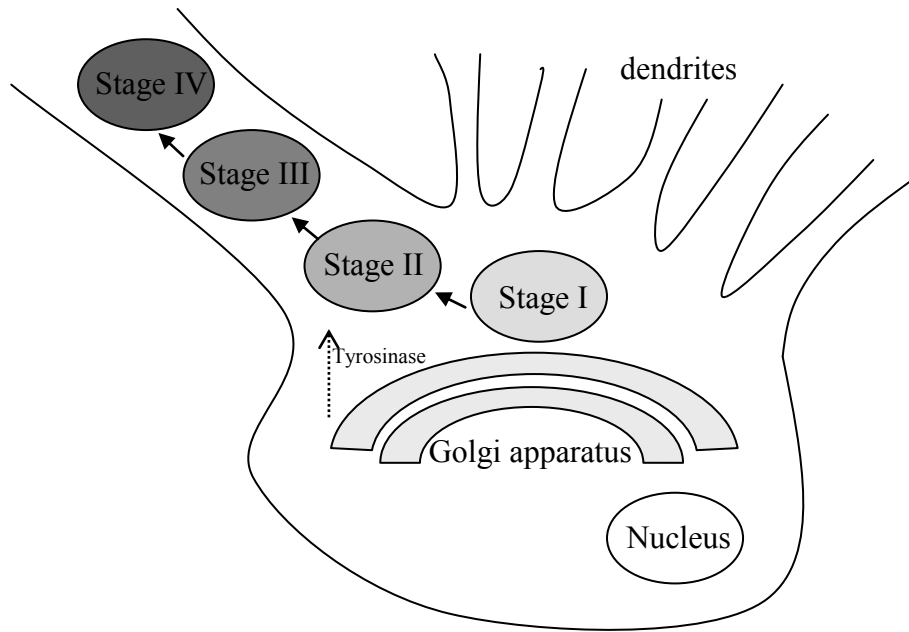


Figure 1. Schematic illustration of a melanocyte with melanosomes at the four developmental stages, moving toward the periphery of the cell within the dendrites.

In general, highly pigmented skin contains numerous single large melanosomal particles (0.5–0.8 μm in diameter), which are ellipsoidal and intensely melanotic (stage IV). Lighter pigmentation is associated with smaller (0.3–0.5 μm in diameter) and less dense melanosomes (stages II and III), which are clustered in membrane-bound groups.¹¹ These distinct patterns of melanosome type and distribution are present at birth and are not determined by external factors (such as sun exposure). They are responsible for the wide variety of skin complexions.

The variation in skin color among various races is determined mainly by the number, melanin content, and distribution of melanosomes produced and transferred by each melanocyte to a cluster of keratinocytes surrounding it.¹² Once in keratinocytes, the melanin granules accumulate above the nuclei and absorb harmful UV-R before it can reach the nucleus and damage the DNA. When melanin is produced and distributed properly in the skin, dividing cells are protected at least in part from mutations that might otherwise be caused by harmful UV.¹³

1.1.3. Pheomelanins as result of *MC1R* mutation

The melanin content of human melanocytes varies not only among different skin types but also among different sites of the skin for the same individual. This heterogeneity is highly regulated by gene expression, which controls the overall activity and expression of melanosomal proteins within melanocytes.¹⁴

The melanocortin 1 receptor (MC1R) is a 317 amino acid transmembrane G-protein coupled receptor member of the melanocortin family.¹⁵ MC1R is expressed on melanocyte and melanoma cells where it plays a role in pigmentation, but it is also expressed on a variety of other cell types relevant to skin (keratinocytes, fibroblasts,...) as well as in other organs (e.g. in the testis and the periaudeductal grey matter in brain).¹⁶ After UV-R exposure, melanocytes increase their expression of proopiomelanocortin, the precursor of α melanocytes stimulating hormone (α -MSH).^{17,18} The ligand α -MSH, via activation of MC1R, stimulates adenylyl cyclase, leading to an increase in cAMP (cyclic adenosine monophosphate), which in turn causes transcription of a number of enzymes, notably members of the tyrosinase family, important in melanin biosynthesis.¹⁶ In animals such as the mouse, overexpression of agouti, a peptide that acts as an inverse agonist at MC1R, results in a reduction in eumelanin production and an increase in the synthesis of pheomelanin.¹⁹ Although there is evidence that agouti signaling peptide, the homologue of agouti, is expressed in human skin, its role in human pigmentation remains unclear.²⁰

The MC1R is encoded for within a single exon of the *MC1R* gene on chromosome 16q24.3. The observation by Robbins et al.²¹ that alterations in the murine *Mclr* gene resulted in different coat colours in mice led to the hypothesis that part of the variation of normal human pigmentation within and between populations may arise from polymorphisms/variants in the human *MC1R* gene. Several association and population genetic studies have shown this to be the case over 30 variants in this gene identified to date.^{16,22} In general, black-skinned populations have two wild-type *MC1R* alleles, as do a number of Asian and darker skins Caucasian. However, within Caucasian populations, a single variant *MC1R* allele is associated with fairer skin type and an inability to tan, whereas two variant *MC1R* alleles are associated with a red hair phenotype.²²

Many of the reported changes, causally associated with a particular phenotype, are not complete loss-of-function mutations but rather show diminished function of signaling to varying degrees; that is, they show quantitative reduction of function rather than absence signaling activity. Although the number of partial loss-of-function mutations at the *MC1R* is large, three are relatively common in Northern European populations: the p.R151C, the p.R160W, and the p.D294H.^{16,22-25} These sequence variants are not however, functionally equivalent.^{22,26}

Recently the complete loss of function mutant *MC1R* alleles, as c.86_87insA and c.534_538insC, with insertion/deletion frameshift or premature stop codon, were studied. They are extremely rare, but Sturm et al. were able to find one case in the homozygote state, actually heterozygote for two rare insertions, that was the first case of *MC1R* null individual, showing red hair and fair skin.²⁷

On this basis, several studies have been focused at assessing the relationship of genotype with measurements of the type and amount of melanins in hair, as determined by quantitation of melanin markers. This approach will not only allow assessment of the quantitative contribution of a locus to variation, but also identification of those variations which have not so far been considered.²⁶

1.1.4. Structure and biosynthesis of pheomelanin

Within melanosomes, at least three enzymes are definitely required to synthesize different types of melanin. While tyrosinase is responsible for the critical steps of melanogenesis, tyrosinase-related protein 1 and dopachrome tautomerase are further involved in modifying the melanin into different types. Besides these, melanosomes contain other melanocyte-specific proteins that have structural functions or probably are involved in regulating the pH within melanosomes.

Eumelanin and pheomelanin both derive from the common precursor dopaquinone (DQ) formed by hydroxylation and oxidation of the common amino acid L-tyrosine by tyrosinase (**Fig. 2**).

DQ, through intramolecular addition of the amino group of the alanyl side chain and further oxidation steps, leads to 5,6-dihydroxyindole intermediates, which in turn give rise to eumelanin by oxidative polymerization.⁴

The biosynthesis of pheomelanin proceeds through several steps at the monomer levels (**Fig. 2**). The process is initiated by the conjugation of cysteine to DQ leading to 5-*S*-cysteinyl-dopa (5SCD) (74%) as main product, with small amount of 2-*S*-cysteinyl-dopa (2SCD) (14%) and other isomers.^{28,29}

Under physiologically relevant conditions, the major pheomelanin precursor 5SCD is converted to cysteinyl-dopa-quinone (CDQ) via a redox exchange with DQ, followed by cyclization and dehydration of CDQ to form the ortho-quinonimine (QI).³⁰ Rearrangement with or without decarboxylation of transient QI leads to 7-(2-amino-2-carboxyethyl)-5-hydroxy-2*H*-1,4-benzothiazine (BTZ) and 7-(2-amino-2-carboxyethyl)-5-hydroxy-2*H*-1,4-benzothiazine-3-carboxylic acid (BTZCA).³¹⁻³³ BTZ and BTZCA are the ultimate monomer precursor of pheomelanin. Before being incorporated into pheomelanin, a minor part of the benzothiazines may undergo a structural modification to form 7-(2-amino-2-carboxylethyl)-5-hydroxy-3-oxo-3,4-dihydro-2*H*-1,4-benzothiazine (ODHB) and 6-(2-amino-2-carboxyethyl)-4-hydroxy-benzothiazole (BT). The four monomeric units, BTZ (and BTZCA), ODHB, and BT, are eventually polymerized to form pheomelanin (**Fig. 2**).^{5,33,34}

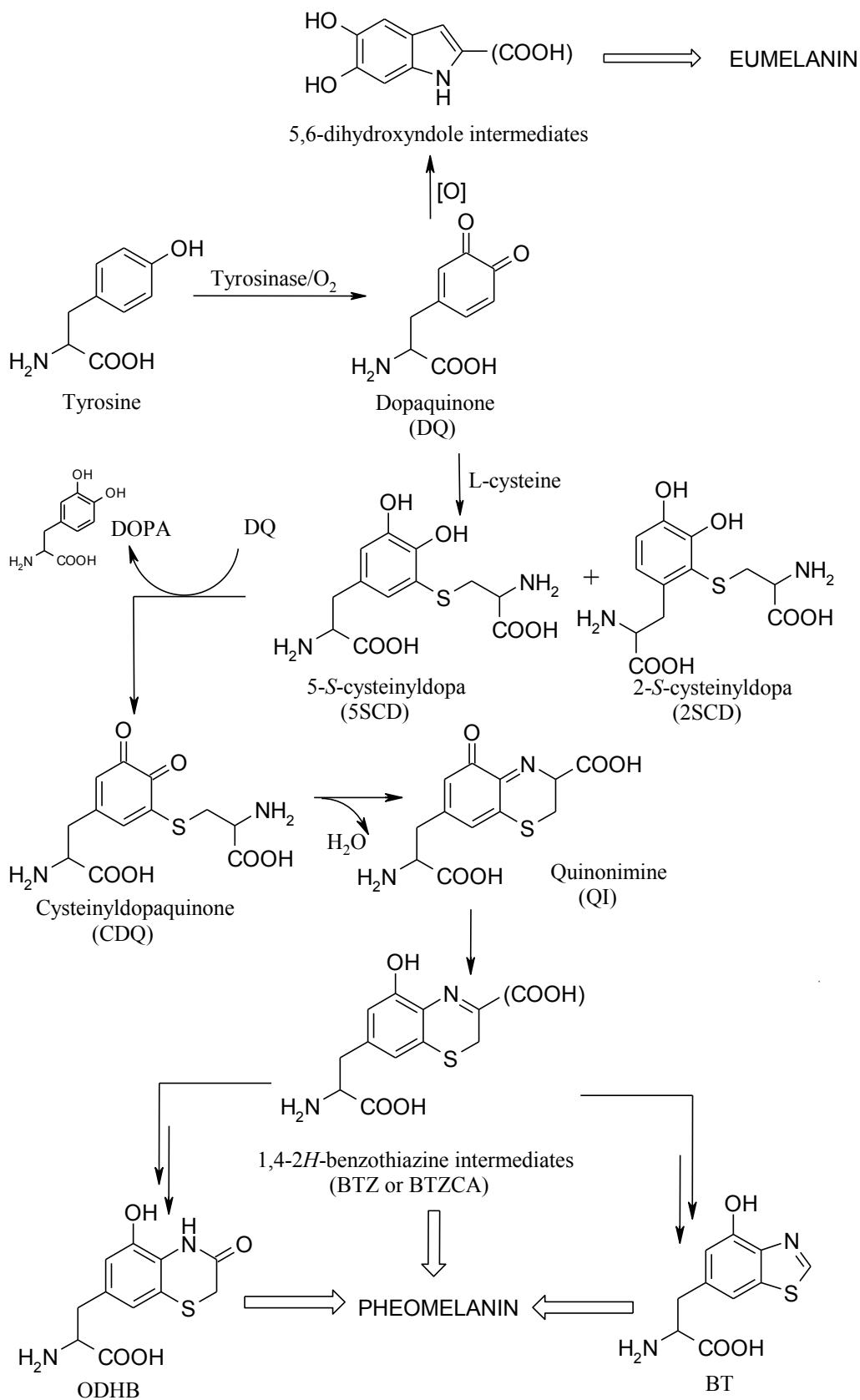


Figure 2. Eumelanogenesis and pheomelanogenesis pathways.

Most of the studies on pheomelanin beyond the monomer level were carried out on 5SCD, the main precursor. In studies carried out in the nineties, the evolution pathways of benzothiazine intermediates were investigated by analysis of the oxidation of 5SCD under biomimetic conditions. The couple peroxidase/H₂O₂, an enzyme involved in pheomelanogenesis *in vivo*, but extremely more efficient than tyrosinase in the oxidation of cysteinyl-dopa,³¹ was chosen as oxidant system. In the early stages of the oxidation BTZ is mainly formed, that rapidly evolves leading to a complex pattern of oligomeric compounds, the major of which was isolated after reductive treatment with 10% yields and characterized as the dimer I shown, while other minor compounds were identified as the related trimers II and III (Fig. 3).³⁵

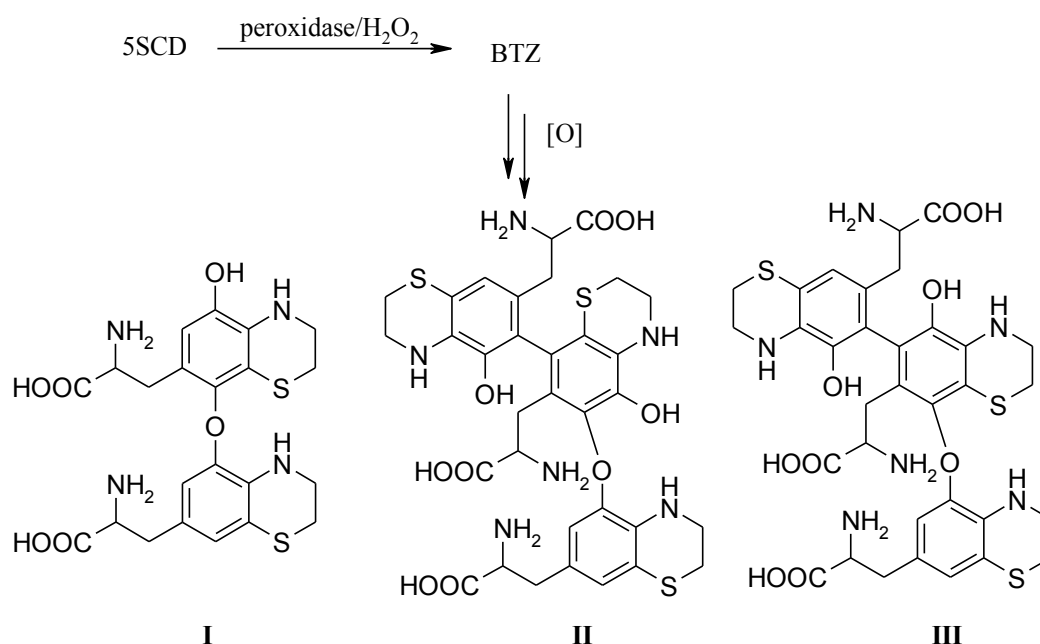


Figure 3. Oligomer compounds arising from oxidation of 5SCD by the peroxidase/H₂O₂ couple.

All the oligomeric structures are characterized by C-C and C-O bonds between the benzothiazine units, suggesting that the polymerization proceeds through phenolic coupling of aryloxy radicals generated by an initial monoelectronic oxidation of 5SCD. In addition to enzymatic factors some metal ions, particularly zinc and iron, are shown to profoundly affect the kinetics and course of fundamental steps of

pheomelanogenesis.³⁶ 5SCD is shown to form strong complexes with a series of metal ions including Zn^{2+} , Cu^{2+} , Fe^{3+} , Al^{3+} , Co^{2+} , Cd^{2+} . Some of these, and particularly the 5SCD–zinc complex, undergoes oxidation at higher rates with respect to free 5SCD, leading to BTZCA.³⁷

This finding is of particular interest as it provides a clue to the formation of trichochromes, a group of low molecular weight pigments, isolated from red feathers, featuring a peculiar pH dependent chromophore, which could unambiguously be formulated as $\Delta^{2,2'}$ -bibenzothiazines(**Fig. 4**).³⁸

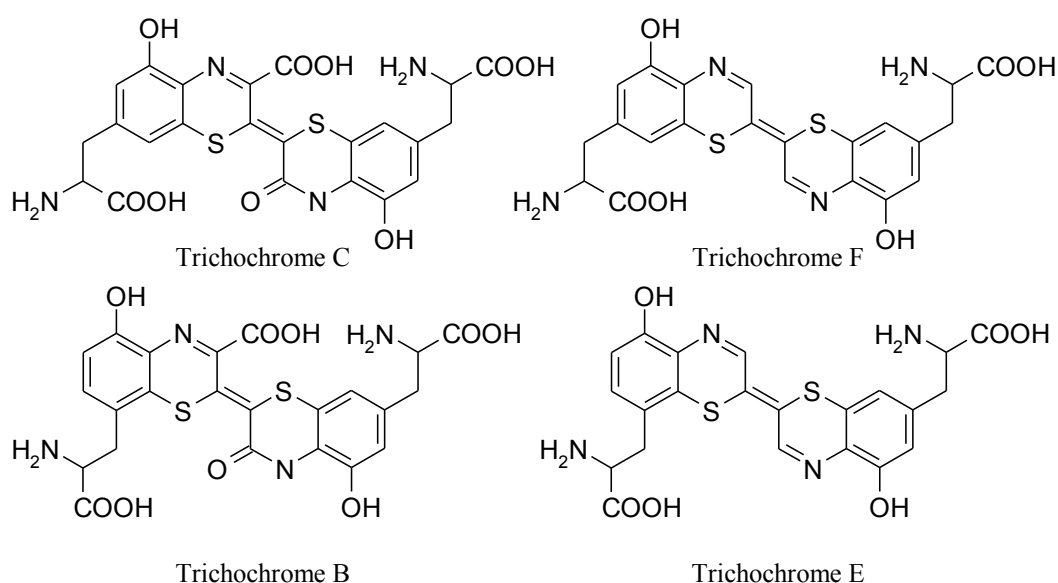


Figure 4. Structures of trichochromes isolated from red avian feathers.

Indeed, Trichochrome C, the most abundant trichochrome isolated in red hair, was obtained when BTZCA was allowed to stand in air in the presence of acids by the intermediacy of 2,2'-bi(3-carboxy-1,4-benzothiazine), BTZCA-dimers (actually a pair of diastereomers), derived by coupling at two position of BTZCA (**Fig. 5**).³⁷

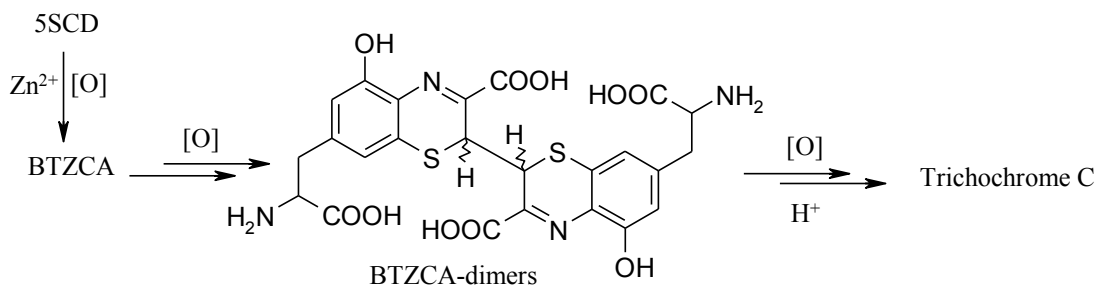


Figure 5. Formation of Trichochrome C by oxidative dimerization of BTZCA in the zinc-catalyzed oxidation of 5SCD.

1.1.5. Chemical degradation studies

Direct investigation of the natural pigments was largely based on chemical degradation studies. Chemical degradation has the advantage to allow direct analysis of melanins from natural sources, which is different from the biogenetic type approach so far illustrated. Yet, exposure to the degradation agent, often an efficient oxidant in strong alkaline or acid media, may produce artifactual alterations of the pigment backbone which are reflected in the structure of the final products. This is indeed a major limitation unless the chemical reactivity of the monomer units of the pigment polymer under the degradation conditions is well characterized and taken into account in the structural interpretation. Thus, when combined with the results of the biogenetic studies, chemical degradation is a valuable tool not only for structural determination but also for identification of melanins in tissues. Indeed, the specificity of the degradation products makes isolation of the pigments from tissues generally not needed, and allows straightforward discrimination of true pheomelanins from pheomelanin-looking pigments, e.g. light brown eumelanins.

Different useful degradation methodologies has been set up. One is the reductive hydrolysis with HI, which produces 4-amino-3-hydroxyphenylalanine (4-AHP) and 3-amino-4-hydroxyphenylalanine (3-AHP).³⁴

The second one is the oxidation by alkaline hydrogen peroxide, that gives 6-(2-amino-2-carboxyethyl)-2-carboxy-4-hydroxybenzothiazole (BTCA), thiazole-4,5-dicarboxylic acid (TDCA) and thiazole-2,4,5-tricarboxylic acid (TTCA) (**Fig. 6**).³⁹

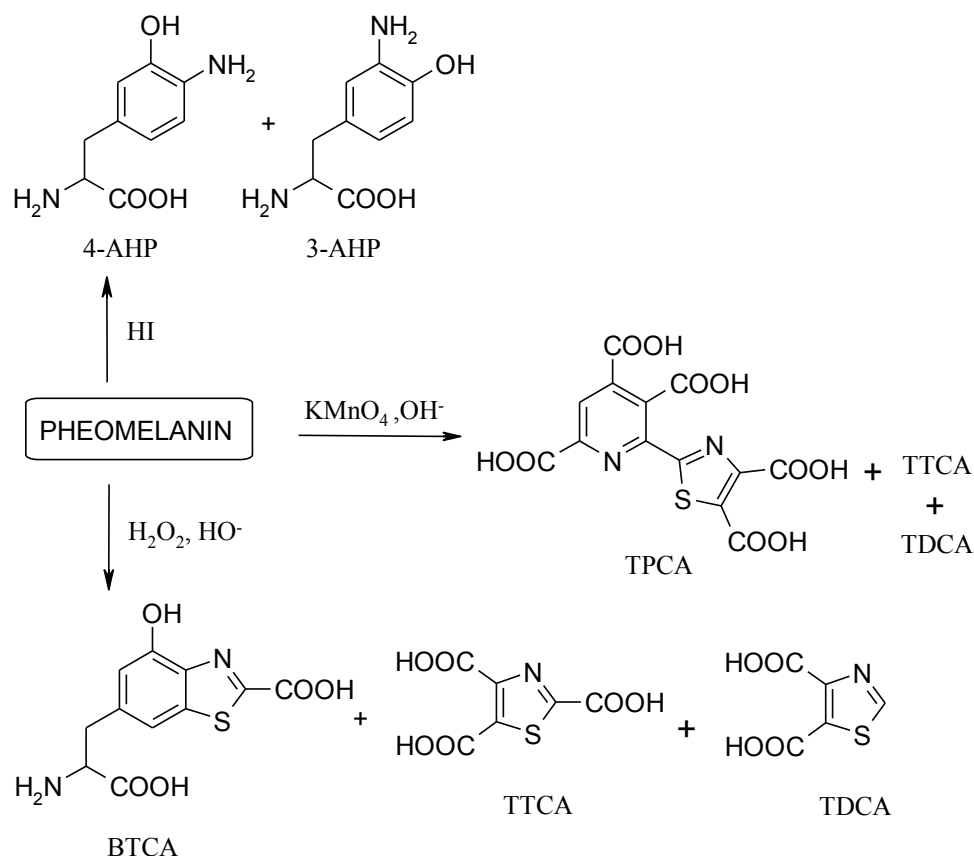


Figure 6. Main chemical degradation products of pheomelanins.

An advantage of this oxidative degradation is that pheomelanin degradation products are produced together with degradation products arising from eumelanin, pyrrole-2,3,5-tricarboxylic acid (PTCA) and pyrrole-2,3-dicarboxylic acid (PDCA). This allows to estimate relative ratios of pheomelanin to eumelanin in tissue samples (**Fig. 7**).^{39,40}

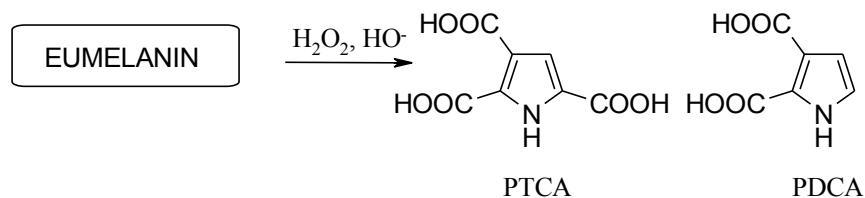


Figure 7. Products from alkaline hydrogen peroxide oxidation of eumelanins.

An intriguing, and so far overlooked, structural issue relates to the identification in an early seminal paper⁴¹ of a series of pyridinecarboxylic acids, including pyridine-2,3,4,6-

tetracarboxylic acid and 2-[2'-(4',5'-dicarboxythiazolyl)]-3,4,6-pyridinetricarboxylic acid (TPCA), by permanganate degradation of pheomelanin isolated from red chicken feathers (**Fig. 6**). This oxidative degradation lead also to TDCA and TTCA.⁴²

Identification of pyridine fragments allowed the authors to postulate the presence of isoquinoline units in natural pheomelanins, but this hypothesis has remained so far unverified (**Fig. 8**). In fact, pyridine-yielding units have never been demonstrated in human red hair pheomelanin or synthetic pheomelanins, the origin of the main pyridine-containing degradation products has never been elucidated since the original study and no isoquinoline derivative has ever been isolated or detected spectroscopically in model chemical studies of pheomelanin synthesis.⁵

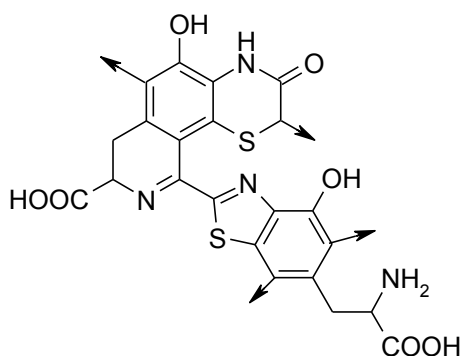


Figure 8. Proposed structural model of pheomelanin.⁴¹

These considerations prompted us to re-examine the structure of pheomelanins. Furthermore more attention was given to the contribution of 2SCD, a minor pheomelanin precursor, in pigment construction.

1.1.6. Casing model for mixed melanogenesis

Over the past 30 years, chemical analyses have been performed that enable the quantification of the amount of eumelanin and pheomelanin present in a naturally occurring sample of melanin.⁴³ These works collectively reveal that more often than not, natural melanin pigments consist of both eumelanin and pheomelanin in varying ratios.^{26,44,45} Thus, rather than focus just on the structural and functional properties of

pure eumelanin or pheomelanin, there is a need to understand how “mixed melanins” are made, and how their molecular and functional properties differ from those of pure melanins.⁵

By use of advanced technologies, in particular photoelectron emission microscopy (PEEM) coupled to a free-electron laser (FEL),^{46,47} it was shown that human eumelanosomes from black hair have a surface oxidation potential of -0.2 V vs. the normal hydrogen electrode. On the other hand, human melanosomes from red hair contain a mixture of eumelanin and pheomelanin, which is reflected by oxidation potentials of -0.2 and +0.5 V, respectively. Because FEL–PEEM is a surface technique, the results indicate that melanosomes from red hair have both types of melanin on or near their surface.⁴⁸

Wakamatsu et al. recently reported the eumelanin/pheomelanin ratios for uveal melanocytes isolated from eyes of varying color.⁴⁹ A variety of spatial imaging studies of the melanosomes isolated from the stroma of blue-green (hazel) and dark brown irides, which are characterized by eumelanin:pheomelanin ratios of 1.3 and 14.8, respectively, were performed.⁵⁰ The photoemission image only reveals the presence of eumelanin on the surface of the melanosome.

Therefore, an explanation is needed for how eumelanin grows on pheomelanin. Recently a three-step pathway for the mixed melanogenesis has been proposed.^{51,52} After DQ production, the first stage is the production of cysteinyl dopas, which continues as long as the cysteine concentration is above 0.13 μM . The second stage is the oxidation of cysteinyl dopas to produce pheomelanin, which continues as long as cysteinyl dopas are present at concentrations above 9 μM . The third stage is the production of eumelanin, after most cysteinyl dopas and cysteine are depleted.⁵³ The morphological consequence of this ‘casing model’ for the chemistry/biochemistry and time course of mixed melanogenesis is schematically represented in **Figure 9**, in which the assembly of the pigment involves a pheomelanin core surrounded by a eumelanin outer coat.

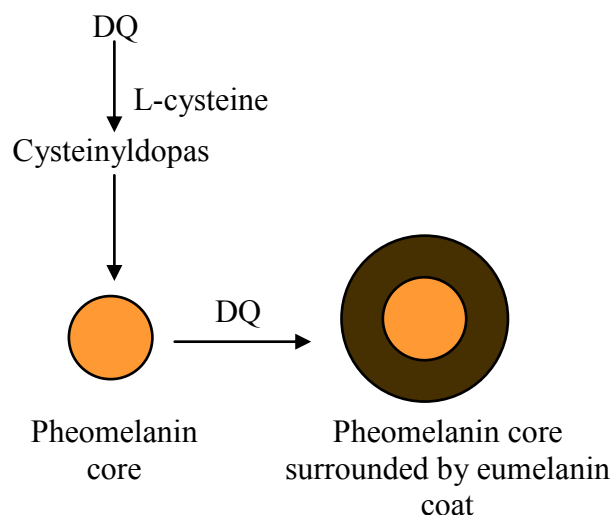


Figure 9. Schematic representation of the casing model for mixed melanogenesis.

This organization has been proved for neuromelanin, a dark pigment present in the substantia nigra and some other regions of the brain, consisting of dopamine with some incorporation of cysteinyldopamine⁵⁴⁻⁵⁶ and iridal stroma melanosomes, both resulting from mixed melanogenesis, suggesting that the casing model may be independent on the tissue type. However, this model has still to be proved for skin and hair pigment with interesting consequences. Indeed, oxidative damage of the eumelaninic surface could expose pheomelanin, which can lead to additional oxidation stress. Subsequent exposure of the photoreactive and pro-oxidant pheomelanin coupled to the lower total amount of melanin in lighter colored tissues could critically contribute to the observed tendency to actinic damage and skin cancers of fair complexioned individuals.

1.1.7. Photochemical properties of pheomelanin

A commonly held view is that pheomelanins may act as potent UV photosensitizers leading to intense production of reactive oxygen species (ROS) which contribute directly to the increased susceptibility of red haired individuals to actinic damage and skin cancer. This concept was pioneered by Chedekel et al.,⁵⁷ and has spurred unabated interest in the photochemical and photobiological properties of pheomelanins.⁵⁸⁻⁶¹

Experiments on congenic mice of black, yellow, and albino coat colors after exposure to predominantly UVB (280–320 nm) or UVA (320–400 nm) radiation have shown that pheomelanin had 3-fold greater specific activity in photosensitizing adjacent cells to caspase-3 independent apoptosis, and this occurs at a frequency greater than the apoptosis induced by UV absorption on DNA.⁶¹

Simon and coworkers demonstrated that different molecular components may be involved in the transient absorption, emission and oxygen photoconsumption responses of pheomelanin.⁶²⁻⁶⁴ Moreover, pheomelanin-containing melanosomes from human hair were shown to display low photo-ionization threshold values relative to eumelanins⁶⁵ supporting a possible role of pheomelanins in the onset of UV-induced skin cancer in redheads.

In this framework the implication of oxidant and photo-oxidant properties of pheomelanins in mixed melanogenesis and in the proposed casing model has not so far been clarified.

1.1.8. Melanoma and melanosis

Melanoma, one of the most widely spread cancers, is derived from pigment-producing melanocytes. There is accumulating evidence that constitutive pigmentation is highly involved in the development of melanoma, with the highest risk being associated with pheomelanin pigmentation.

Diffuse melanosis is a rare condition which may occur in metastasizing melanoma and is associated with a very poor prognosis. The median survival after the appearance of diffuse melanosis is only about six months, with a range of a few days to one year.⁶⁶ The process of diffuse melanosis may involve the total skin, mucous membranes and internal organs, resulting in a characteristic slate-gray discoloration. The color of the patients' urine is dark brown when freshly voided. In 1864 the German pathologist Ernest Wagner was the first to describe a 30-year-old patient with a melanoma arising in a congenital nevus who subsequently acquired a generalized bluish-gray discoloration.⁶⁷ Despite various explanations for the diffuse melanosis,⁶⁷⁻⁷⁰ the process resulting in diffuse melanosis from metastatic melanoma is still unknown.⁷¹

The formation of cysteinyl-dopa in melanocytes was proven by their occurrence in melanoma and epidermal tissues⁷² but also in biological fluids such as urine and serum,^{73,74} where they are found at ratios that compare fairly well with those obtained during *in vitro* pheomelanogenesis (5:1).^{29,33} Of particular interest in this connection is the rise of urinary and serum levels of cysteinyl-dopas in melanoma patients.⁷⁴ Studies carried out on thousands of patients have indicated that determination of 5SCD levels is a powerful tool for monitoring melanoma progression and prognosis, but it appears also as a sensitive and specific predicting factor of distant metastases.⁷⁵

BTCA obtained from oxidative degradation of 5SCD derived units⁴⁰ proved to be a specific structural marker for the analysis of pheomelanin containing tissues together with AHPs.^{76,77} The conditions for chemical degradation and analysis of these compounds were recently improved by introduction of wetttable octadecylsilane columns³⁹ simpler eluents, hydrophilic interaction liquid chromatography (HILIC)⁷⁸ and GC/MS analysis.⁷⁹ Using the latter methodologies evidence was obtained for the presence of pheomelanin pigments in the urine of melanoma patients.⁷⁷

1,4-Benzothiazole compounds were obtained in melanoma patients on HI degradation of urinary pigments followed by ethyl chloroformate derivatization and GC/MS analysis.⁷⁹ The presence of an active pheomelanogenic pathway associated with melanoma was also indicated by the occurrence of trichochromes in the urine of melanoma patients⁸⁰ particularly when diffuse melanosis occurs in metastasizing melanoma.⁸¹

However the pheomelanogenic pathway associated with melanosis of melanoma is still poorly unknown.

1.2. Thioconjugates from dietary polyphenols of plant origin

1.2.1. Classification and occurrence of dietary polyphenols

Dietary polyphenols are the most abundant antioxidants in human diets. With over 8,000 structural variants, they are secondary metabolites of plants and denote many substances with aromatic ring(s) bearing one or more hydroxyl moieties. They are ranked into groups (**Fig. 10**) based on the number of phenolic rings and of the structural elements that connect these rings:⁸² (1) the phenolic acids with the subclasses derived from hydroxybenzoic acids such as gallic acid and from hydroxycinnamic acid, containing caffeic, ferulic, and coumaric acid; (2) the large flavonoid subclass, which includes flavonols, flavones, isoflavones, flavanones, anthocyanidins, and flavanols; (3) the stilbenes; (4) the lignans and the polymeric lignins.

The main dietary sources of polyphenols include some common fruits, vegetables and beverages (fruit juice, wine, tea, coffee, chocolate and beer) and, to a lesser extent, dry legumes and cereals. Phenolic acids account for about one third of the total intake and flavonoids account for the remaining two thirds. The most abundant flavonoids in the diet are flavanols (catechins plus proanthocyanidins), anthocyanins, glycosylated derivative of anthocyanidin, present in highly pigmented flowers and fruits, and their oxidation products.⁸³

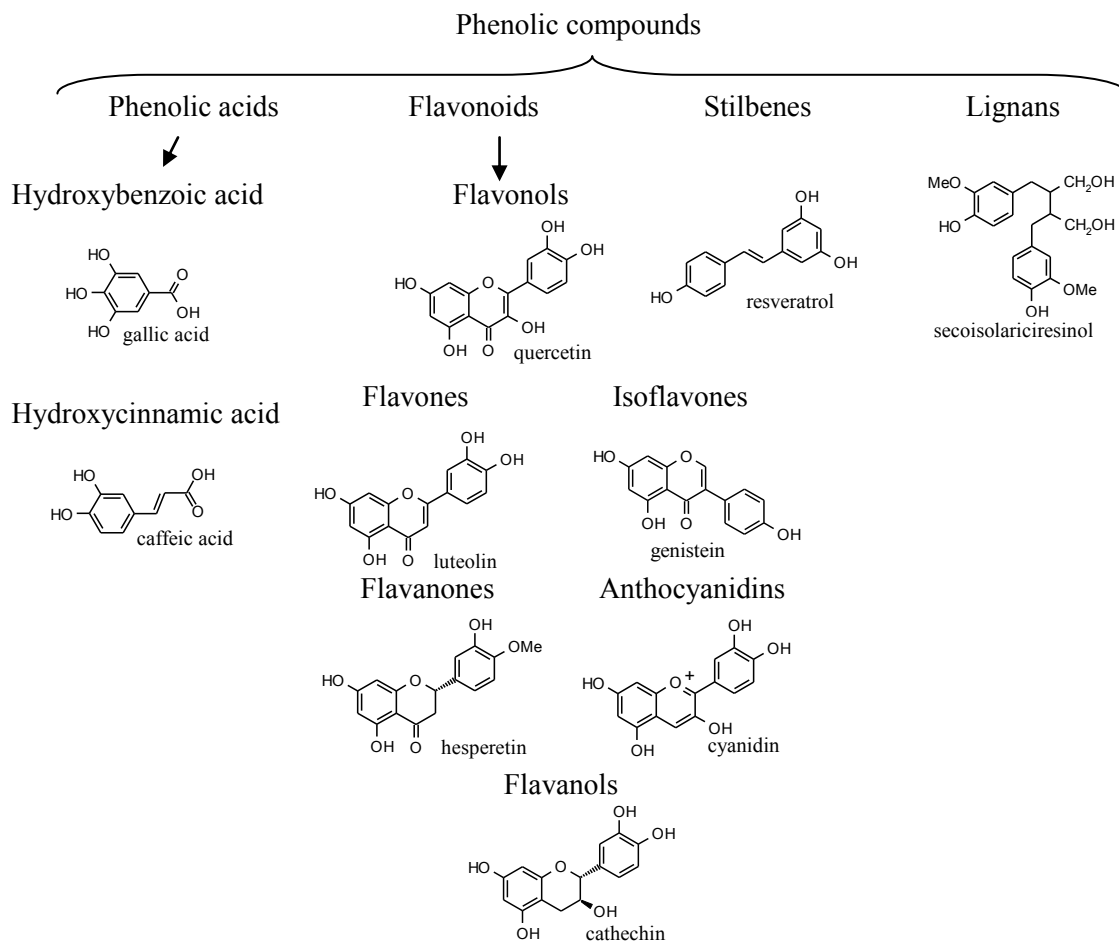


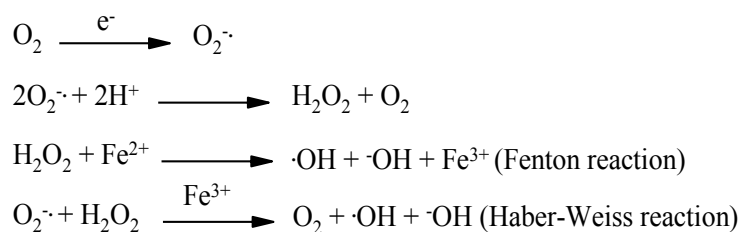
Figure 10. Classification of dietary polyphenols.

1.2.2. Reactive oxygen species (ROS) and bioactivities of dietary polyphenols

Oxidative stress is a condition of over-production of reactive oxygen species (ROS) and is considered to play a pivotal role in the pathogenesis of aging and several degenerative diseases, such as atherosclerosis, cardiovascular disease, type II diabetes and cancer.⁸⁴⁻⁸⁶ ROS are products of normal cellular metabolism and are well recognised for being both deleterious and beneficial species, since they can be either harmful or beneficial to living systems.⁸⁷⁻⁹¹ Beneficial effects of ROS occur at low/moderate concentrations and involve physiological roles in cellular responses to noxious stimuli as, for example, in defence against infectious agents and in the functioning of a number of cellular signalling systems.

The harmful effect of free radicals occurs in biological systems when there is a deficiency of enzymatic and non-enzymatic antioxidants to readily detoxify the reactive intermediates or to repair the resulting damage.⁸⁸ The excess ROS can damage cellular lipids, proteins or DNA inhibiting their normal function.

Oxidative stress is the result of the metabolic reactions that use oxygen and represents a disturbance in the equilibrium status of prooxidant/antioxidant reactions in living organisms. Because of this, oxidative stress has been implicated in a number of human diseases as well as in the ageing process. Free radicals can be defined as molecules or molecular fragments containing one or more unpaired electrons in atomic or molecular orbitals.⁹² This unpaired electron(s) usually gives a considerable degree of reactivity to the species. The addition of one electron to dioxygen forms the superoxide anion radical ($O_2^{\cdot-}$),⁹³ which is generated mostly within mitochondria. Superoxide anion, arising either through metabolic processes or following oxygen “activation” by physical irradiation, is considered the “primary” ROS, and can further interact with other molecules to generate “secondary” ROS, prevalently through enzyme- or metal-catalysed processes.⁹⁰ Superoxide can disproportionate by action of superoxide dismutase to yield hydrogen peroxide (H_2O_2). In the presence of partially reduced metal ions, in particular iron, hydrogen peroxide is subsequently converted through Fenton and Haber-Weiss reactions to a hydroxyl radical ($\cdot OH$) according to equations below:



The hydroxyl radical has a high reactivity, making it a very dangerous radical with an exceedingly short *in vivo* half-life of approx. 10^{-9} s,⁹⁴ that is near diffusion rate. Thus when produced *in vivo* $\cdot OH$ reacts close to its site of formation and can interact with nucleic acids, lipids, and proteins. The hydroxyl radical is known to react with all components of the DNA molecule, damaging both the purine and pyrimidine bases and also the deoxyribose backbone.⁹⁰

Oxygen consumption in peroxisomes leads to H₂O₂ production, which is then used to oxidize a variety of molecules. These organelles also contain catalase, which decomposes hydrogen peroxide and presumably prevents accumulation of this toxic compound. When peroxisomes are damaged and their H₂O₂-consuming enzymes downregulated, H₂O₂ is released into the cytosol which significantly contributes to oxidative stress.

Additional reactive radicals derived from oxygen that can be formed in living systems are peroxy radicals (ROO·). The simplest peroxy radical is ·OOH, which is the protonated form of superoxide (O₂^{·-}) and is termed hydroperoxy radical. It has been demonstrated that hydroperoxy radical initiates the process of lipid peroxidation *in vivo*, a process that generates a variety of products including reactive electrophiles such as epoxides and aldehydes.⁹⁵

In order to cope with an excess of free radicals produced upon oxidative stress, humans have developed endogenous and exogenous mechanisms in order to maintain redox homeostasis. Among these, dietary polyphenols have been largely studied for their strong antioxidant capacities and other properties by which cell activities are regulated.⁸³

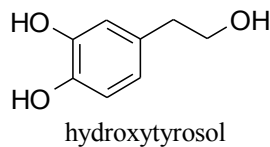
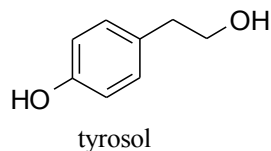
In literature several data are reported about the mechanisms with which dietary polyphenols exhibit their antioxidant activities.^{96,97} In particular, it was shown that they, thanks to the *o*-diphenol function, are able to chelate metal ions such as Fe²⁺ and Cu²⁺ involved in Fenton-type oxidation processes. They can also act as hydrogen donors, interrupting, for example, the processes of chain propagation in lipidic peroxidation⁹⁸ and can act as a scavenger of radical species.⁹⁹

In the following sections the characteristics of the main classes of polyphenols will be discussed in more details.

1.2.3. Polyphenolics of olive oil. Hydroxytyrosol

Hydroxytyrosol (2-(3,4-dihydroxyphenyl)ethanol, HTYR) and related polyphenolic constituents of extra virgin olive oil are endowed with several biological properties that

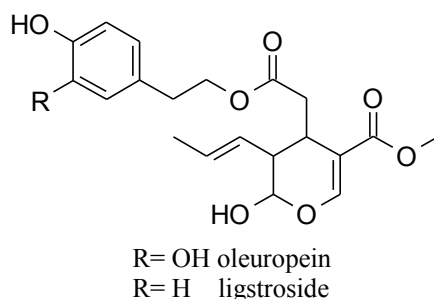
may contribute to the reduced risk of cardiovascular diseases and malignant neoplasms in the populations of Mediterranean countries.¹⁰⁰⁻¹⁰²



The beneficial role of olive phenols in cancer prevention is ascribed to their potent antioxidant properties enabling them to counteract the geno- and cytotoxic effects of ROS generated in settings of oxidative stress.^{96,97} Extra virgin olive oil constituents can contribute to lower the incidence of coronary heart diseases as well as of prostate and colon cancer.¹⁰⁰ HTYR and related (poly)phenolic components can also inhibit the formation of carcinogenic and mutagenic heterocyclic amines.¹⁰³ The scavenging potential of HTYR towards ROS has recently been determined.¹⁰⁴ The marked antioxidant properties of HTYR are also exemplified by its ability to inhibit the copper sulphate induced oxidation of low density lipoproteins as shown by the reduced short chain aldehydes formation, sparing of vitamin E and decrease of the levels of malondialdehyde-lysine and 4-hydroxynonenal-lysine adducts indicating protection of the apoprotein layer.¹⁰⁵ Another mechanism by which HTYR may exert its effects is metal chelation, particularly Cu^{2+} and Fe^{2+} ions which are able to promote peroxy/hydroxyl formation by decomposition of hydroperoxides by the Fenton and Haber-Weiss reactions. The ability of HTYR to chelate ferric ions accounts for the marked inhibition of hydroperoxide formation promoted by enzymatic and non enzymatic process including lactoferrin and iron in liposomes and oil-in-water emulsions¹⁰⁶ or hemoglobin, enzymatic NADH-iron and non enzymatic ascorbate-iron.¹⁰⁷ Free iron sequestering by HTYR may therefore represent an important route by which this compound exerts the documented beneficial effects towards those pathological conditions and chronic diseases associated with oxidative stress.¹⁰⁸

The concentration of phenols in extra virgin olive oil varies from 50 to 800 mg/Kg, with a mean value for commercial oil of 180 mg/kg,^{97,109} a daily consumption of 50 g olive oil (a mean value in the Mediterranean countries) would therefore result in an intake of about 9 mg of olive oil phenols per day, of which it is estimated that 1 mg is derived

from HTYR and tyrosol and about 8 mg from the aglycones of oleuropein and ligstroside. Extra virgin olive oil is also rich in the antioxidant compound α -tocopherol, whose concentration varies between a few ppm to 350 ppm.

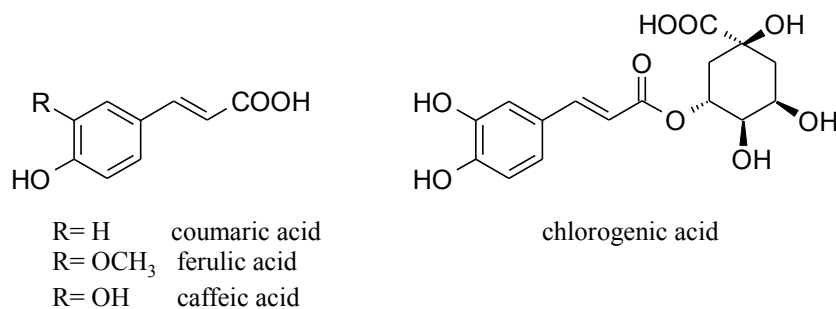


HTYR was reported to be absorbed by 66%: this would lead to a maximum concentration of $0.06 \mu\text{M}$ of this compound in plasma after a 50 g intake of olive oil.¹⁰⁹ Although low molecular weight phenols are found in virgin olive oil, a high percentage is discarded in olive mill wastewaters (OMW), a by-product of the extraction process of olive oil. Most OMW are accumulated over a short period (typically November–December) then spread over fields or dumped into rivers, thus causing pollution of soils and aquatic area. Olive phenols are partially responsible for this pollution due to their toxicity to plants, bacteria and aquatic organisms. Hence, chemical and biotechnological processes (*e.g.*, Fenton reaction or oxidation catalyzed by fungal enzymes) have been developed to degrade OMW phenols. An interesting alternative could be the extraction of phenols from OMW and their valorization as antioxidants in the food and pharmaceutical industries.¹¹⁰

1.2.4. Hydroxycinnamate compounds

The total polyphenol intake has been reported to reach 1 g/d in people who eat several servings of fruit and vegetables per day. Hydroxycinnamate compounds, including *p*-coumaric acid, ferulic acid, caffeic acid and its ester chlorogenic acid (5-caffeoyl-D-quinic acid), are widely diffused at relatively elevated levels in various agricultural products and contribute significantly to the total polyphenol intake: for example,

chlorogenic acid is present in quantities of 3.4-14 mg/100 g fresh weight in potatoes, 60 mg/kg in broccoli, 12-31 mg in 100 mL of apple juice, 89 mg/100 g in dry tea shoots, and 70-350 mg in a cup of coffee. Caffeic acid is present in fruit such as pears (19 mg/g) and apples (1.3 mg/g), while ferulic acid is the most abundant phenolic acid found in wheat grain (0.8-2 g/kg dry weight).¹¹¹

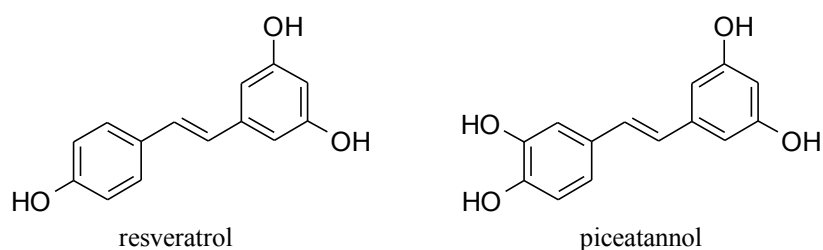


Hydroxycinnamic acids have been suggested to play a role in the apparent association between the regular consumption of polyphenol-rich foods and beverages and the prevention of inflammatory and proliferative diseases. In particular, chlorogenic acid reportedly prevents type 2 diabetes mellitus by inhibiting intestinal glucose absorption¹¹² and exerts anticarcinogenic effects by attenuating injury from carcinogenic N-nitroso compounds and DNA damage.^{111,113,114} However, ~33% of chlorogenic acid is absorbed in the intact form intestinally, with the remaining 67% being metabolized to caffeic acid in the colon.¹¹¹ In contrast, ~95% of caffeic acid is absorbed intestinally. These bioavailability data suggest that the biological effects of chlorogenic acid in the body would manifest after it has been metabolized to caffeic acid.

Caffeic acid is a selective inhibitor for biosynthesis of leukotriene, involved in immunoregulation and in a variety of diseases, including asthma, inflammation and various allergic conditions. In addition, caffeic acid is a strong and selective activity and transcription inhibitor of matrix metalloproteinase, that are directly involved in human hepatic tumorigenesis and metastasis.¹¹⁵

1.2.5. Red wine stilbenes

Resveratrol (5-[2-(4-hydroxyphenyl)vinyl]benzene-1,3-diol) is the most well-known and well-characterized stilbene. Primarily found in peanuts, red wine, and grapes,^{116,117} resveratrol is a polyphenolic phytoalexin produced by various plants in response to microbial attack, excessive ultraviolet exposure and disease.¹¹⁸ Currently, has been shown how resveratrol can act as a potent anti-inflammatory, anti-cancer and chemoprotective agent.



Stilbenes (diarylethenes) exist as stereoisomers in *E* and *Z* forms, but naturally occurring stilbenes exist in the *E* (*trans*) form. Research has revealed the *E* form to exhibit more potent activity compared to the *Z* form across various anti-cancer and anti-oxidant assays.

Studies of structure-activity relationships indicate that the antioxidant activity of resveratrol stems from the peculiar oxygenation pattern on the planar stilbenic skeleton, featuring as a crucial determinant of the radical scavenger activity the 4'-OH group, synergistically supported by the 3- and 5-OH groups on the resorcin moiety. The efficiency of the 4'-OH group as a hydrogen donor is enhanced by the *trans* double bond, which increases both its acidity and the resonance stabilization energy of the phenoxy radical derived from H-atom abstraction.^{119,120}

Based on encouraging therapeutic evidence, resveratrol research has fuelled a great deal of interest in characterizing structurally similar stilbene compounds and in synthesizing modified stilbenes substituted with various functional groups. Among these one of the best known is piceatannol (4-[2-(3,5-dihydroxyphenyl)vinyl]benzene-1,2-diol).

Piceatannol is synthesized in response to fungal attack, ultraviolet exposure, and microbial infection. Induction of piceatannol synthesis is also evident during the

ripening of grapes and increases during the fermentation process of wine production due to β -glucosidase activity of bacteria. Constitutive piceatannol has also been identified in white tea, sugar cane, rhubarb, and some varieties of berries.¹²¹

Resveratrol and piceatannol have been detected in red wine and have long been associated with cardioprotection. The “French paradox” was described as an anomaly in which southern French citizens, who smoke regularly and enjoy a high-fat diet, boast a very low mortality rate of coronary heart disease. Scientists have attributed this unlikely relationship to moderate consumption of the anti-inflammatory and anti-oxidant polyphenolic compounds, such as piceatannol and resveratrol, in red wine.^{122,123} Piceatannol and resveratrol have been shown to elicit a number of cardioprotective activities including inhibition of low-density lipoprotein (LDL) oxidation, mediation of cardiac cell function, suppression of platelet aggregation, and attenuation of myocardial tissue damage during ischemic events.⁸³

It has been estimated that the concentration of resveratrol in wine ranges from as little as 0.2 mg/L up to 10.6 mg/L, depending largely on grape type and environment while that of piceatannol is about 0.45 mg/L.¹²⁴

One study employing human liver microsomes found that *trans*-resveratrol metabolism produces two main metabolites, with one being piceatannol. The rate of resveratrol hydroxylation forming piceatannol was rapid, leading investigators to postulate that resveratrol may act as a pro-drug for production of piceatannol and other stilbenes.¹²⁵

Piceatannol is an antagonist of the aryl-hydrocarbon receptor, implicated in dioxin toxicity. Due to its estrogen structural similarity piceatannol acts as a selective estrogen receptor modulator in human breast cancer cell lines. Further investigations revealed piceatannol to be a potent superoxide scavenger. Recent researches have shown piceatannol to be a more effective scavenger of nitric oxide and hydrogen peroxide and significantly more potent in inhibiting Cu^{2+} induced lipid peroxidation in low-density proteins compared to resveratrol. It is commonly believed that the additional hydroxyl group of piceatannol makes it more reactive and is therefore a more potent free radical scavenger compared to resveratrol.⁸³

1.2.6. Thioconjugates of polyphenols with dihydrolipoic acid

In the field of antioxidants research, development of new antioxidants with enhanced activity and lower toxicity is highly desirable for the prevention and/or treatment of a number of diseases and, in food chemistry, for better food preservation.

In particular recent efforts are directed to the preparation and properties evaluation of thioconjugates of polyphenols from natural sources.

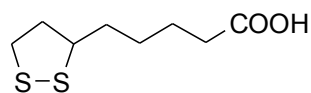
It was shown that conjugation of catechins with cysteine generates compound with higher antiradical capacity and enhanced neuroprotective activity than their underivatised counterparts.¹²⁶

In a recent paper it was elucidated that the presence of an alkylthio group in *para*-position of phenolic systems produces a marked enhancement of the chain breaking antioxidant activity, by decreasing the bond dissociation enthalpy of the OH group and affecting the reaction rate with peroxylic radicals.¹²⁷ Nevertheless, it is not yet clear the effect of an alkylthio group in *ortho*-position of phenolic systems on their antioxidant activity and on the reactivity of *ortho*-catechols.

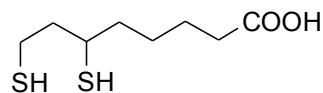
All naturally occurring antioxidant are strongly hydrophilic and this makes their incorporation into fat and oil matrices difficult. To overcome this problem in recent years preparation of lipophilic antioxidants from natural sources, as clovamide derivatives, poly(lauroyl(+)-catechin)s or hydroxytyrosol fatty acid esters, as the hydroxytyrosol acetate, palmitate, oleate and linoleate has largely been pursued.¹²⁸⁻¹³⁰ Yet, improvement of the antioxidant activity of polyphenols through modification of the catecholic nucleus has scarcely been pursued, the only derivatives so far prepared being esters at the phenolic or alcoholic functionality.

With this in mind new experiments were directed to the synthesis of a new derivative of polyphenols by conjugation with dihydrolipoic acid (DHHLA) and evaluation of its antioxidant properties.

Lipoic acid (1,2-dithiolane-3-pentenoic acid, LA) and its reduced form dihydrolipoic acid (DHHLA) are naturally occurring compounds.



lipoic acid

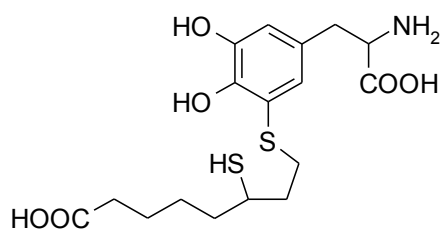


dihydrolipoic acid

LA has long been known as a coenzyme of multienzymatic mitochondrial complexes catalyzing oxidative decarboxylation of α -ketoacids.¹³¹ Therapeutic action of LA is based on unique antioxidant properties of LA/DHLA system, which possesses one of the lowest standard biological redox potentials ($E_0 = -0.29$ V). Thus, DHLA is able to reduce not only ROS but also the oxidized forms of other antioxidant.¹³² It is worth remembering that LA has antioxidant properties as well. Owing to its easy absorption from the gastrointestinal tract and ability to cross the blood-brain barrier, exogenous LA can reach the majority of tissues. Moreover, LA and DHLA are easily soluble both in fats and water, which is a unique features among antioxidants, and are therefore active both at membrane level and in aqueous phases of cytoplasm.

Due to its unique properties, LA has also been administered in the treatment of various oxidative stress related diseases such as alcoholic liver disease, heavy metal poisoning, mushroom poisoning, diabetes, glaucoma, ischemia/reperfusion injury of heart and neurodegenerative disorders.¹³³ The most important exogenous source of LA are potatoes, spinach and red meats.

Examples of conjugate of DHLA with polyphenols have been reported in literature e.g. the 5-S-lipoyl-DOPA, obtained by the reaction of DHLA with 3,4-dihydroxyphenylalanine (DOPA), which was found to act as inhibitor of DOPAchrome formation, with possible applications as depigmentating agent for skin.¹³⁴



5-S-lipoyl-DOPA

2. Results and discussion

2.1. Isomeric cysteinyl dopas provide a (photo)degradable bulk component and a robust structural element in red human hair pheomelanin

Traditional models of pheomelanogenesis postulated a major involvement of 5SCD in pigment build-up, whereas 2SCD was usually dismissed as a minor side product in the process. Borges et al.,¹³⁵ however, recently analyzed melanin composition in various human hair samples using 4-AHP and 3-AHP as markers, and reported that the pheomelanin component of the total melanin pool consisted mainly of 2SCD-derived units, up to 80%. Though apparently confirmed in subsequent studies,⁷⁶ this observation passed virtually unnoticed because of the questionable reliability of 3-AHP as a marker of 2SCD due to a possible background contribution from 3-nitrotyrosine in proteins.

2.1.1. Identification of a new structural marker

Analysis of red hair was carried out according to a recently improved procedure based on alkaline hydrogen peroxide degradation of pheomelanin followed by HPLC determination of BTCA, a marker of 5SCD-derived units.⁴⁰ The peak area ratio at 254 and 280 nm ($A(280)/A(254)$ for BTCA = 0.6) was a valuable parameter for reliable identification of this structural marker even in the most complex degradation mixtures.

Figure 11 shows HPLC/UV traces of degradation mixtures from red human hair and isolated pheomelanin from red human hair, as well as black human hair and albino hair as controls. Inspection of the chromatographic trace from red hair revealed the formation, besides BTCA (R_T 52 min), of an additional major peak (R_T 45 min) not detectable in black and albino hair samples. This component was also well

distinguishable in the pigment isolated from red human hair by a mild proteolytic procedure.³⁹ Both peak area ratio (A(280)/A(254)= 0.6) and pseudomolecular ion peak of the product by LC-MS analysis with electrospray ionization in the positive ion mode (ESI+) ($[M+H]^+$, $m/z= 283$) were identical to those of BTCA, suggesting an isomer.

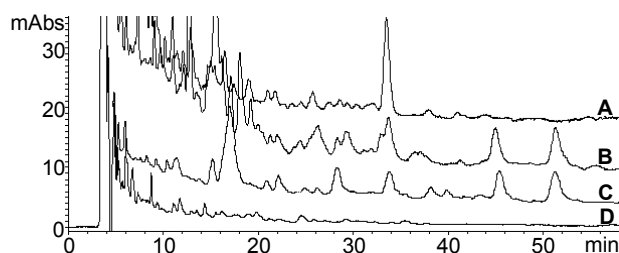


Figure 11. HPLC/UV (254 nm) traces of the degradation mixtures of black human hair (A), red human hair (B), pheomelanin isolated from red human hair (C), and albino human hair (D). Elutographic profiles are shown with different intensities.

On this basis, a likely candidate was a benzothiazole carboxylic acid arising from an isomeric cysteinyl-dopa. To check this hypothesis, a synthetic pheomelanin from 2SCD was prepared by tyrosinase catalyzed oxidation of 2SCD under oxygen with catalytic dopa.¹³⁶ The pigment thus obtained was subjected to chemical degradation with $H_2O_2/NaOH$. HPLC analysis of the reaction mixture (**Fig. 12**) indicated the presence of the same peak found in red hair mixtures, but no detectable BTCA. Moreover, the peak was clearly missing in the oxidation mixture from 5SCD and was much lower in synthetic pheomelanin from dopa and cysteine.

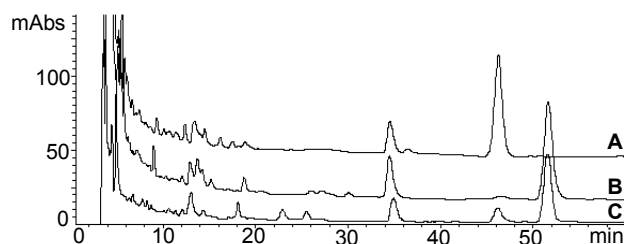
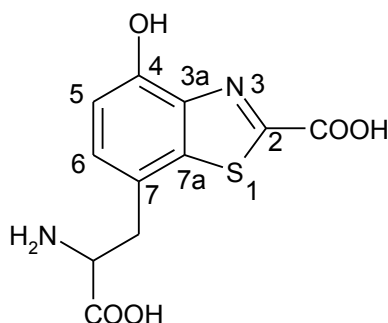


Figure 12. HPLC/UV traces of the degradation mixtures of a synthetic pheomelanin from 2SCD (A), 5SCD (B) and dopa + cysteine (C). Elutographic profiles are shown with different intensities.

The product eluted under the unknown peak was then isolated by oxidative degradation of a large sample of synthetic pheomelanin from 2SCD and was identified as 7-(2-amino-2-carboxyethyl)-2-carboxy-4-hydroxybenzothiazole (2-BTCA) by extensive spectral analysis (**Table 1**).

Table 1. ^1H and ^{13}C NMR data ($\text{D}_2\text{O}/\text{DCl}$) of 2-BTCA.



	δ_{H} (multiplicity, J , Hz)*	δ_{C} *
2		158.0
C-2-COOH		163.2
3a		142.4
4		151.9
5	6.65 (d, 8.0)	114.2
6	7.13 (d, 8.0)	132.6
7		120.5
7a		139.6
-CHCH ₂	3.11 (dd 15.2, 10.4)	36.8
	3.38 (dd 15.2, 4.4)	
-CHCH ₂	4.50 (dd 10.4, 4.4)	54.4
-CHCOOH		172.4

*Chemical shift values are given in ppm.

The identity of the 2-BTCA with the species eluted under the new peak in the red hair degradation mixture was secured by LC-MS with single ion monitoring (SIM) detection

(**Fig. 13**). The identification of 2-BTCA by degradation of isolated, partially purified natural pheomelanin and its lack in control experiments on white hair (**Fig. 11**) and pure 2SCD would rule out any artifactual formation from free 2SCD into the pigment sample.

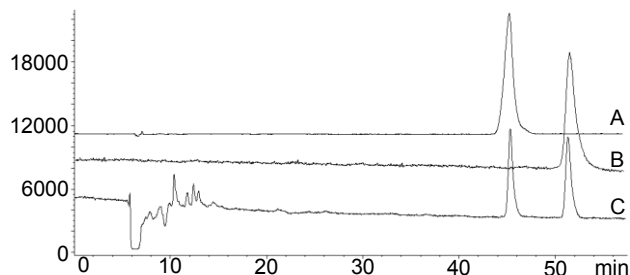


Figure 13. *LC-MS profiles with SIM detection at m/z 283 of the degradation mixtures of a synthetic pheomelanin from 2SCD (A) or 5SCD (B) and of pheomelanin isolated from red human hair (C). Elutographic profiles are shown with different intensities.*

The structures of BTCA and 2-BTCA and their relationships with 5SCD- and 2SCD-derived structural components are illustrated in **Figure 14**.

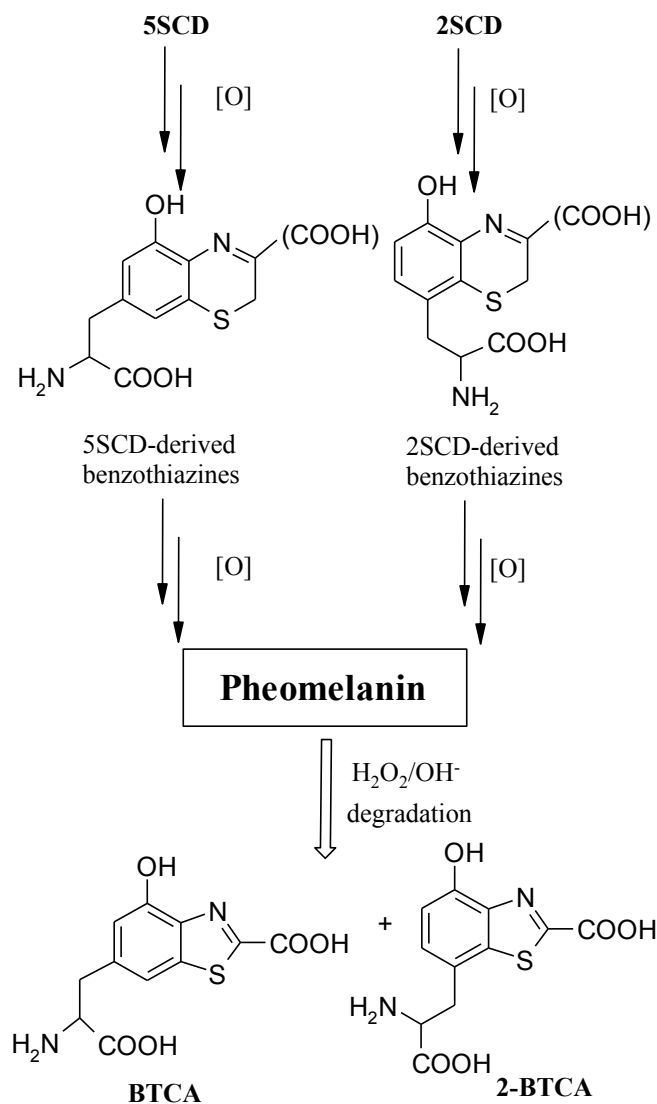


Figure 14. Origin of BTCA and 2-BTCA from degradation of 5SCD- and 2SCD-derived units in pheomelanin.

2-BTCA, as novel structural marker of pheomelanins, does not suffer from the aforementioned ambiguities related to 3-AHP determination,⁷⁶ and provides definite evidence of the involvement of 2SCD in pheomelanogenesis.

2.1.2. Pheomelanin analysis

The simultaneous determination of BTCA and 2-BTCA was assessed through a series of control experiments with a view to setting up an improved methodology for pheomelanin analysis. It was shown that 1) the rate of formation of BTCA and 2-BTCA are comparable under the degradation conditions adopted, and plateau after 24 h in line with results of previous studies⁴⁰ (**Table 2**); 2) exposure of BTCA and 2-BTCA at 250 μM to the degradation conditions resulted in a comparable decay of about 30% after 24 h; 3) oxidation of 5SCD and 2SCD gives the corresponding pigments in similar yields (approx 60% on a w/w basis), indicating the same degree of conversion to pigment polymers; and 4) the amounts of BTCA and 2-BTCA obtained by hydrolytic treatment of synthetic pheomelanins from 5SCD or 2SCD under non-oxidative conditions that is on exposure to 1 M sodium hydroxide with exclusion of oxygen for 24 h did not exceed 15% of those obtained under the standard degradation conditions. No significant reactivity of either BTCA or 2-BTCA was observed under different oxidation conditions including prolonged exposure to oxygen at alkaline pHs and ferricyanide oxidation.

Table 2. Yields of formation of BTCA and 2-BTCA from 5SCD and 2SCD pheomelanins, respectively at different degradation times.

Time (h)	Yields ($\mu\text{g}/\text{mg}$)*	
	BTCA	2-BTCA
1	71	85
5	119	131
10	137	145
24	151	165

*Shown are the mean values for three separate experiments with $\text{SD} \leq 10\%$.

On this basis, pheomelanin containing tissues of different origin and a synthetic sample were analyzed with the novel methodology. For comparison, pheomelanin analysis was repeated on the same samples using the classic reductive method based on HI reduction

followed by determination of 4-AHP and 3-AHP as markers of 5SCD and 2SCD derived units, respectively.⁷⁶

Data in **Table 3** show that all natural pheomelanins provide in addition to BTCA substantial amounts of 2-BTCA. Recessive and lethal yellow mouse hair, chicken feathers and synthetic dopa-cysteine pheomelanin gave yields of BTCA and 2-BTCA at ratios that reflected the formation ratio of 5SCD to 2SCD as observed by tyrosinase oxidation of dopa in the presence of cysteine.²⁹ By contrast, the yields of BTCA and 2-BTCA from red human hair were in an approximate 1.5:1 ratio.

Table 3. Yields of degradation products from pigmented tissues and synthetic pigments.

Sample	Yields (ng/mg) ^a			
	BTCA	2-BTCA	4-AHP	3-AHP
Red human hair ^b	600	420	600	330
Recessive yellow mouse hair	4000	830	1370	380
Lethal yellow mouse hair	3200	700	1640	480
Chicken feathers	7700	1400	3100	840
Dopa/cys pheomelanin	285500	51000	205000	32500

^aShown are the mean values for three separate experiments with SD ≤ 10%. ^b The sample was taken from the tip of the lock at about 7 cm from the scalp.

A key to the “anomalous” BTCA/2-BTCA values from human hair came from analysis of a very short red hair sample (ca. 5 mm from scalp) which gave a BTCA/2-BTCA ratio close to 5:1 differently from the hair sample shown in the **Table 3** that was taken from the tip of the lock at a distance of about 7 cm from the scalp. On the other hand murine hairs (approximately 1 cm long) were analysed as a whole. Based on this observation BTCA and 2-BTCA values were determined in different segments of red hair locks taken at various distances from the scalp from 19 subjects.

The results, summarized in **Figure 15**, showed in all cases in spite of a significant individual variability an abrupt drop of BTCA yields on passing from the segment near the root to the tip of the hair, whereas 2-BTCA values remained virtually constant throughout the entire hair length. Such trend was well apparent in a representative long (ca 30 cm) red hair lock (see *Inset* in **Figure 15**).

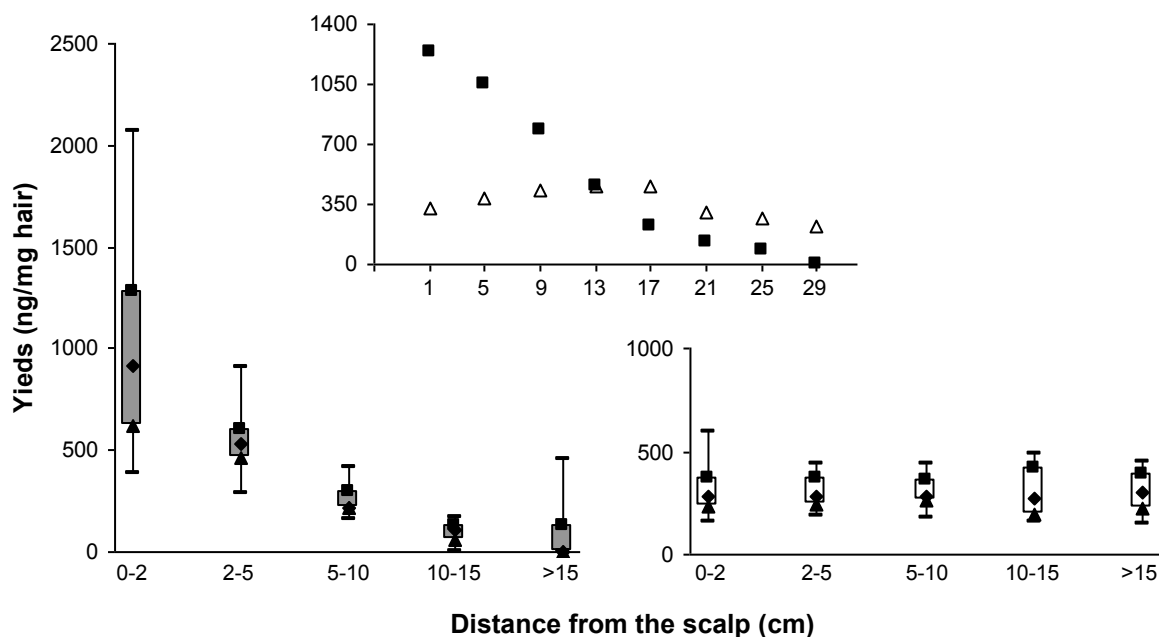


Figure 15. Yields of BTCA (left) and 2-BTCA (right) from degradation of different segments of hair locks taken at various distances from the scalp for 19 red haired individuals. \blacktriangle = 25th percentile; \blacklozenge = median; \blacksquare = 75th percentile; horizontal bars = minimum and maximum values. (*Inset*) BTCA (\blacksquare) and 2-BTCA (\triangle) yields from degradation of 4 cm segments of a representative red hair lock. Values on the x axis refer to the distance from scalp of the start of each segment.

Analysis of 4-AHP and 3-AHP showed a closely similar trend. **Figure 16** compares the yields obtained for the four markers in a hair lock long enough to allow obtaining segments at very different distances from the scalp. A significant decrease of the yields of BTCA and 4-AHP with increasing the distance from the scalp is observed whereas 2-BTCA and 3-AHP yields are not changed significantly.

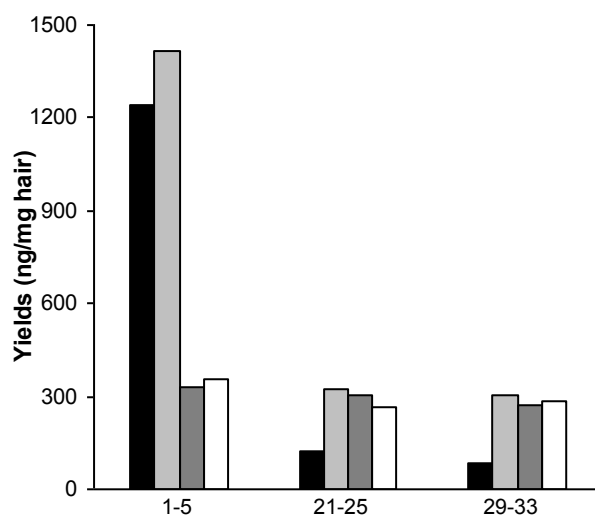


Figure 16. Yields of BTCA (black bars), 4-AHP (light grey bars), 2-BTCA (dark grey bars) and 3-AHP (open bars) from degradation of 4 cm-segments of a representative hair lock.

Data for other hair samples examined are reported in **Table 4** along with the yields obtained for TTCA, another typical degradation product of pheomelanin.⁴⁰ Data show a marked increase of TTCA yields with increasing distance from the scalp, whereas the yields of the other markers confirm the trend observed and shown in **Figure 15** and **16**.

Table 4. Yields of pheomelanin markers from degradation of red human hair locks taken at various distances from the scalp.

Sample #	Distance from the scalp (cm)	Yields (ng/mg)*				
		BTCA	2-BTCA	4-AHP	3-AHP	TTCA
1	1-3	618	159	1052	266	230
	7-9	324	176	616	223	245
2	3-6	612	421	602	331	258
	18-20	/	335	141	196	614
3	1-5	1239	331	1415	353	266
	21-25	125	306	324	265	477

*Shown are the mean values for three separate experiments with $SD \leq 10\%$.

Exposure of three locks from different individuals to intense sun light over 2 weeks (ca 140 h exposure) resulted in a decrease of BTCA while 2-BTCA remained almost unchanged, with a well apparent lightening of the red color. **Figure 17** shows the changes occurring at different distances from the scalp of a representative hair sample after sun exposure.

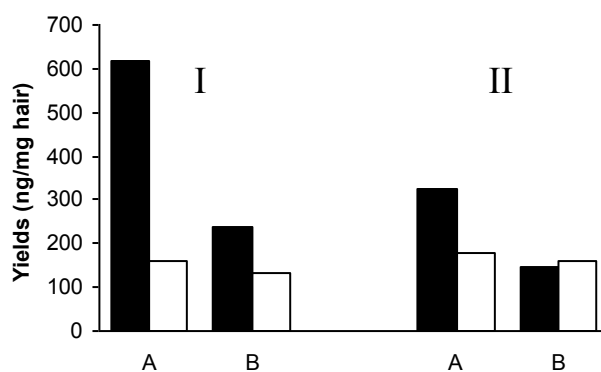


Figure 17. Yields of BTCA (black bars) and 2-BTCA (open bars) obtained by degradation of a representative red hair lock at (I) 1-3 cm and (II) 7-9 cm from the scalp before (A) and after (B) 140 h exposure to sun light. Shown are the mean values of experiments run in triplicate with $SD \leq 10\%$.

A similar trend was observed for the other two locks examined, with individual variability in the yields of BTCA and 2-BTCA at the root and tip of hair as apparent also from data of **Figure 15**. In all cases BTCA yields significant decreased (at least halving of the initial value) following solar exposure. These data confirmed the relative stability of the 2SCD component even under conditions favoring photodegradation processes. Prolonged storage of red hair samples over periods of months, on the other hand, did not affect BTCA and 2-BTCA values. Reproducible BTCA values were determined on red hair samples that had been stored in the dark for more than three years.

2.1.3. Model chemical studies

A vis-à-vis analysis of the oxidative conversion of 5SCD and 2SCD to pheomelanin was carried out with a view to gaining an insight into the different behavior of the two main pheomelanin components. Autoxidation in phosphate buffer at pH 9.0 was selected as the model reaction to compare the intrinsic reactivity of the substrates independent of the oxidizing system used. HPLC monitoring of the oxidation mixtures with substrates at 200 μ M showed comparable rates of substrate consumption with a decay > 90% after 4 h. Spectrophotometric analysis however revealed quite different reaction courses: whereas 2SCD gave after 2 h a broad absorption at 400 nm suggesting extensive benzothiazine formation and after 4 h significant melanization, 5SCD was poorly melanized after 4 h (**Figure 18**).

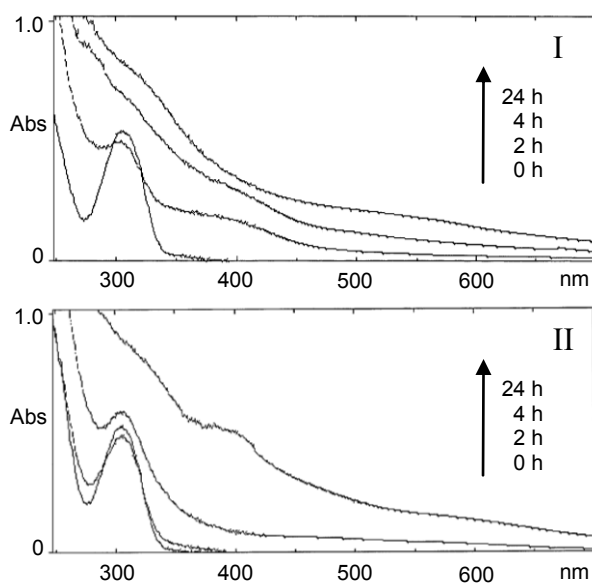


Figure 18. Spectrophotometric analysis of the mixture of autoxidation of (I) 2SCD and (II) 5SCD at 200 μ M in 0.1 M phosphate buffer pH 9.0 at various times.

These results clearly show that oxidation of isomeric cysteinyl dopas proceeds with different chromophoric changes during the early phases, but leads eventually (24 h) to pheomelanin-like pigments with similar absorption properties.

In further experiments 5SCD and 2SCD were allowed to autoxidize at 1:1 molar ratio and the pigment that separated from the mixture in the very early stages was subjected to chemical analysis. The results at 24 h showed a BTCA/2-BTCA ratio of 1:1 whereas after 72 h the ratio decreased to 0.5:1, indicating a substantial oxidative degradation of the pheomelanin constituents leading to BTCA. No appreciable amounts of either BTCA or 2-BTCA were obtained from degradation of the supernatants after pigment separation at different times.

Finally, a typical experiment of pheomelanogenesis *in vitro* was carried out in which a dopa-cysteine reaction promoted by tyrosinase was monitored at various intervals of time to probe the relative stability of the 5SCD and 2SCD components. At 9 h reaction time an approximately 5:1 BTCA/2-BTCA ratio was observed which dropped to nearly 3:1 after two week (**Fig. 19**). After an additional week the ratio was not significantly

changed (not shown). 2-BTCA yields varied less than 10% over the whole experimental time, suggesting an intrinsic chemical instability of the BTCA-forming structures.

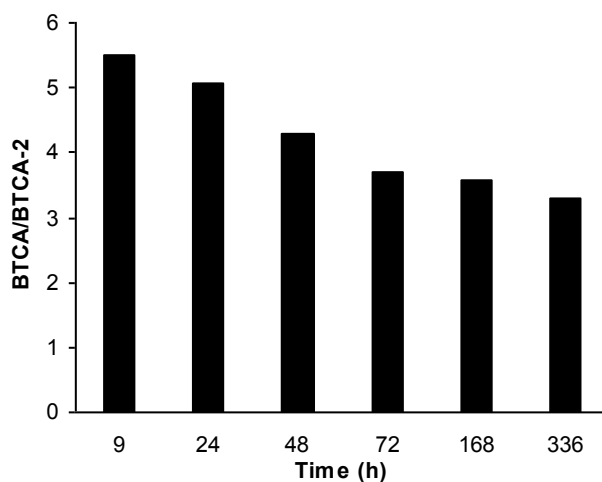


Figure 19. Ratios of BTCA/2-BTCA yields from degradation of an oxidation mixture of dopa and cysteine at different times of incubation in air.

2.1.4. BTCA/2-BTCA as aging- and UV- index

In this study it was demonstrated that 2SCD provides human pheomelanin with a stable structural constituent, whereas the bulk 5SCD-derived component is degraded during hair growth and represents an index of pigment aging.

The noticeable persistence of the 2SCD component during red hair growth might reflect an intrinsic stability to ROS attack or UV-induced degradation, which appear to affect preferentially the dominant 5SCD component.

The marked drop in BTCA yields indicates an irreversible change in pheomelanin structure which occurs in hair with aging. The high BTCA/2-BTCA values in mouse hair, approximating those in native pheomelanin set by the 5SCD/2SCD formation ratio, can be explained considering the short hair cycle (about 3 weeks)¹³⁷ compared to the human case (years).

In spite of a marked individual variability in the yields of either the BTCA/2-BTCA or the 4-AHP/3-AHP markers obtained at the hair root or tip the general trend was confirmed in all the red haired subjects examined.

The age (and UV)-dependent change of components giving BTCA (and 4-AHP) may be interpreted in terms of bond formation involving the benzene moiety. In this connection, it should be mentioned that 5SCD-derived benthiazine/bentothiazole components have *ortho*- and *para*-positions to the hydroxyl group intact while 2SCD-derived counterparts have only *ortho*-position intact. Other possibilities accounting for the decrease of BTCA include degradation of the alanyl moiety¹³⁸ and oxidative fission of the benzene moiety of benzothiazine/benzothiazole structural components. The latter process is compatible with the increased yields of TTCA.

Pheomelanin degradation is likely to be the consequence of photodegradation processes. However, the abrupt decrease in BTCA yield observed in hair segments near to the scalp and supposedly little exposed to direct sunlight suggests that other mechanisms, probably related to oxidative stress, may be also involved. An attractive hypothesis implicates the abnormal accumulation of iron in red hair pheomelanin as a possible vulnerability factor.¹³⁹ Pheomelanin precursors and components are strong transition metal chelators^{37,140} and may cause a “lens effect” enhancing site-directed Fenton-type reactions with hydrogen peroxide on the pigment granules and their immediate environment.^{60,141}

A major implication of the present results is in relation to pheomelanin roles and fate in the skin of red haired individuals. As pointed out by Slominski et al.,¹⁴² hair shaft melanin components are a long-lived record of precise interactions in the hair follicle pigmentary unit involving follicular melanocytes, keratinocytes, and dermal papilla fibroblasts. Melanin synthesis and transfer to bulb keratinocytes are regulated by signal transduction pathways intrinsic to skin and hair follicle. In an oxidative stress setting with elevated ROS production, e.g. in sunburn, extensive degradation of the 5SCD component of pheomelanin may be a significant event accompanying the inflammatory response. In this context, the 2SCD-derived component might survive ROS attack during aging or sun exposure, providing a stable (photo)protective effect even after the 5SCD portion of pheomelanin is degraded.

2.2. A melanin-inspired pro-oxidant system for aerial catechol(amine)-polymerization: implementing a non-enzymatic mimic of the natural casing model

According to a currently accepted kinetic model, assembly of pigment-containing organelles, the melanosomes, occurs by a casing process in which a pheomelanin core is initially formed and is then encapsulated into a eumelanin coating (**Fig. 9**).⁴⁸ Support to this model came from photoemission electron microscopy imaging studies of iridial melanosomes and neuromelanin granules indicating eumelanin-type surface properties despite a large pheomelanin content.^{46,50,143} Recently, eumelanins have attracted increasing interest because of their intriguing physico-chemical properties, including broad band monotonic absorbance, extremely low radiative quantum yield, and condensed phase electrical and photoconductivity, that suggested possible applications as bio-inspired high-tech materials for bioelectronics, chemical sensing, photon detection and radioprotection.¹⁴⁴⁻¹⁴⁹ Several papers have also reported use of catecholamines such as dopamine, dopa and epinephrine for the preparation of eumelanin-like multifunctional coatings and adhesive films that stick to a broad variety of organic and inorganic surfaces, e.g. silica, dimethyldiethoxysilane emulsions, nanotubes, etc.¹⁵⁰⁻¹⁵⁸ In most of these surface modification systems, however, catecholamine polymerization is obtained through a lengthy oxygen-induced process (autopolymerization) subject to substrate and oxygen availability as main determinants of coat thickness.^{159,160}

2.2.1. Pheomelanin promoted oxidative polymerization of catechol(amines)

A peculiar redox system based on pheomelanin that implements a non-enzymatic mimic of the natural casing process of melanin pigments was observed which enables efficient deposition of eumelanin-like coatings. The new system is built upon the discovery that a finely suspended, partially solubilized pheomelanin-type polymer obtained by oxidation of 5SCD (5SCD-pheomelanin) markedly accelerates the oxygen-dependent

polymerization of catecholamines at pH 7.4 leading to a faster eumelanin coating formation. The catecholamines object of this studies were DOPA and 5,6-dihydroxyindole-2-carboxylic acid (DHICA), intermediates of eumelanin, dopamine (DA), the main precursor of neuromelanin and epinephrine (EN), a neurotransmitter.

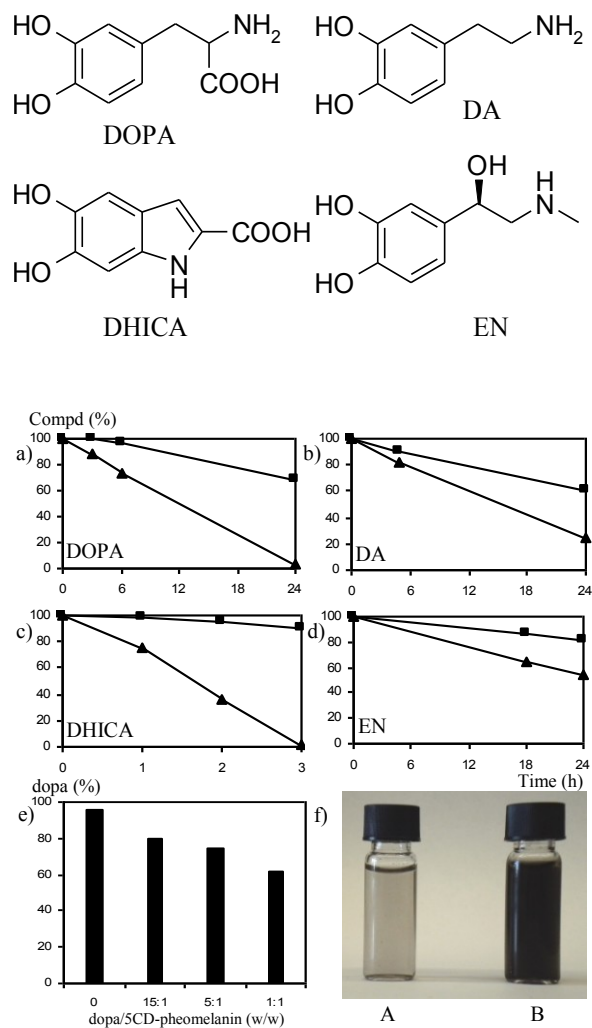


Figure 20. Catechol(amine) oxidation promoted by synthetic 5SCD-pheomelanin. a) Time course of 1 mM DOPA oxidation in the presence (▲) and in the absence (■) of pheomelanin (5:1 w/w). b) As in a), with DA. c) As in a) but with DHICA. d) As in a) but with EN. e) DOPA consumption at 6 h as a function of the amount of 5SCD-pheomelanin added. Shown are the mean values for three separate experiments with $SD \leq 5\%$. f) Color changes of DOPA solutions after 24 h without (A) or with (B) added pheomelanin (5:1 w/w).

The key observation underpinning this study is provided in **Figure 20**. The rate of oxidation of various catechol substrates at 1 mM concentration in air-equilibrated phosphate buffer at pH 7.4 is markedly increased in the presence of 20% (w/w) 5SCD-pheomelanin (panels a-d), leading to dark insoluble eumelanin-like polymers visually identical to those obtained by spontaneous oxidation (panel f). Despite differences in the relative rates of catechol oxidation, the accelerating effect was significant in all cases examined, being higher with DHICA and DOPA, and varies with the added amount of pheomelanin (panel e), doubling on passing from a 1:15 to 1:1 w/w pheomelanin/DOPA ratio.

Separate experiments (not shown) indicated that: a) catechol(amine) consumption is not affected by SOD and catalase under the usual conditions for inhibition experiments; b) the process is virtually inhibited under an argon atmosphere; and c) synthetic eumelanin, obtained by oxidation of DOPA (DOPA-eumelanin) has no detectable effect on DOPA oxidation. From these data, it was concluded that catechol(amine) consumption is due to an oxygen-dependent process, but is not mediated to any significant degree by superoxide and hydrogen peroxide and is not associated to physical adsorption phenomena.

2.2.2. Analysis of pheomelanin-induced oxidation of dopa and dopamine

Figure 21a, panel a, reports the decay profile of 1 mM DOPA after multiple additions to the pheomelanin-containing buffer at pH 7.4. When all of the DOPA from the oxidation reaction was consumed (24 h), addition to the mixture of a fresh solution of DOPA at the same initial concentration resulted in a markedly slower consumption rate. No significant accelerating effect was eventually observed following a third addition of freshly prepared DOPA (48 h), indicating complete inactivation of the pheomelanin system. Based on these data, it was estimated that the system can promote oxidation of up to 4.5 mg of DOPA/mg of pheomelanin at a 6.5:1 w/w initial ratio before inactivation, the remainder of DOPA being consumed by the concurrent slower spontaneous autoxidation (dashed line panel a).

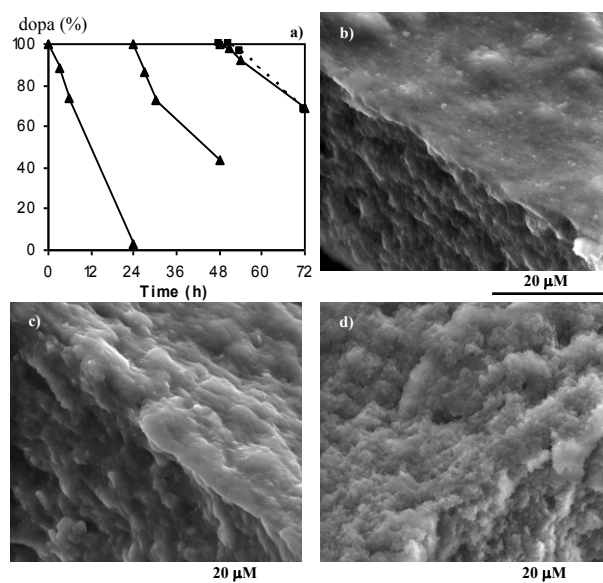


Figure 21a. a) Kinetic profile of DOPA decay following repeated addition to 5SCD-pheomelanin solution (initial condition: DOPA/pheomelanin 5:1 w/w; at time 0, 24 h and 48 h DOPA concentration is taken to 1 mM); dashed line: 24 h DOPA decay in absence of 5SCD-pheomelanin added, reported in the range 48-72 h. Shown are the mean values for three separate experiments with $SD \leq 5\%$. b) SEM image of 5SCD-pheomelanin; c) as b) but 24 h after addition of the same weight amount of DOPA; d) as b) but 24 h after oxidation of a 10-fold weight excess of DOPA.

The polymer produced by pheomelanin-promoted oxidation of DOPA was then investigated by scanning electron microscopy (SEM). The morphological features of 5SCD-pheomelanin are shown in **Figure 21a**, panel b. The image reveals compacted grains which generate a well defined continuous structure. Interestingly, a globe-like morphology became apparent in the case of polymers obtained by 5SCD-pheomelanin promoted oxidation of DOPA (1:1 w/w, panel c), which was much more pronounced with a 10-fold weight excess of the catechol (panel d). The latter images indicated a close similarity of the polymer morphology with that of a pure DOPA-eumelanin, suggesting encasement of the 5SCD-pheomelanin component into the DOPA-eumelanin coating (**Fig. 21b**).

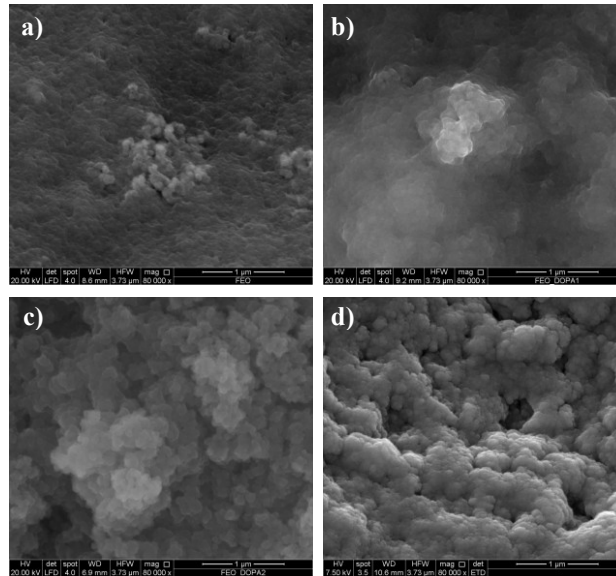


Figure 21b. a) SEM image of 5SCD-pheomelanin b) as a) but 24 h after addition of the same weight amount of DOPA; c) as a) but 24 h after oxidation of a 10-fold weight excess of DOPA; d) DOPA-eumelanin.

The casing process was confirmed by additional experiments in which the polymer obtained by pheomelanin-induced oxidation of DOPA (DOPA/pheomelanin 5:1 w/w) was washed sequentially on a filter with phosphate buffer pH 8, pH 9, and with 1 M NaOH, (4 times each), and the washings were separately analyzed for melanin content by the alkaline H₂O₂ degradation protocol³⁹ in comparison with the untreated material (Fig. 22).

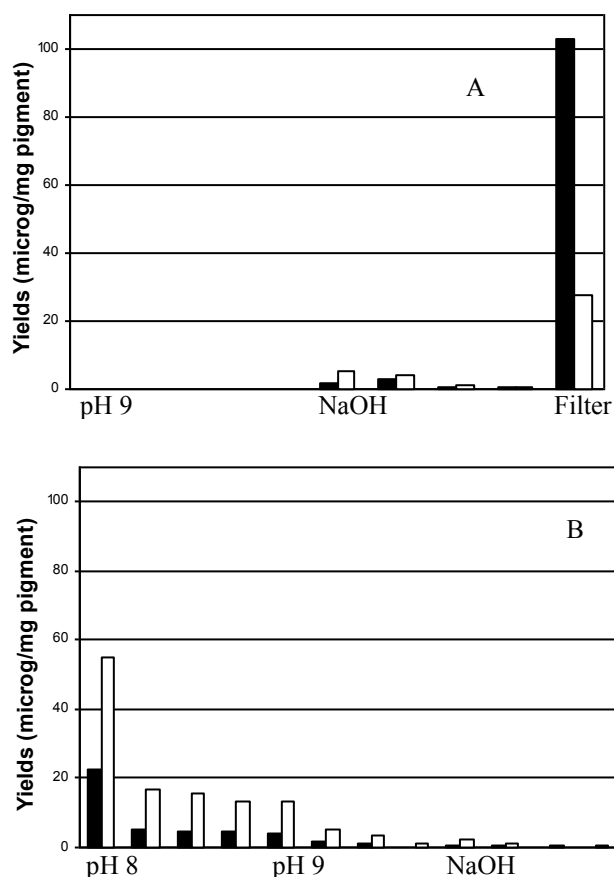


Figure 22. Yields of PTCA (black bars) and BTCA (open bars) from alkaline oxidative degradation of eluates deriving from washing with phosphate buffer pH 8, pH 9 and NaOH 1 M of polymer obtained by pheomelanin-induced oxidation of dopa (panel A) and of 5SCD-pheomelanin (panel B). In panel A the degradation of the insolubilized material is reported. Shown are the mean values for three separate experiments with SD $\leq 10\%$.

HPLC determination of eumelanin and pheomelanin markers, PTCA and BTCA, consistently indicated an approximately 2.5:1 eumelanin/pheomelanin ratio in both the crude and washed polymers, but no trace of pheomelanin or eumelanin released into the washings. Since in control experiments pure 5SCD-pheomelanin was completely released from the filter following washing with alkali, it was concluded that all of the pheomelanin component was encased and preserved from alkali-induced solubilization by the insoluble polycatecholamine coating.

Table 5. Yields of PTCA and BTCA from alkaline oxidative degradation of eluates deriving from washing with phosphate buffer pH 8, pH 9 and NaOH 1 M of polymer obtained by pheomelanin-induced oxidation of dopa and of 5SCD-pheomelanin. The yields of the melanin markers from degradation of the pigments not subjected to solubilization treatments are reported.

	Polymer by pheomelanin-induced oxidation of dopa		5SCD-pheomelanin	
	Yields ($\mu\text{g}/\text{mg}$ pigment)*		Yields ($\mu\text{g}/\text{mg}$ pigment)*	
	PTCA	BTCA	PTCA	BTCA
pH 8	/	/	22.39	55.25
	/	/	5.29	16.79
	/	/	4.84	15.36
	/	/	4.55	13.31
pH 9	/	/	3.89	13.50
	/	/	1.47	5.49
	/	/	1.15	3.64
	/	/	0.24	0.95
NaOH 1M	1.52	5.52	0.76	2.09
	2.68	3.97	0.64	1.29
	0.59	0.98	0.21	0.81
	0.39	0.63	0.12	0.66
Filter (insoluble material)	102.93	27.40	/	/
Pigment without washings	99.2	43.5	56.2	104.6

*Shown are the mean values for three separate experiments with SD \leq 10%.

Overall, the above data would suggest that catecholamine oxidation and coating formation is an oxygen-dependent process occurring on the surface of the finely dispersed 5SCD-pheomelanin, e.g. via redox cycling of benzothiazine units⁵ sustained by oxygen (**Fig. 23**). The proposed redox mechanism is compatible with the oxidation potentials of eumelanosomes and pheomelanosomes (-0.2 V and $+0.5$ V, respectively, vs normal hydrogen electrode),^{47,161} indicating that pheomelanin, but not eumelanin, may be competent to act as an oxidizing system. Unfortunately, current gaps in the

knowledge of pheomelanin structure and the heterogeneous character of the pigment prevent a more detailed characterization of the redox system at this time.

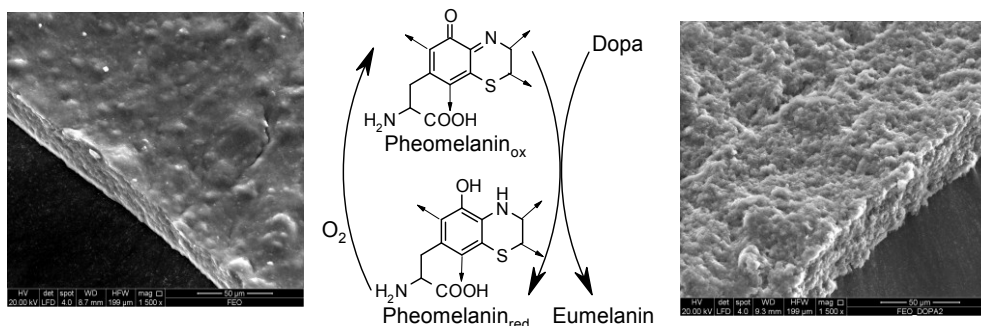


Figure 23. Left panel: SEM image of 5SCD-pheomelanin; Right panel: SEM image of 5SCD-pheomelanin plus a 10-fold weight excess of DOPA (at 24 h reaction time). In the middle: proposed redox mechanism of 5SCD-pheomelanin oxidation of DOPA and eumelanic coating formation.

Assuming a 4.5:1 eumelanin/pheomelanin ratio as indicated above and a uniform density for the fundamental cased aggregates, it could be predicted that the thickness of the eumelanic exterior formed by deposition of polymerized DOPA is about 0.75 times the radius of the pheomelanic core (**Fig. 24**).

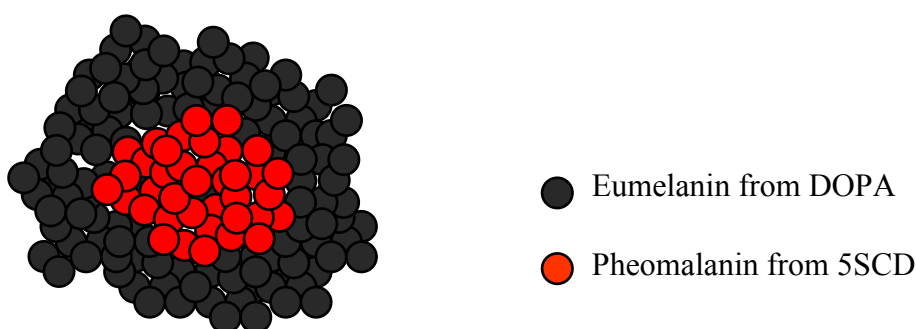


Figure 24. Schematic illustration of eumelanic coating on pheomelanic core.

This value falls within within the recently reported range for iridal melanosomes.⁵⁰ These results may be relevant to the origin of the casing architecture in the DA-derived neuromelanin of human substantia nigra. Based on preliminary data, it can be

speculated that a 5-*S*-cysteinyl-dopamine-derived melanin, generated under an oxidative-stress condition in dopaminergic neurons,⁴⁸ may trigger DA polymerization and neuromelanin accumulation without enzymatic assistance (**Fig. 25**). The similarity in organization of neuromelanin granules and iridial stroma melanosomes suggests that the morphological consequence of mixed melanogenesis may be independent of tissue type, biosynthetic origin, time scale of synthesis and enzymatic assistance.

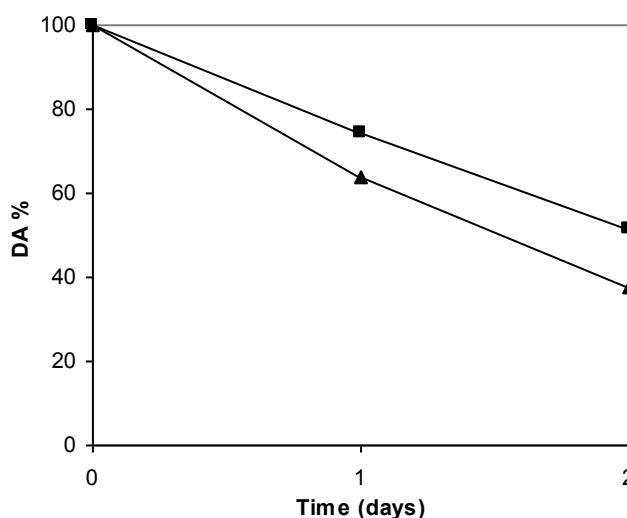


Figure 25. Time course of 1 mM dopamine oxidation in the presence (▲) and in the absence (■) of 5-*S*-cysteinyl-dopamine-pheomelanin (5:1 w/w). Shown are the mean values for three separate experiments with $SD \leq 5\%$.

On this basis it is tempting to speculate that the casing mechanism is a consequence of the intrinsic chemical reactivity during melanization in any mixed eumelanin/pheomelanin-forming system. Besides the biological relevance, the results disclosed herein may be of interest in relation to the potential utility of added oxidants for improved polycatecholamine coating methodologies. So far, this aspect has been little investigated, though certain limitations of chemical oxidants have been recently highlighted. To this aim, the technological prospects deriving from inclusion in catecholamine polymerization protocols of a pheomelanin-inspired non-enzymatic system enabling controlled coating formation¹⁶² are worthy of further attention.

2.3. Oxidative chemistry of cysteinyl dopas and properties of related synthetic pheomelanins

As illustrated in the paragraph 2.1, it was demonstrated that 2SCD provides human pheomelanin with a stable structural constituent, whereas the bulk 5SCD-derived component is degraded during hair growth and represents an index of pigment aging. To give a molecular interpretation to this phenomenon, the oxidative reactivity of 2SCD was examined in biomimetic condition, also in comparison with the more extensively investigated 5SCD isomer. The pro-oxidant properties of 5SCD-pheomelanin in promoting catecholamine oxidation (paragraph 2.2) were studied also for 2SCD-pheomelanin, in the oxidation of the catecholamine pheomelaninic precursors themselves, 5SCD and 2SCD. Model experiments led to formulate a pheomelaninic casing model as interpretation of the instability of 5SCD-derived components observed in hair growth.

2.3.1. Oxidative chemistry of 2SCD

In order to assess possible differences in the reactivity between 2SCD and 5SCD, and then the relative tendency to take part in the formation of pheomelaninic pigment, a first stage of this work was directed at investigating the oxidative chemistry of 2SCD under the conditions typically used to prepare synthetic pigments.^{40,163} This analysis showed in all cases a marked tendency of 2SCD to oxidation. Particular attention was focused to reaction carried out with tyrosinase in the presence of L-DOPA in phosphate buffer pH 6.8, bubbled with O₂. At 30 minutes reaction time, the reverse-phase HPLC analysis of the mixture, after reductive treatment with NaBH₄, showed the presence of three main products: one poorly retained with *t_R* 12 min and two eluted between 30 and 40 min. The reaction was then carried out on 50 mg of 2SCD. The mixture was reduced after 30 min, lyophilized, the residue was taken up in water and eventually purified by semi-preparative HPLC-RP.

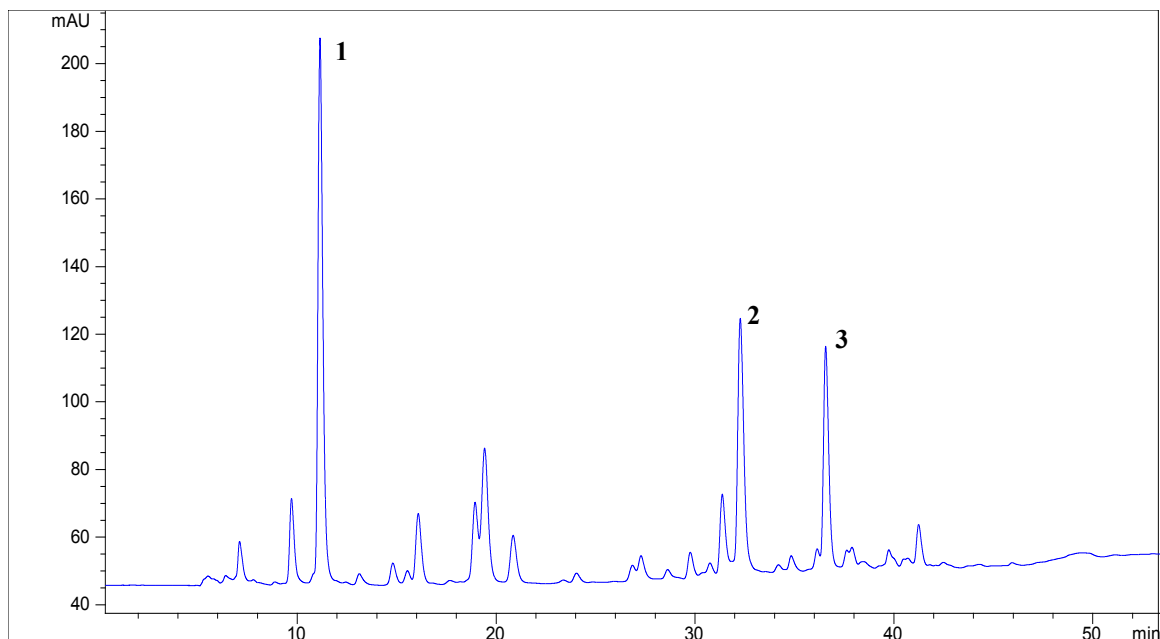


Figure 26. HPLC/UV traces of the reaction oxidation mixture of 2SCD, after reductive treatment with NaBH_4 at 30 min reaction time.

^1H NMR analysis and ESI(+)-MS analysis of the product eluted at 11.2 min allowed its identification as 8-(2-amino-2-carboxyethyl)-5-hydroxy-3,4-dihydro-1,4-benzothiazine (**1**), while the two components eluted at 32.3 and 36.6 min showed very similar proton spectra and were identified as two diastereoisomers of 8-(2-amino-2-carboxyethyl)-3-carboxy-5-hydroxy-3,4-dihydro-1,4-benzothiazine (**2** and **3**). The products isolated likely derived from reduction of the 2*H*-1,4-benzothiazine and the 3-carboxy derivative, respectively, arising from intramolecular cyclization of 2SCD. This was confirmed also by the 1:1 formation ratio of two diastereoisomers produced by borohydride reduction (**Fig. 27**).

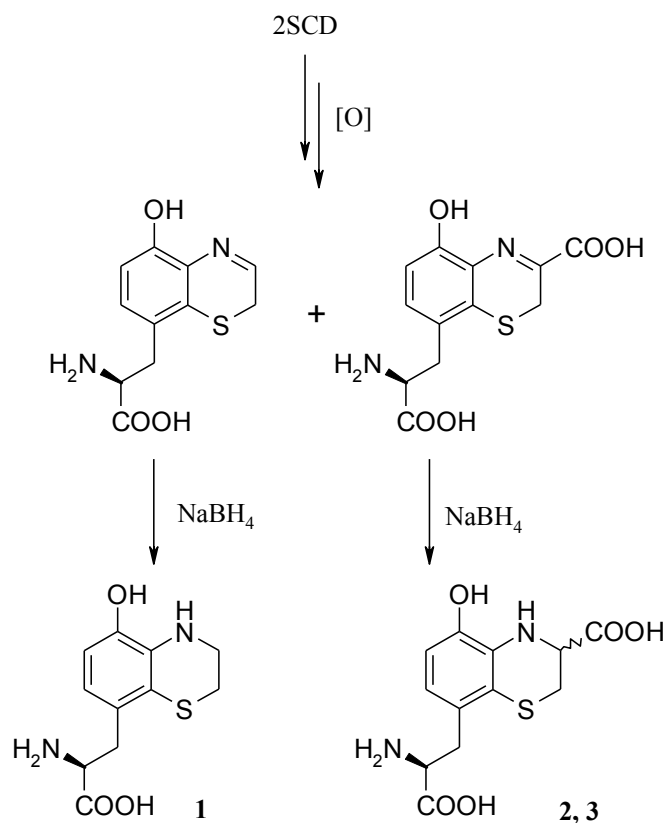


Figure 27. Products arising from the early stages of 2SCD biomimetic oxidation, after reductive treatment.

The analysis of the reaction mixture after 24 h after reductive treatment showed the disappearance of the benzothiazines initially formed and the presence of a complex pattern of products (**Fig. 28**). However, all the attempts to isolate the main components in sufficient quantities to carry out the spectroscopic characterization failed because of the extreme instability of these species, that after chromatographic fractionation of the mixture and removal of the solvent (even by lyophilization) were converted into several other species.

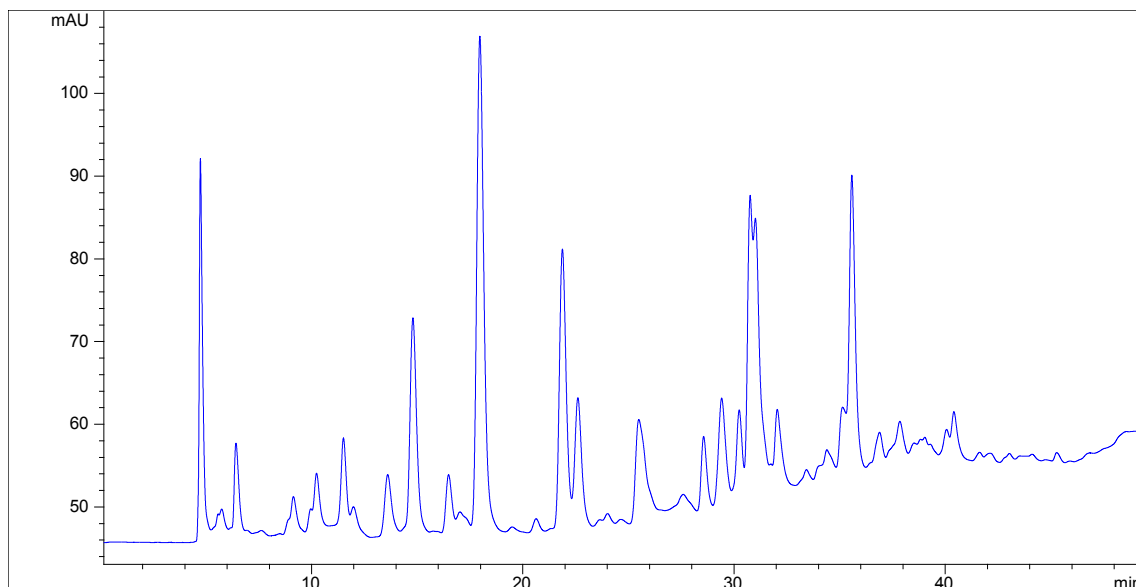


Figure 28. HPLC/UV traces of the reaction oxidation mixture of 2SCD, after reductive treatment with NaBH_4 at 24 h reaction time.

Overall, this preliminary investigation showed that the early stages of biomimetic oxidation of 2SCD are quite similar to those characterized in detail in the case of 5SCD.

2.3.2. Aerial oxidation of 5SCD and 2SCD

In a subsequent series of experiments a direct comparison between the tendency to oxidation of 2SCD and 5SCD was carried out. To avoid effects due to substrate specificity of the isomers, as observed in the case of tyrosinase (which operates more effectively on 5SCD than on 2SCD), it was preferred not to use enzymes as oxidizing systems. Aerobic oxidation was therefore chosen and the reaction was carried out using solutions of the two isomers at 0.5 mM under conditions of neutral pH of physiological relevance (phosphate buffer, pH 7.4), kept under vigorous stirring. The consumption rate was determined by monitoring the reaction mixtures by HPLC at 30 min intervals. For both compounds a relatively low and comparable consumption rate was observed: after 24 h the residual compounds were up to 80%.

2.3.3. Oxidation of 5SCD and 2SCD in the presence of synthetic and natural pheomelanins

Due to the similarity in the reactivity between 5SCD and 2SCD, the research work was directed toward examination of the properties of pigments obtained from cysteinyl-dopa isomers. Preliminary, pheomelanins were prepared by treating a 12 mM solution of the substrate (5SCD or 2SCD) with the oxidizing system peroxidase/H₂O₂ for 2 h according to a procedure previously developed.^{40,163} The pigment formed was precipitated by cautious acidification, recovered by centrifugation (7000 rpm, 30 min, 4°C), washed three times with 1% acetic acid, once with H₂O and lyophilized.

The pheomelanin pigments prepared, together with the one synthesized by oxidation of DOPA with cysteine by the enzyme tyrosinase,¹³⁶ commonly considered as the reference pheomelanin, were used in all experiments described below.

1 mM solutions of 5SCD or 2SCD in phosphate buffer at pH 7.4 were taken under air stirring, in the presence and in the absence of the pigments, with w/w ratio cysteinyl-dopa/pigment of 5:1. Cysteinyl-dopa consumption was followed by HPLC-RP. Data in **Figure 29** show the significant increase in the rate of cysteinyl-dopa decay in the presence of the pigment: after 4 h the consumption of cysteinyl-dopa was complete, while in the absence of the pigment was not detectable. In the case of 2SCD the effect of the pigment was more pronounced, but the type of precursor from which the pigments were obtained did not affect the oxidation to a significant extent (data not shown). The effect observed in the case of pheomelanin promoted oxidation of cysteinyl-dopa was much more apparent than in the case of the previously studied catecholamines (paragraph 2.2).

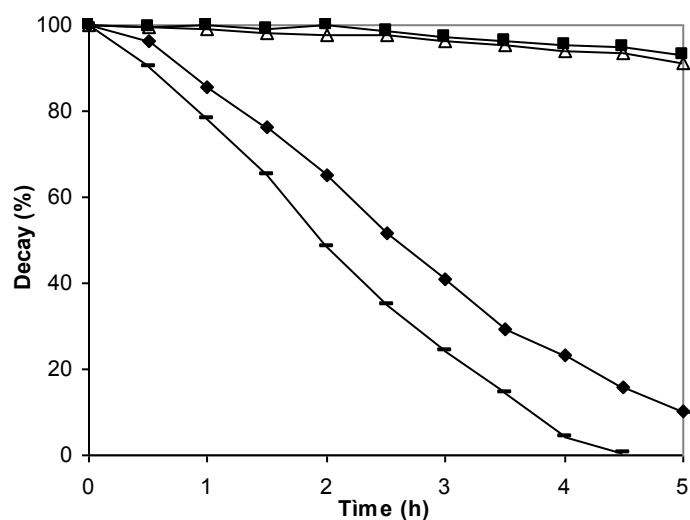


Figure 29. Time course of 1 mM 5SCD oxidation in the presence (◆) and in the absence (■) of synthetic pheomelanin (5:1 w/w) and of 1 mM 2SCD oxidation in the presence (-) and in the absence (Δ) of synthetic pheomelanin (5:1 w/w). Shown are the mean values for three separate experiments with $SD \leq 5\%$.

The same experiments were carried out in the case of 5SCD in the presence of natural melanin isolated from red hair and black hair.

The effect of natural pheomelanin in the oxidation of 5SCD, at 5SCD/pigment ratio of 1:2, was significantly higher than that observed for synthetic pigment (**Fig. 30**). It is important to consider that in the natural pigment even after purification there is a relevant contribution of the matrix protein, so the weight corresponds to a smaller quantity of pheomelanin.

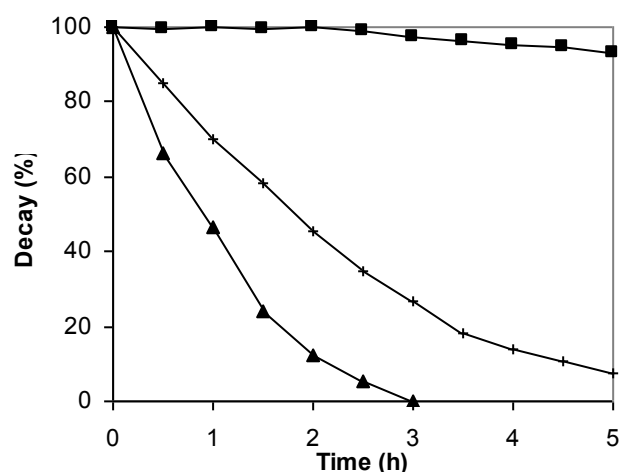


Figure 30. Time course of 1 mM 5SCD oxidation in the presence of synthetic pheomelanin (+), natural pheomelanin from red hair (▲), or in the absence of pigment (■) (5SCD/pigment ratio 1:2 w/w). Shown are the mean values for three separate experiments with $SD \leq 5\%$.

The eumelanin isolated from black hair did not effect the oxidation of 5SCD, using the same 5SCD/pigment ratio of 1:2 (**Fig. 31**), as previously observed for the pheomelanin promoted oxidation of a series of catecholamines (paragraph 2.2.1).

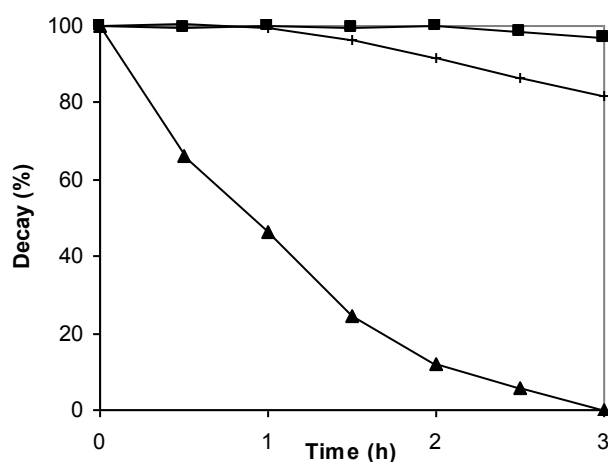


Figure 31. Time course of 1 mM 5SCD oxidation in the presence of natural pheomelanin from red hair (▲), natural eumelanin from black hair (+), or in the

absence of pigment (■) (5SCD/pigment ratio 1:2 w/w). Shown are the mean values for three separate experiments with SD $\leq 5\%$.

2.3.4. Proposed mechanism of growth of synthetic pheomelanins from 2SCD and 5SCD

To explain the different trend to (photo) degradation observed for the components of the pheomelanin pigment of red hair, it was initially hypothesized that 2SCD and 5SCD might exhibit a different oxidative chemistry, leading to different pigments with different structural characteristics and hence diverse susceptibility to (photo) degradation. This hypothesis, however, was not supported by the results of the comparative examination of the oxidation reactivity of the two isomers, that showed a broad similarity of the course of early stages of the process.

A similar photoreactivity of 2SCD- and 5SCD-pigments was also shown recently by electron paramagnetic resonance (EPR) oximetry and EPR-spin trapping experiments indicating that either pigments had a pronounced but comparable tendency to reduce molecular oxygen to ROS.¹⁶⁴

The possibility was then considered that the two pigments are differently exposed to sunlight and air, as a result of the intervention of a coating mechanism during pigment growth closely parallel to that proposed in the case of eumelanin and pheomelanin (paragraph 2.2).

To test this hypothesis, an experimental protocol was designed based on the preparation of two different synthetic pheomelanins, termed *mixed* because containing both 5SCD units and 2SCD units.

The *mixed pheomelanin A* was prepared by peroxidase/H₂O₂ oxidation of a solution of 5SCD in 0.01 M phosphate buffer at pH 6.7 in the presence of pheomelanin from 2SCD previously synthesized, while the *mixed pheomelanin B* derived from oxidation of a solution of 2SCD in the presence of pheomelanin from 5SCD. In both cases the ratio of 2SCD (or its pheomelanin) and 5SCD (or its pheomelanin) was 1:5, reflecting the formation ratio of cysteinyl dopas *in vivo*.²⁹

It was then assumed that the pigments thus prepared were made, in the first case, of a core of pheomelanin from 2SCD and a surface of pheomelanin from 5SCD (*mixed pheomelanin A*), while the latter, had a pheomelanin core from 5SCD and a surface of pheomelanin from 2SCD (*mixed pheomelanin B*) (**Fig. 32**).

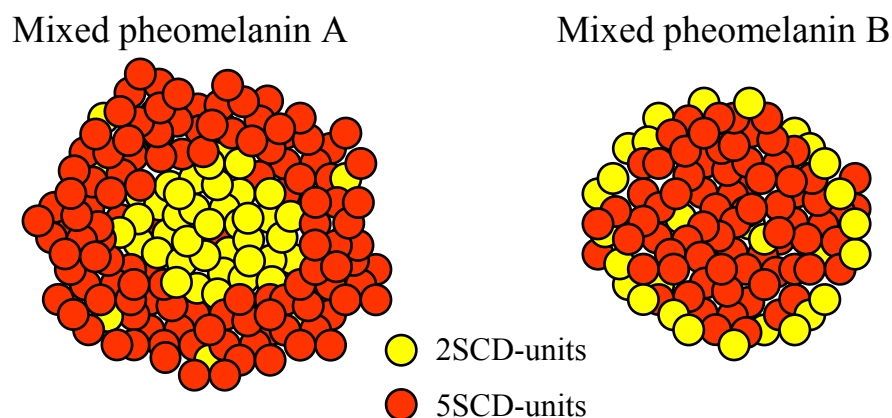


Figure 32. Schematic illustration of *mixed pheomelanin A* and *mixed pheomelanin B*.

The pheomelaninic pigments are slightly soluble in dilute alkali, under which conditions they do not undergo structural changes. On this basis, in order to assess a possible stratification between the two components, each mixed pheomelanin was subjected to the following steps: 2 mgs of dry sample were loaded on a nylon filter (Millex-GV, 0:22 mm) and dissolved by the rapid treatment with solutions at increasing pHs, including 4 aliquots of H₂O, 4 aliquots of phosphate buffer at pH 8, 4 aliquots of phosphate buffer at pH 9 and 4 aliquots of NaOH 1 M (each aliquots of 200 μ L). Each eluate was then subjected to oxidative degradation with NaOH/H₂O₂ and degradation products analyzed by HYDRO-RP HPLC-UV. The solubilized components present in each sample were identified by the amounts of BTCA and 2-BTCA arising from the degradation reaction. For each pheomelanin the oxidative degradation of the pigment without washings was carried out, in order to determine the ratio of the 2SCD-units and 5SCD-units "in the whole pigment".

Initially mixed pheomelanin A was studied. Analysis of the degradation mixture of the entire pigment showed a BTCA/2-BTCA ratio of 5:1 (grey dashed line, **Fig. 33**, panel

b). When pheomelanin A was subjected to the solubilization treatment degradation of the eluates showed that 5SCD- and 2SCD-derived components were solubilized differently, in particular at lower pHs only the 5SCD-derived units were solubilized (**Fig. 33**, panel a).

In the eluates obtained at lower pHs a BTCA/2-BTCA ratio of about 10:1 was obtained which decreased up to 3:1 in the NaOH eluates (**Fig. 33**, panel b). It is worth noting that in the absence of any coating the BTCA/2-BTCA ratio should remain constant at a value of 5:1.

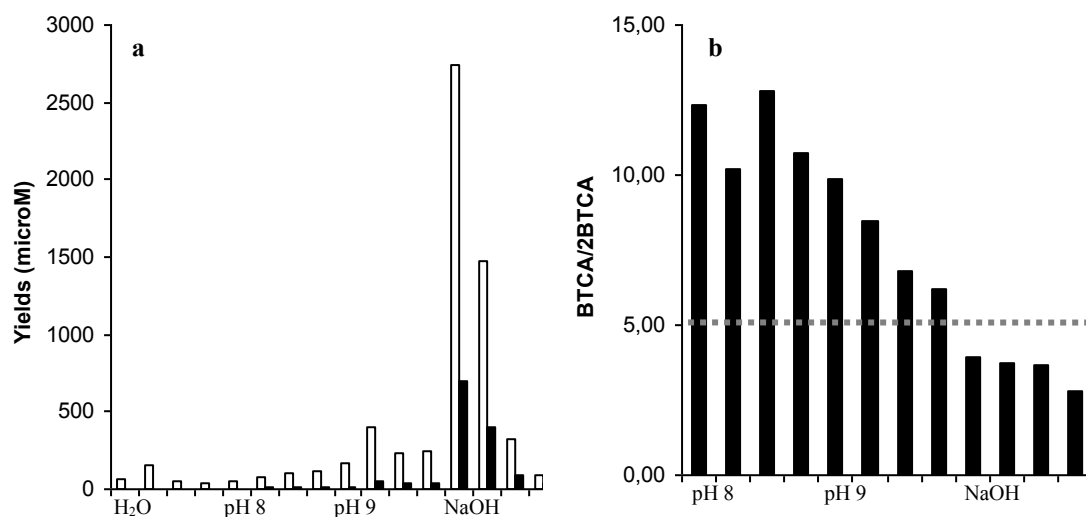


Figure 33. Yields of BTCA (black bars) and 2-BTCA (open bars) from alkaline oxidative degradation of eluates at increasing pH of mixed pheomelanin A (panel a) and reported as BTCA/2-BTCA ratio (panel b). Grey dashed line is in correspondence of BTCA/2-BTCA ratio of the entire pigment.

This trend can be interpreted as an evidence of a coating process: at the beginning the solubilization of 5SCD-units occurs and, only after these components had been washed away, the 2SCD-units are exposed to the action of the washing solutions and pass into the eluates. A complete recovery of the pigment from the filter was obtained following this procedure. Moreover the average BTCA/2-BTCA ratio from all eluates was 5:1.

Subsequently the mixed pheomelanin B was analyzed. Analysis of the degradation mixture of the entire pigment afforded a BTCA/2-BTCA ratio of 3.3:1 (grey dashed

line, **Fig. 34**, panel b). When this mixed pheomelanin was subjected to the solubilization treatment and subsequent oxidative degradation of the eluates it was observed that, differently from the case of mixed pheomelanin A, the 5SCD and 2SCD components showed a comparable solubility (**Fig. 34**, panel a). Analysis of the BTCA/2-BTCA ratio showed in the first eluates values slightly in favor of 2-BTCA, but at higher pHs they remained constant to a ratio of 3.3 (**Fig. 34**, panel b). This trend would indicate that in this case the coating process did not occur. Also in this case the recovery of the pigment from the filter was complete.

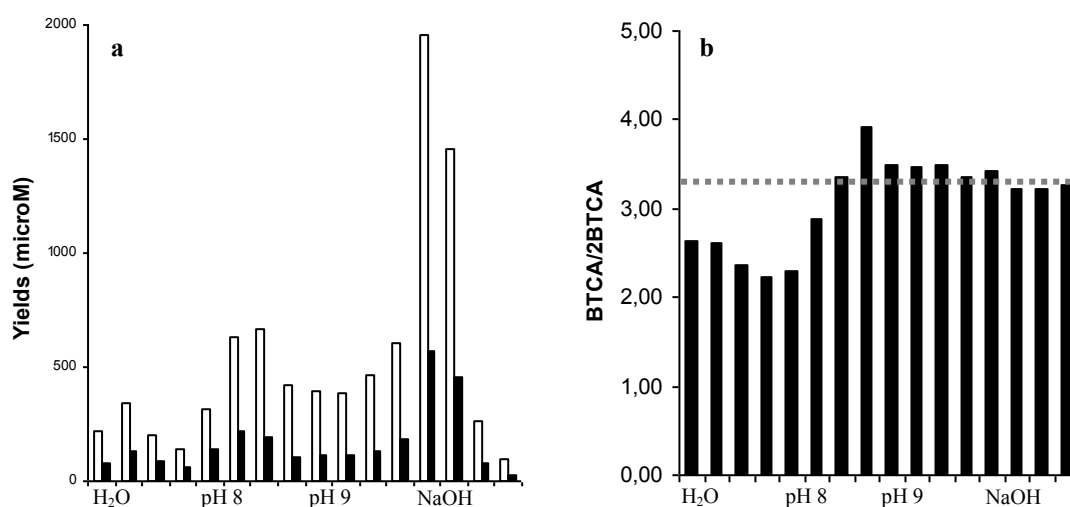


Figure 34. Yields of BTCA (black bars) and 2-BTCA (open bars) from alkaline oxidative degradation of eluates at increasing pH of mixed pheomelanin B (panel a) and reported as BTCA/2-BTCA ratio (panel b). Grey dashed line is in correspondence of BTCA/2-BTCA ratio of the entire pigment.

Control experiments with pheomelanin from 2SCD and 5SCD allowed to rule out that the observed behavior for the mixed pheomelanins was due to different solubility properties of the two pigments.

The mixed pheomelanin A represents a valid model of the pheomelanin casing, according to which the 2SCD-pheomelanin core is protected by a 5SCD-pheomelanin surface, that results much exposed to (photo)degradation. In **Figure 35** the degradation of 5SCD-units, observed during hair growth, is represented.

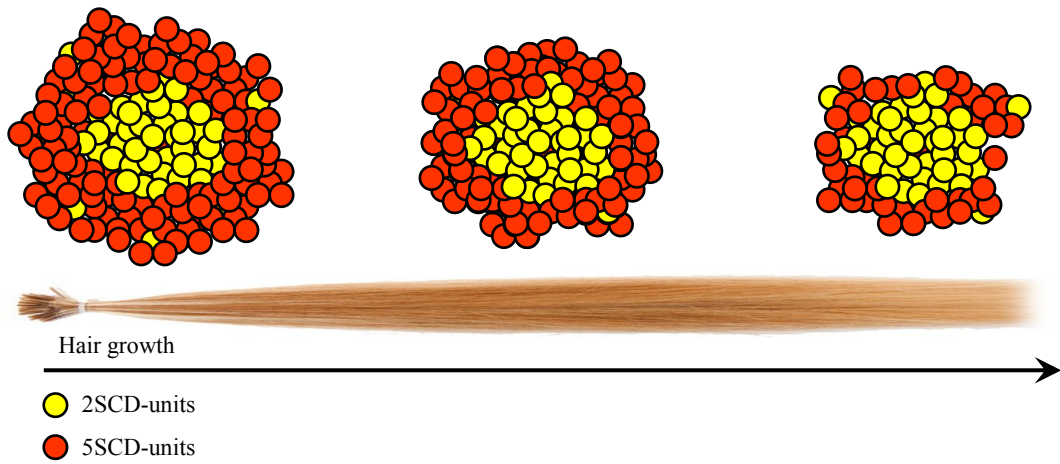


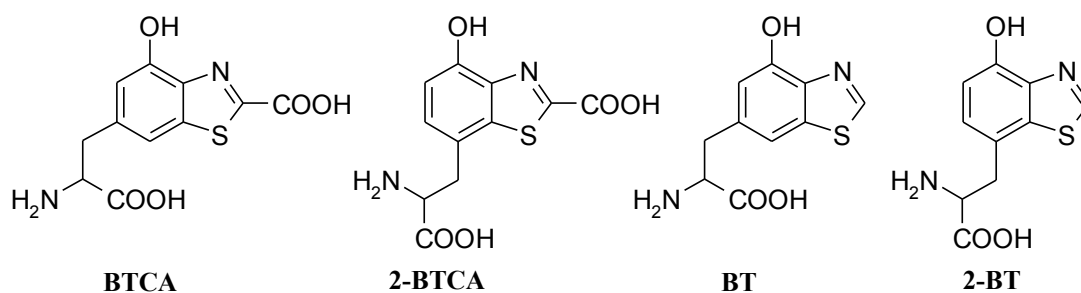
Figure 35. *Schematic illustration of pheomelanin with a 5SCD-units surface on a 2SCD-units core and degradation of exposed 5SCD-units during red hair growth.*

The pheomelanin casing is just one of the possible interpretation of the 5SCD-units degradation during red hair growth but other processes may well contribute.

2.4. Biosynthesis-inspired one-pot access routes to 4-hydroxybenzothiazole aminoacids, red hair-specific markers of UV susceptibility and skin cancer risk

4-Hydroxybenzothiazole aminoacids BTCA and 2-BTCA are specific structural markers of pheomelanins.^{163,165} They can be obtained in small amounts by oxidative degradation of red hair or synthetic pigments.¹⁴¹ On the other hand, available syntheses of the 4-hydroxybenzothiazole system are lengthy and require several steps (from six to eight to obtain BTCA and 2BTCA).¹⁶⁶⁻¹⁶⁸ This is a most critical gap since BTCA and 2-BTCA appear to be selective markers for red-haired individuals⁴⁰ at higher risk for skin cancer, and the current lack of straightforward synthetic routes has hampered their use for routine population screenings, and for genetic and epidemiologic correlations studies. For biomedical research purposes, synthetic procedures for analytical marker preparation should in fact be facile, cheap and easy to do even by non-experts.

Prompted by the urgent and increasing demand for these markers, the feasibility of the biosynthetic pathway leading to 4-hydroxybenzothiazole aminoacids was explored as a practical access route to BTCA and 2-BTCA as well as their decarboxylated derivatives 6-(2-amino-2-carboxyethyl)-4-hydroxybenzothiazole (BT) and 7-(2-amino-2-carboxyethyl)-4-hydroxybenzothiazole (2-BT).



2.4.1. Access protocol to 4-hydroxybenzothiazole aminoacids

The protocol to BTCA involves a rationally devised sequence of enzymatic and chemical steps that have been elaborated into a remarkable one-pot procedure. The developed methodology involves *i*) oxidation of L-DOPA and L-cysteine in 0.05 M phosphate buffer (pH 7.4) with mushroom tyrosinase; *ii*) treatment of the mixture with potassium ferricyanide/zinc sulfate; and then *iii*) acidification and oxidation with sodium persulfate. HPLC-RP purification eventually gives the desired compound in pure form (57% yield) (**Fig. 36**, route a). By a simple additional operation, i.e. *iv*) heating of the final mixture at 90 °C for 1.5 h, the decarboxylated derivative BT can be obtained instead in similar (55%) yield, after HPLC-RP purification.

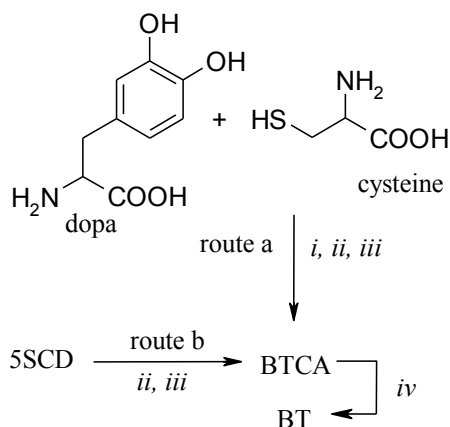


Figure 36. Reagents and conditions: *i*) tyrosinase, O_2 ; *ii*) $K_3Fe(CN)_6/ZnSO_4$; *iii*) $Na_2S_2O_8/HCl$; *iv*) 90 °C, 1.5 h.

Three critical steps underpin the synthetic methodology: *a*) the enzymatic conversion of L-DOPA to dopaquinone (DQ) followed by the addition of L-cysteine to give 5SCD (the prevalent isomer); *b*) the ferricyanide-promoted oxidative cyclization of 5SCD to a benzothiazine intermediate stabilized by Zn^{2+} ions; *c*) the persulfate-induced oxidative ring contraction of the benzothiazine- Zn^{2+} complex *I* to give BTCA (**Fig. 37**).

Consistent with the proposed mechanism is an alternate procedure to BTCA/BT which has been developed in the course of this study based on the oxidation of 5SCD, prepared following a reported procedure,¹⁶⁹ according to the above steps *ii*) and *iii*) (and *iv*, if appropriate) to give the products in quite similar yields (**Fig. 36**, route b).

The successful conversion of L-DOPA and L-cysteine to BTCA/BT reflects a careful choice of oxidation methods and sequential operation times that have been optimized within the one-pot protocol after a thorough and careful screening of oxidizing systems and experimental conditions. Thus, for example, commercially available mushroom tyrosinase proved to be the most efficient oxidizing system for *in situ* conjugation of L-cysteine to L-DOPA,²⁹ but was ineffective in promoting subsequent oxidation of cysteinyl-dopa. On the other hand, ferricyanide was effective on the latter step but not in the initial conjugate formation.

The crucial experimental expedient favouring efficient benzothiazole formation is the addition of Zn^{2+} which is known to stabilize 3-carboxy-4-hydroxybenzothiazines by forming a chelate complex, such as *I*, as evidenced by the typical absorption maximum at around 390 nm.^{37,163} Thus, in the presence of Zn^{2+} , the key benzothiazine intermediate can be accumulated in suitable amounts for the oxidative ring contraction (Fig. 37).¹⁴¹

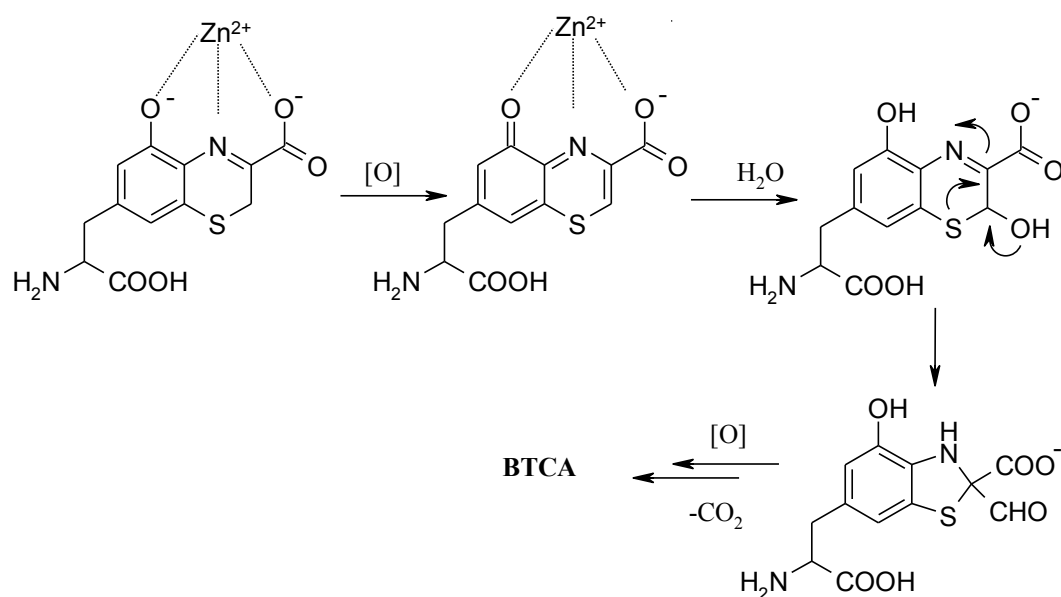


Figure 37. Proposed routes of formation of BTCA from benzothiazine- Zn^{2+} complex *I*.

The latter step was efficiently achieved by using persulfate combined with acid conditions while other oxidants or reaction media proved much less effective. Interestingly, the acid-promoted ring contraction of a remarkably stable 2-alkoxy-7-

hydroxy-2*H*-[1,4]benzothiazine intermediate is the key step in a strategically similar synthesis of 6-hydroxybenzothiazole-2-carboxylic acid.¹⁷⁰

Extension of the L-DOPA + L-cysteine coupling route to the synthesis of 2-BTCA/2-BT was precluded by the low formation ratio of 2SCD/5SCD (1:5) in the tyrosinase promoted conjugation.²⁹ After extensive unfruitful efforts to direct the coupling reaction, we eventually resorted to use 2SCD as the precursor. This was made possible by the facile synthesis recently described for this melanogen.¹⁷¹ As expected, oxidation of 2SCD as in **Figure 36**, route b, afforded the desired 2-BTCA/2-BT in similar yields (52-57%).

2.5. Pheomelanin-related benzothiazole isomers in the urine of patients with diffuse melanosis of melanoma

Currently used as structural markers for pheomelanin identification and quantitation, benzothiazole compounds have been indicated by recent in vitro studies as new potential pheomelanogenesis intermediates.

The conditions for chemical degradation and analysis of these compounds were recently improved by introduction of wetttable octadecylsilane columns³⁹ simpler eluents, hydrophilic interaction liquid chromatography (HILIC)⁷⁸ and GC/MS analysis.⁷⁹ Using the latter methodologies evidence was obtained for the presence of pheomelanin pigments in the urine of melanoma patients.⁷⁷ 1,4-Benzothiazole compounds were obtained in melanoma patients on HI degradation of urinary pigments followed by ethyl chloroformate derivatization and GC/MS analysis.⁷⁹ The presence of an active pheomelanogenic pathway associated with melanoma was also indicated by the occurrence of trichochromes in the urine of melanoma patients⁸⁰ particularly when diffuse melanosis occurs in metastasizing melanoma.⁸¹

On this basis and relying on the newly developed analytical methodologies urine from 3 patients with melanosis due to melanoma and from 16 patients with metastatic melanoma without melanosis were examined to assess the presence of pheomelanin-related metabolites and particularly benzothiazole isomers.

2.5.1. Method development and identification of BTCA and 2-BTCA in the urine of melanoma patients

Standards of BTCA (BTCA-5), 2-BTCA (BTCA-2), BT (HBTA-5) and 2-BT (HBTA-2) obtained as described (paragraph 2.4) were injected on a ZIC-HILIC column. Baseline separation was obtained (**Fig. 38**). The HPLC method developed for the analysis of AHP isomers⁷⁸ was initially used for peak purity determination and quantification of BTCA-5 and BTCA-2 in human urine from a patient with diffuse melanosis. To achieve the sensitivity and selectivity required for the analysis of the

isomers in biological samples, a photo-diode array detector (PDA) was employed. This allowed monitoring at several wavelengths and provided UV spectra which could be used to assess peak purity and safely identify the compounds by comparison of the peculiar spectral features against those of standard samples. The absorption spectra of BTCA isomers showed maxima at approximately 210, 250, 285 and 325 nm (**Fig. 38**).

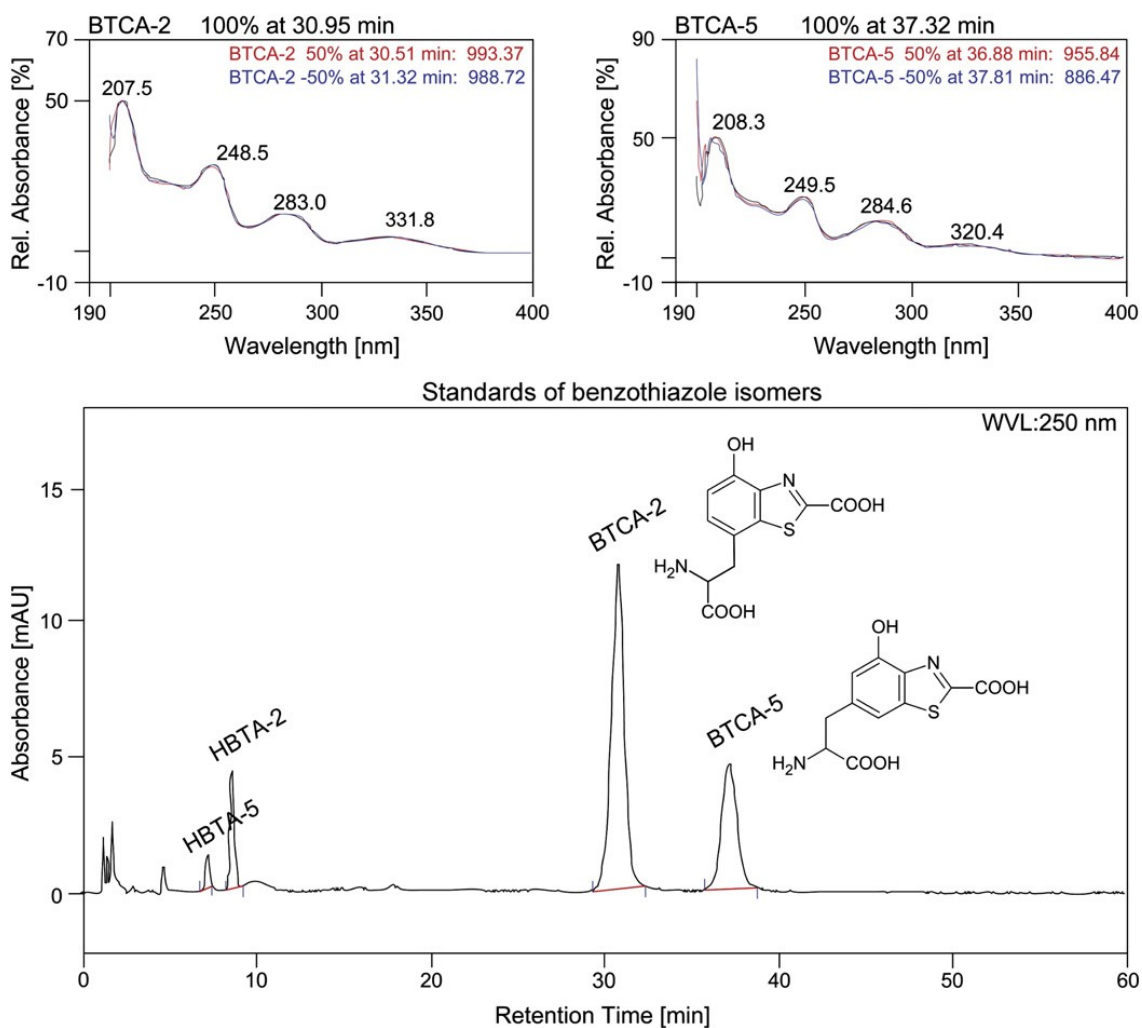


Figure 38. LC-PDA profile of a calibrator of benzothiazole isomers separated with the HILIC. Spectra at 50% of the peak height before and after peak apex are compared with spectrum at the apex. The match degree of all three spectra is a criterion for the peak purity.

By direct injection of urine (diluted with mobile phase before injection) the peaks with the same spectra as standards of BTCA-5 and BTCA-2 were observed but peaks

fronting and interferences from other compounds from urine were considerable. BT and 2-BT could not be identified in the urine with this method. Small changes in mobile phase composition (pH or aqueous phase content and even sample matrix) influenced separation vigorously. Retention times for BTCA isomers increased when mobile phases with lower contents of aqueous phase were used. This is probably due to the hydrophilic character of BTCAs and also due to the ionic interactions with the stationary phase. Lower pH resulted in shorter retention time but poorer separation from interfering peaks. With a mobile phase composition of acetonitrile:ammonium acetate buffer pH 5 (82:18, v/v), BTCA isomers were eluted as single peaks with the retention times of approximately 31 and 37 min when flow rate was set at 300 μ l/min.

In order to obtain higher sensitivity and purer peaks a solid phase extraction (SPE) step was employed using 200 mg of C18 sorbent. Optimization of the elution conditions led us to choose a ratio of 1 ml urine/ 100 mg sorbent. The BTCA isomers were eluted in a 1 ml fraction. To obtain detectable levels of BTCA isomers in samples with expected low BTCA concentrations the eluates were evaporated and analyzed after dilution with mobile phase.

In peak purity studies we found that a wavelength of 285 nm gave the best selectivity and purest chromatographic peak despite that sensitivity was higher at lower wavelengths (**Fig. 39**, panel a). After SPE treatment of the samples, chromatograms extracted at 250 nm were improved, and due to good sensitivity and pure peaks 250 nm was used for quantification of BTCA (**Fig. 39**, panel b).

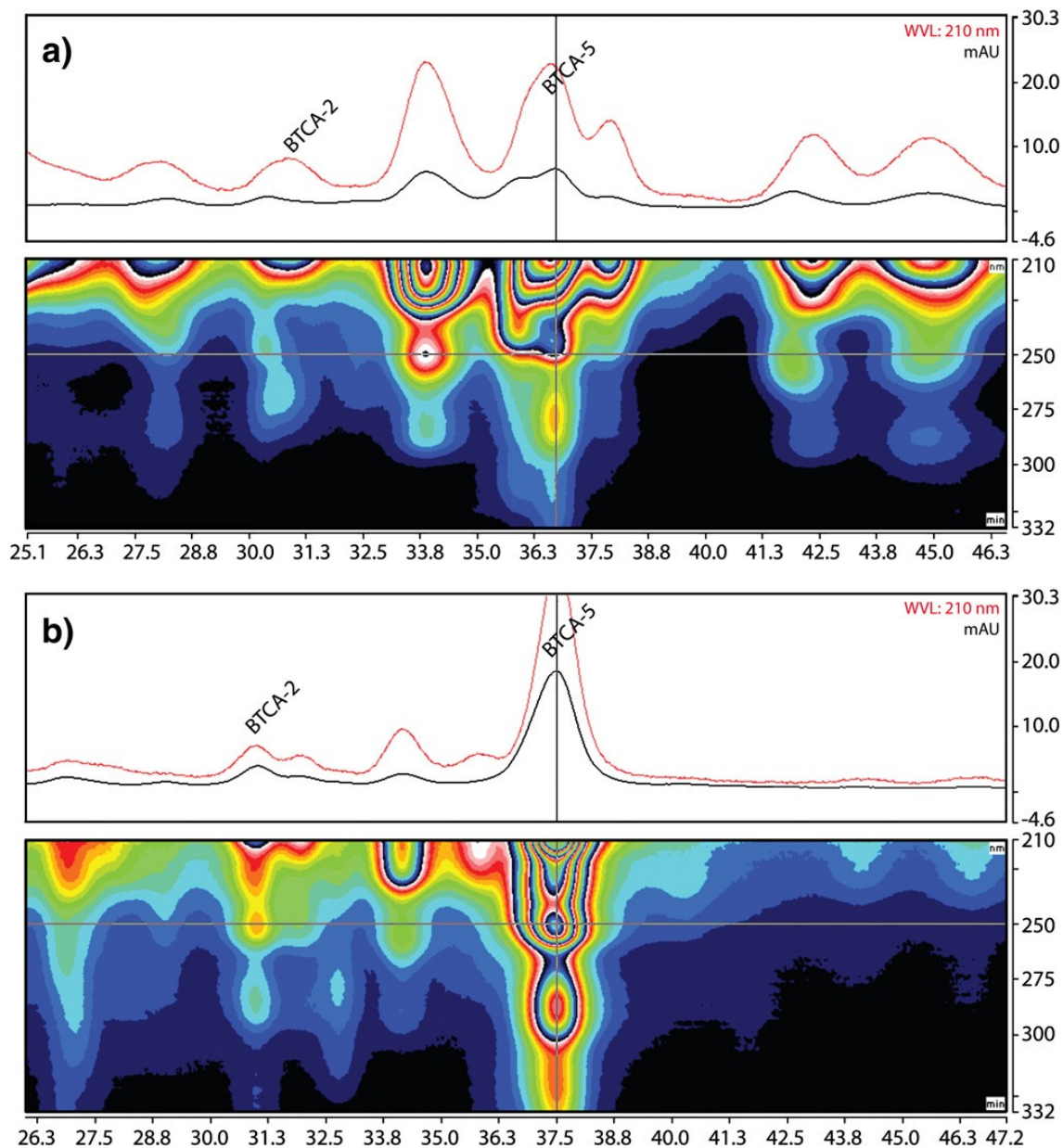


Figure 39. Chromatograms and 3D spectra of a urine sample from a patient with melanoma a) before sample preparation, b) after sample purification. 3D spectra were obtained for 190–400 nm. The black lines show recordings at 210 nm and the red lines are obtained after flexible screening of 3D spectra and plotted at 250 nm.

The HILIC-PDA method was validated with respect to linearity, limit of detection (LOD), extraction, recovery, precision, and interferences. Calibration curves were built using the areas of the chromatographic peaks (y) from standards of 4 increasing

concentrations in the range 0.05–2.5 mM (x). The responses were linear with following equation $y=30.8x-0.136$ ($R^2=0.9996$) and $y=73.9x+0.073$ ($R^2=0.9995$) for BTCA-5 and BTCA-2 respectively at all four wavelengths tested, but for quantification the wavelength 250 nm was optimal. This wavelength gave the best sensitivity, and the selectivity was significantly improved after interfering peaks were removed with SPE. The LODs were calculated using the $3 \times S/N$ criterion. Results were based on the responses and the slopes of specific calibration curves containing the analytes. The estimated LOD values were 5.98 μg and 2.13 μg for BTCA-5 and BTCA-2 at 250 nm. For comparison LODs at 285 nm were also calculated and were 11.22 μg and 5.48 μg respectively. For recovery studies aqueous samples with known amounts of the standard solution of BTCA-5 were extracted according to the described SPE protocol. Extraction recovery was estimated by analysis of the peak area of the samples before and after extraction. Urine from a healthy subject was spiked with known amount of the standard solution of BTCA-5 before extraction and analytical recovery was estimated as 85% by comparison with a pure standard. For comparison 0.05 M acetic acid was also used the medium following the same spiking protocol and a recovery of 93% was obtained. Intra-day relative standard deviation (RSD) was calculated from repeated analysis of one patient's sample and was 4.55% for BTCA-5 and 1.89% for BTCA-2. Inter-day assay was calculated from mean variance of three patients' samples analyzed repeatedly at four occasions during one month. The total RSD was less than 10% for BTCA isomers. These data suggests that the method was reproducible for the determination of BTCAs in the urine of melanoma patients. Since 5SCD is a known marker of melanoma progression and a precursor of BTCA its possible conversion to BTCA in urine samples of melanoma patients was assessed at different temperatures (between -20 and $+20$ °C) and storage time (up to 1 month). Stability of 5SCD has been studied before.¹⁷² An aqueous solution of 5SCD 650 μM was prepared in 0.01 M acetic acid and in the urine of a healthy subject. The urine was analyzed for BTCA isomers before spiking. No detectable amounts of BTCA-5 were formed from 5SCD with the exception of very low amounts obtained in a single sample after one month storage at 4 °C.

2.5.2. Free BTCAs and 5SCD concentrations in the urine from patients with melanoma and diffuse melanosis

Urines from three patients with diffuse melanosis and 16 patients with melanoma but not diffuse melanosis were analyzed using the above developed methodologies. In all three urines from patients with diffuse melanosis and from one patient with melanoma (no information of melanosis was available) significant amounts of BTCA-5 and BTCA-2 were found (**Table 6**).

Table 6. Urinary free BTCAs, 5SCD and S100 protein concentrations in melanoma patients with or without melanosis and healthy subjects.

Sample	BTCA-5 $\mu\text{mol/l}$	BTCA-2 $\mu\text{mol/l}$	5SCD $\mu\text{mol/l}$	5SCD/creatinine ^a $\mu\text{mol/mol}$	S100 protein ^b $\mu\text{mol/l}$	Stage ^c
Melanosis Pt 1	342.7	81.4	831.0	75400	3.2	IV, M1c
After 4 m	95.4	80.5 ^d	754.0	87474	10.0	Progress
Melanosis Pt 2	118.7	37.4	713.0	169762	9.4	IV, M1c
Melanosis Pt 3	28.9	6.8	52.0	8966	-	IV, MX
Melanoma Pt 1	/	/	8.6	587	0.09	III, N1b
After 5 m	/	/	26.7	1701	0.25	Stable
After 6 m	/	/	7.2	1600	0.33	Stable
After 10 m	4.8	/	23.3	2678	0.23	IV, M1c
After 17 m	6.8	1.6	54.9	6949	-	Progress
Melanoma Pt 2	/	/	15.9	3118	-	IV, M1c
After 14 days	/	/	49.3	4695	-	Progress
After 1 m	/	/	66.0	6055	0.25	Progress
Melanoma Pt 3	/	/	7.1	826	0.69	IV, M1c
After 1 m	/	/	9.4	1133	0.93	Progress
After 1.5 m	/	/	12.8	1164	0.62	Progress
Melanoma Pt 4	/	/	9.7	4217	-	III, N1b
Melanoma Pt 5	/	/	1.1	396	0.17	III, N1b
After 2 m	/	/	2.8	2000	-	IV, M1b
Melanoma Pt 6	/	/	4.3	286	-	IV, M1a
Melanoma Pt 7	/	/	11.4	726	0.88	IV, M1c
Melanoma Pt 8	/	/	20.2	2220	-	IV, M1bc

Melanoma Pt 9	/	/	4.7	564	-	IV, M1c
Melanoma Pt 10	/	/	8.3	1587	0.83	IV, M1c
Melanoma Pt 11	/	/	22.2	1531	5.10	III, N2b
Melanoma Pt 12	/	/	5.9	426	0.13	IV, N1b
Melanoma Pt 13	/	/	18.9	867	0.44	IV, M1a
Melanoma Pt 14	/	/	8.1	976	5.29	IV, M1abc
After 11 m	/	/	33.1	1715	7.00	Stable
Melanoma Pt 15	/	/	60.0	3704	-	IV1a
Melanoma Pt 16	/	/	0.8	130	1.06	IV, M1bc
Red haired	/	/	0.3	<70		
normal						
Black haired	/	/	0.2	<70		
normal						
Brown haired	/	/	0.3	<70		
normal						

^a Normal reference range <70 $\mu\text{mol/mol}$.

^b Normal reference range <0.12 $\mu\text{g/l}$.

^c Highest stage regarding N and M is reported.

^d This peak was not purely separated from interfering peaks.

Data in **Table 6** do not show a straightforward correlation between the levels of excreted BTCAs and 5SCD, although patients with significant amounts of BTCA isomers in the urine had generally high levels of 5SCD. Similar results were obtained when excretion of trichochromes and 5SCD in patients with diffuse melanosis were compared.^{80,81,173} It should be noted also that abnormally high levels of 5SCD were observed in melanoma patients with melanosis as reported in previous studies.^{80,174} No detectable amounts of BTCAs were found in the urine of healthy subjects either belonging to the pheomelanic or the eumelanic phenotype. The BTCA-5/BTCA-2 ratios found for patients with melanosis ranged from 3 to 4. The urine from one of the patients was analyzed after four months and a lowering of the concentrations of BTCA-5 in the last urine was observed. However, this urine was more diluted than the former one and a correction to BTCA-5/creatinine ($\mu\text{mol/mol}$), revealed that the total excretion of BTCA-5 was similar between the two samples, 77.8 $\mu\text{mol/mmol}$ creatinine and 73.4 $\mu\text{mol/mmol}$ creatinine. Interestingly enough the quotient between free BTCA and BTCA in the sediment varied greatly. This may be due to how much free BTCA and

trichochromes relative to pigment with higher molecular weight is formed and excreted. The absence of BTCAs in the urines of melanoma patients without melanosis, even those with high 5SCD, indicates that BTCA formation may not primarily be the result of a process related to melanoma cell proliferation. It may be that, different from most melanoma patients, those with diffuse melanosis have melanoma cells overactive in pheomelanin formation. Diffuse melanosis may therefore be the result of spread of such melanoma cells through the body. These cells may continue to produce melanosomes which eventually are deposited in dermal macrophages.^{68,69} Another possible interpretation would invoke an increased tyrosinase activity associated with metastatic malignant melanoma, which might lead to an accelerated conversion of tyrosine to melanin precursor and the formation of metabolic intermediates that accumulate in the blood and are excreted into the urine.^{66,175} The fact that in most cases the higher BTCA levels are associated with the higher cysteinyl-dopa levels may point to a non-enzymatic oxidative conversion of this metabolite to benzothiazines and hence benzothiazoles as evidenced by in vitro studies.³⁴ This conversion could be induced by reactive oxygen species whose levels have been shown to rise in malignant transformations such as in dysplastic nevi compared to dermal nevi producing a chronic oxidative stress condition.^{68,176}

2.5.3. Analysis of urinary soluble pigments and sediment by chemical degradation

The urines of melanoma patients were subjected to chemical degradation according to the alkaline hydrogen peroxide procedure currently used for identification of pheomelanin in pigmented tissues.³⁹ As with analysis of BTCAs in untreated urine, separation was greatly improved by SPE pretreatment (**Fig. 40**). Oxidation mixtures were also analyzed using conventional chromatographic conditions previously employed for BTCAs analysis.¹⁶³ However, peak separation was not satisfactory and we decided to continue with the HILIC-PDA methodology for BTCA-5 and BTCA-2 quantification.

The yields of BTCA-5 and BTCA-2 are reported in **Table 7**. When compared with the concentrations of free BTCAs, BTCAs obtained after chemical degradation of mixed

urine are around 2.5 fold higher. It should be observed that BTCAs were analyzed quantitatively in the three compartments: mixed urine (total BTCA), urinary sediment, and supernatant obtained after centrifugation. Thus separate chemical degradation of the sediment and the supernatant showed that most of the pigment remained in solution.

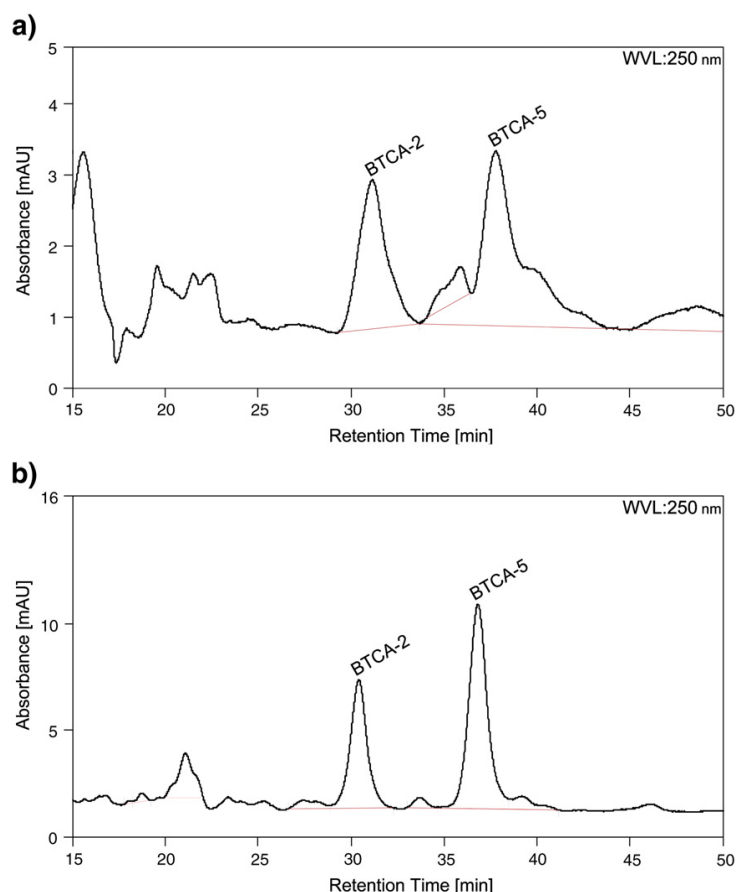


Figure 40. Chromatogram of urine from a patient with melanoma after chemical degradation a) before SPE, b) after SPE.

The relation between different fractions is more clearly shown for melanosis patients in **Table 8**. When considering BTCA amount from supernatant and sediment together they constitute close to 100% of BTCA from mixed urines. Assuming that free BTCA was un-affected by oxidation (as observed in separate control experiment) we subtracted this concentration from that obtained after oxidation of the supernatant from centrifuged urine. This fraction was called LowMW pigment and we think that this corresponds to soluble low-molecular weight components, possibly including trichochromes and

dimers formed from both 5SCD and 2SCD. The quotients between BTCA-5 and BTCA-2 were calculated for all the fractions (except for the second free urine fraction of patient 1). The ratio between the two markers varied between 2.0 and 4.9, which corresponds fairly well with the ratio of BTCA-5 and BTCA-2 obtained after oxidative degradation of synthetic pheomelanin obtained from L-dopa and cysteine. By comparing the yields of BTCAs of the sediment with those obtained from a synthetic pheomelanin it was estimated that pheomelanin represented about 15% of the sediment.

Table 7. BTCAs by oxidative degradation of urinary soluble pigment and sediment in melanoma patients with or without melanosis and healthy subjects.

Sample	Mixed urine		Urine sediment		Centrifugated urine	
	$\mu\text{mol/l}$		$\mu\text{mol/l}$		$\mu\text{mol/l}$	
	BTCA-5	BTCA-2	BTCA-5	BTCA-2	BTCA-5	BTCA-2
Melanosis Pt 1	856.9	240.1	105.7	44.4	681.6	245.9
After 4 m	632.8	290.0	257.2	75.3	457.1	227.0
Melanosis Pt 2	436.7	92.4	60.9	13.3	362.1	74.4
Melanosis Pt 3	101.8	38.2	34.7	10.4	75.3	29.8
Melanoma Pt 1	-	/	/	/	/	/
After 5 m	-	/	/	/	/	/
After 6 m	-	/	/	/	/	/
After 10 m	-	/	/	/	46.1	15.6
After 17 m	-	/	/	/	88.3	29.0
Melanoma Pt 2	-	/	/	/	/	/
After 14 days	-	/	/	/	/	/
After 1 m	-	/	/	/	/	/
Melanoma Pt 3	-	/	/	/	/	/
After 1 m	-	/	/	/	/	/
After 1.5 m	-	/	/	/	/	/
Melanoma Pt 4	-	/	/	/	/	/
Melanoma Pt 5	-	/	/	/	/	/
After 2 m	-	/	/	/	/	/
Melanoma Pt 6	-	/	/	/	/	/
Melanoma Pt 7	-	/	/	/	/	/
Melanoma Pt 8	-	/	/	/	/	/
Melanoma Pt 9	-	/	/	/	/	/

Melanoma Pt 10	-	/	/	/	/	/
Melanoma Pt 11	-	-	/	/	/	/
Melanoma Pt 12	-	-	/	/	/	/
Melanoma Pt 13	-	-	/	/	/	/
Melanoma Pt 14	-	-	/	/	/	/
After 11 m	-	-	/	/	/	/
Melanoma Pt 15	-	-	/	/	/	/
Melanoma Pt 16	-	-	/	/	/	/
Red haired	-	-	/	/	/	/
normal						
Black haired	-	-	/	/	/	/
normal						
Brown haired	-	-	/	/	/	/
normal						
Pheomelanin	-	-	14.9 ^a	2.7 ^a		

^aThese values are calculated in mg BTCA/mg pheomelanin (%).

The possibility that some eumelanin was as well present was indicated by the yields of the typical marker pyrrole-2,4,5-tricarboxylic acid (PTCA) which exceeded those expected for a pheomelanin. In any case eumelanin was only a minor constituent of the whole pigment in the sediment. Analyses of urine of melanoma patients without melanosis shown in **Table 6** did not provide detectable amounts of BTCA. Only in melanoma patient number 4, who could be monitored for a long period, appreciable amounts of BTCA-5 were obtained after 10 months (BTCA-5 110 $\mu\text{mol/l}$) with an increase at 17 months (151 $\mu\text{mol/l}$), a trend already observed for free BTCA (see **Table 6**). Hence it can be concluded first that the BTCA obtained after degradation does not reflect free BTCA already present in the urine, and second that the urinary pigment can be regarded as a pheomelanin giving rise to the BTCAs markers after degradation. This trend was also confirmed in the other melanosis patients. Control healthy patients with pheomelaninic or eumelaninic pigmentation did not provide detectable amounts of BTCA. Our results suggest that several intermediate metabolites involved in pheomelanin formation are excreted into the urine of patients with melanosis from melanoma. As regards cysteinyl dopas and the eumelaninic precursor dihydroxyindole and dihydroxyindole carboxylic acid, their excretions have mainly been considered as

overflow from melanoma cells and their concentration in the urine as proportional to the melanoma load.⁷⁵

Table 8. Relation between analyzed free and by oxidative degradation derived BTCA isomers from different urinary fractions of patients with melanosis. Concentration of low-molecular weight pigment structures (Low_{MW} pigment) were calculated as $BTCA_{\text{Centrifuged urine}} - BTCA_{\text{Free urine}}$.

Sample	Mixed urine		Urine sediment		Centrifugated urine		Free BTCA		Low _{MW} pigment	
	μmol/l	%	μmol/l	% ^a	μmol/l	%	μmol/l	% ^b	μmol/l	% ^b
BTCA-5										
Melanosis Pt 1	856.9	100.0	105.7	12.3	681.6	79.5	342.7	50.3	338.9	49.7
After 4 m	632.8	100.0	257.2	40.6	457.1	72.2	95.4	20.9	361.7	79.1
Melanosis Pt 2	436.7	100.0	60.9	13.9	362.1	82.9	118.7	32.8	243.4	67.2
Melanosis Pt 3	101.8	100.0	34.7	34.1	75.3	74.0	28.9	38.4	46.4	61.6
BTCA-2										
Melanosis Pt 1	262.0	100.0	44.6	17.0	245.9	93.9	81.4	33.1	164.5	66.9
After 4 m	290.0	100.0	75.7	26.1	227.0	78.3	80.5 ^c	35.5	146.5	64.5
Melanosis Pt 2	92.4	100.0	13.3	14.4	74.4	80.5	37.4	50.3	37.0	49.7
Melanosis Pt 3	38.2	100.0	10.4	27.2	29.8	78.0	6.8	22.8	23.0	77.2

^a Calculated as % of mixed urine.

^b Calculated as % of centrifuged urine.

^c This peak was not purely separated from interfering peaks.

The occurrence of free BTCAs in the urine is an entirely new finding. The mechanism by which this excretion occurs is not clear at present although melanuria and melanogenuria are wellknown phenomena.^{66,177} Several earlier studies have shown that other benzothiazine related compounds such as trichochromes are also excreted into the urine of such patients.^{81,173,178} A number of histological studies have revealed dermal

melanin pigment in extracellular connective tissue and within histiocytes and fibroblasts in otherwise normal skin, and it should be noted that diffuse melanosis is observed in almost all organs, including the liver, spleen, gut, lungs, bone marrow, and heart.⁶⁶ Others have also observed melanosomes and pigment even in endothelial cells or as cell-free material in tissues.⁶⁷ An interesting theory is that tumor-derived melanin granules are liberated to the lymph and blood and are circulated to various organs where they are phagocytosed by endothelial cells and the pigment deposited in macrophages and other cells.⁶⁶ In the studies by Gambichler et al.⁶⁶ the histopathologic appearance of the kidney tissue was consistent with acute kidney injury caused by melanin accumulation within the tubules, tubular cells, and endothelial cell of the vessels and glomeruli. Acute lysis syndrome is a rare event that occurs mainly in lymphoproliferative disease. It has been described in less than ten cases of malignant melanoma,¹⁷⁹ and it has been described initially in the development of melanosis.⁷¹ The findings of Busam et al.⁷¹ however, documented that diffuse melanosis may result from tumor lysis, with release of melanosomes into the bloodstream. Although acute lysis syndrome occurs much more seldom in advanced melanoma than melanosis it is possible that lysis of melanoma cells is the cause of melanosis, however rarely resulting in progression to acute renal failure. Even if melanosomes are found circulating as cell-free material to tissues^{67,71} these particles measure up to 1.5 μm in diameter and such subcellular granulae as well as melanin granules of comparable size are unlikely to cross an intact glomerular membrane. We found free BTCAs to constitute 15–40% of total detected BTCAs (mixed urine after chemical degradation) and the soluble fraction (supernatant after centrifugation of urine) constituted around 75% of total (mixed urine). This indicates that at least most of the pheomelanin pigment and pigment precursors are excreted into the urine as low-molecular compounds and not as high molecular weight pigments. It could be speculated that part of the low-molecular compounds are dimers of or trichochromes formed from 5SCD and 2SCD.

2.6. Mapping structural diversity in red hair pheomelanin: key elusive benzothiazolyldihydroisoquinoline building blocks and their formation pathway uncovered

A definitive assessment of the actual role of pheomelanin in UV susceptibility and actinic damage awaits complete elucidation of the fundamental molecular components of these heterogeneous and elusive biopolymers.^{63,163} Defining the basic structural motifs of human red hair pheomelanin is of the utmost importance in the prospects of determining what chromophores activate molecular oxygen and mediate phototoxic reactions in cellular systems.⁵⁷

Oxidation of 5SCD and its isomers to pheomelanin proceeds via an array of benzothiazine intermediates (**Fig. 2**). Further oxidation leads to dimers and the trichochromes³⁷ which overall would take part in pheomelanin build-up (**Fig. 4; Fig. 5**).^{63,163} Beyond this level, knowledge of the mechanisms of pheomelanogenesis is virtually lacking.

Direct investigation of the natural pigments, on the other hand, was largely based on spectroscopic analysis coupled with chemical degradation studies^{44,165} (**Fig. 6**), supporting the notion that pheomelanins consist of benzothiazine and benzothiazole units at various oxidative levels and linked through different bondings.⁵

A series of studies carried out in the late 1960's suggested the presence of isoquinoline units in natural pheomelanins, but this hypothesis has remained so far unverified (paragraph 1.1.5).

The lack of information on the occurrence and levels of isoquinoline moieties in human pheomelanin is a serious drawback toward an understanding of the role and implication of this peculiar pigment in photocarcinogenic processes in redheads.⁵

Described herein are the results of an integrated approach which allowed for the first time the demonstration, characterization and quantitation of isoquinoline-containing structural motifs in the human pigment. Evidence is also provided for a possible role of these units as determinants of human pheomelanin chromophore.

2.6.1. Chemical degradation of natural and synthetic pheomelanins

An initial series of experiments was directed to gauge the presence of isoquinoline-containing constituents in human red hair pheomelanin by chemical degradation. To this aim, it seemed of interest to revisit the alkaline KMnO_4 oxidation method successfully applied in the early studies to the characterization of gallopheomelanins.⁴² HPLC analysis of the red hair degradation mixture (**Fig. 41**) revealed the presence of two distinct peaks attributed to known fragmentation products, thiazoletricarboxylic acid (TTCA) and thiazole-4,5-dicarboxylic acid (TDCA), along with other components eluted at higher retention times whose properties did not match with those of other known degradation products of pheomelanins. Among these a major species eluting at around 36 min (I) was well discernible. The same product was generated, together with TTCA and TDCA, by degradation of a set of synthetic pheomelanins prepared under different conditions (**Fig. 41**).

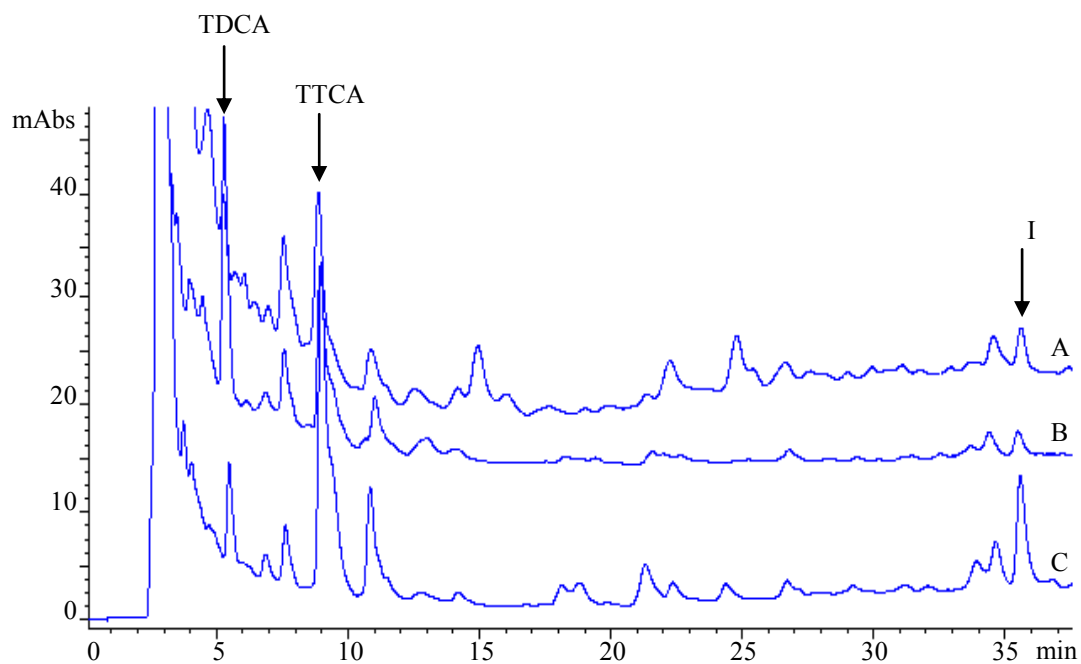


Figure 41. HPLC traces of the alkaline permanganate degradation mixtures of red human hair (A), dopa/cysteine pheomelanin (B), and 5SCD/ Zn^{2+} /peroxidase/ H_2O_2 pheomelanin (C). Elutographic profiles are shown with different intensities.

No detectable amount of the product I, however, was present in the degradation mixtures from black hair eumelanin, indicating that it derived from an important and specific pheomelanin component (**Fig. 42**).

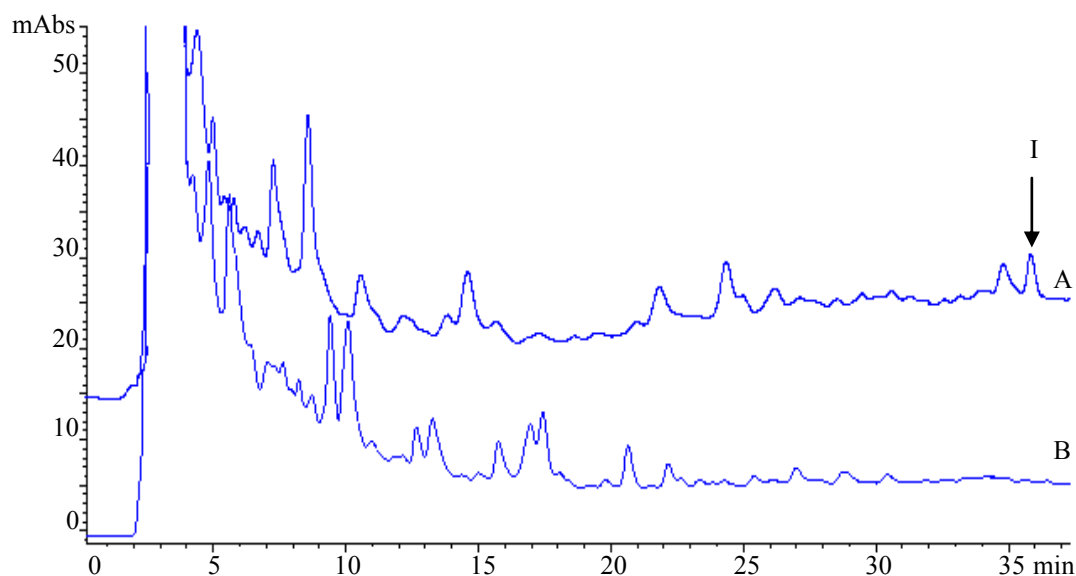


Figure 42. HPLC traces of the alkaline permanganate degradation mixtures of red human hair (A), and black human hair (B). Elutographic profiles are shown with different intensities.

Accordingly, a procedure was set up which allowed the isolation of the main degradation product in sufficient amounts for spectral characterization. For this purpose, 120 mg of pheomelanin obtained by oxidation of 5SCD with peroxidase/H₂O₂ in the presence of Zn²⁺ ions were treated with alkaline KMnO₄ yielded a complex degradation mixture from which the desired product could eventually be isolated in small amounts by preparative HPLC. The mass spectrum (ESI(-)/MS) displayed a pseudomolecular ion peak at *m/z* 381 (HR/MS 380.9672 calcd for C₁₃H₅N₂O₁₀S 380.9670) and an absorption maximum at 292 and 318 nm.⁴¹ The ¹H NMR spectrum was remarkably simple, exhibiting a single resonance (singlet) at δ 8.56. On this basis, the product I was unambiguously formulated as the previously described TPCA.⁴¹ This result allowed to conclude that human red hair pheomelanin contains units akin to those found in gallopheomelanin and giving on degradation the structurally significant TPCA.

The pheomelanin obtained by oxidation of 5SCD with peroxidase/H₂O₂ in the presence of Zn²⁺ ions was selected because of the higher formation yields of the product relative to other synthetic pigments prepared under different oxidation conditions (**Table 9**).

Table 9. Yields of TPCA from alkaline permanganate degradation of red human hair and synthetic pigments.

Sample	TPCA (ng/mg) ^a
Red human hair	690
Dopa/cysteine pheomelanin	25950
5SCD/tyrosinase/O ₂ pheomelanin	15370
5SCD/Zn ²⁺ /tyrosinase/O ₂ pheomelanin	40750
5SCD/peroxidase (16.7 U/mL)/H ₂ O ₂ pheomelanin	23940
5SCD/Zn ²⁺ /peroxidase (16.7 U/mL)/H ₂ O ₂ pheomelanin	95700
5SCD/Zn ²⁺ /peroxidase (50 U/mL)/H ₂ O ₂ pheomelanin	110520

^a Shown are the mean values for three separate experiments with SD ≤ 10%

2.6.2. Biomimetic oxidation of 5SCD and product isolation

Information about the nature of the TPCA precursor units was then sought through careful investigation of the oxidation of 5SCD with peroxidase/H₂O₂ in the presence of Zn²⁺. As shown above, this reaction led to a synthetic pigment which provided the richest source of TPCA on degradation. The role of Zn²⁺ ions was to slow down the kinetics of pheomelanin synthesis favoring the accumulation of benzothiazine intermediates.^{37,163} Such an effect has also been confirmed in studies on catechol compounds model of 5SCD.¹⁸⁰ Besides being chemically convenient for intermediate isolation and characterization, the addition of Zn²⁺ is also of biological relevance since relatively high levels of zinc are found in normal human skin and are known to accumulate in red hair.¹³⁹ HPLC analysis coupled with ESI(+)-MS (**Fig. 43**) showed in the early stages of the reaction the generation of two main products, identified as the reduced 3,4-dihydrobenzothiazine-2-carboxylic acid derivative (BTZCA),¹⁶³ and ODHB.

While compound ODHB accumulated with time, and remained largely unchanged in the mixture, intermediate BTZCA attained its maximum concentration after about 1 h and then gradually decayed, being replaced by a complex pattern of products including BTZCA-dimers and two additional species, A and B, separated by quite different elution times but sharing a pseudomolecular ion peak $[M+H]^+$ in common at m/z 515.0, suggesting isomeric dimers of 5SCD.

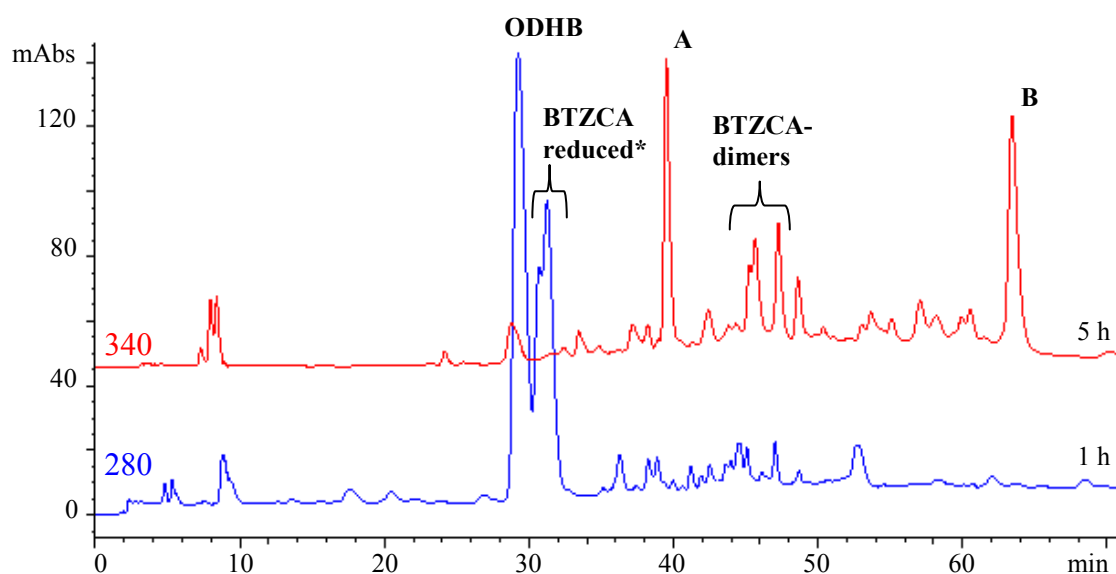


Figure 43. HPLC traces of the oxidation mixture of 5SCD with peroxidase/ H_2O_2 in the presence of Zn^{2+} at 1 h reaction time (after reduction with $NaBH_4$, 280 nm, blue trace), and at 5 h reaction time (340 nm, red trace).

*7-(2-amino-2-carboxyethyl)-3-carboxy-5-hydroxy-3,4-dihydro-2H-1,4-benzothiazine.¹⁶³

To gain insight into the structure of these products, the oxidation of 5SCD was repeated under similar conditions but on a larger scale, and products A and B were isolated accordingly the following procedure. Briefly, when the formation yield of A and B was maximum (ca. 5 h), the mixture was cautiously acidified to pH 2 (care being taken to avoid artifactual side reactions), and the products that precipitated were collected by centrifugation and eventually purified by preparative HPLC. Product A, the most abundant (m/z 515.0 $[M+H]^+$, λ_{max} 248, 282, 346, 392 nm), was obtained as an oil

poorly soluble in water and markedly unstable to acids. It displayed three singlets in the aromatic region of the ^1H NMR spectrum at δ 7.05, 7.09 and 7.65, the latter two exhibiting a distinct cross-peak in the $^1\text{H},^1\text{H}$ COSY spectrum, and two sets of resonances (δ 3.39, 3.50 and 4.73 and δ 3.60, 3.64 and 5.09) belonging to two alanyl side chains, in one of which the CH proton was unusually down field shifted. Product B (m/z 515.0 $[\text{M}+\text{H}]^+$, λ_{max} 245, 330, 394 nm) proved highly unstable and could not be further characterized. Based on these data compounds A and B were tentatively formulated as the isomeric dihydroisoquinolines **4** and **5**.

The unfavorable properties of products A and B prevented a more in-depth spectral analysis.

In a mildly acidic medium, both A and B were rapidly converted into more retained species on reverse phase, featuring a pseudomolecular ion peak $[\text{M}+\text{H}]^+$ at m/z 513.0, suggesting that they were oxidized species (**Fig. 44**).

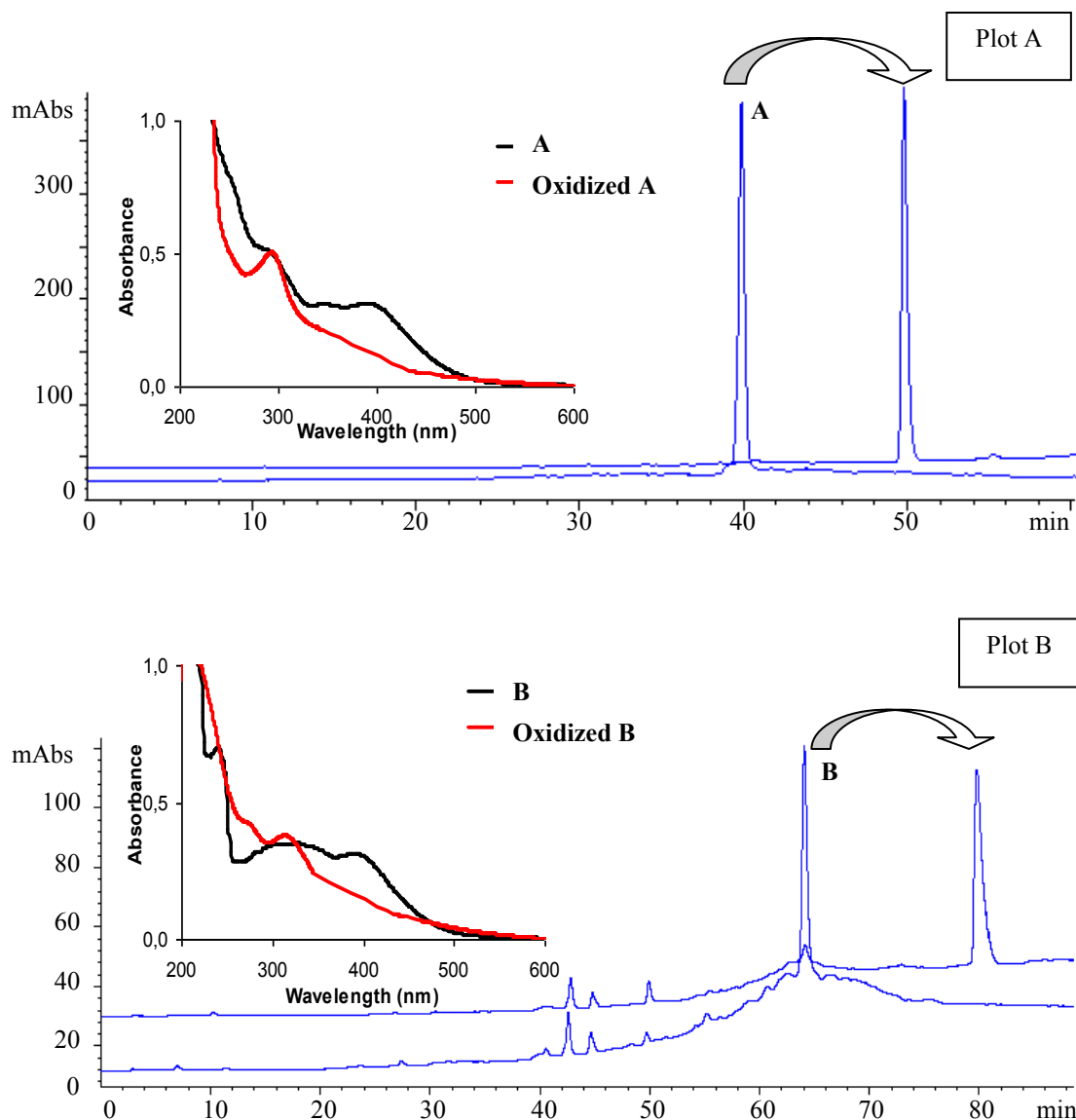


Figure 44. HPLC (detection at 280 nm) traces and UV-vis spectra (HCl 0.1 M) of A (Plot A) and B (Plot B) and their conversion to the oxidized forms, following treatment with acids as described.

Whereas A and B could be reduced to tetrahydroisoquinoline derivatives by treatment with NaBH_4 (Fig. 45), their oxidized forms were fairly stable. Accordingly, a convenient protocol for structural characterization of the oxidized forms was developed, which involved isolation of A and B in pure form followed by quantitative conversion to the oxidized forms.

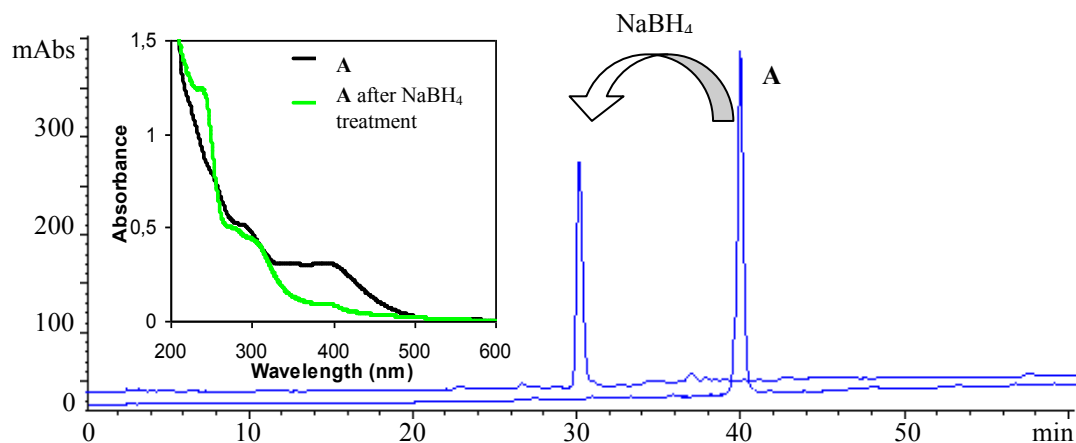
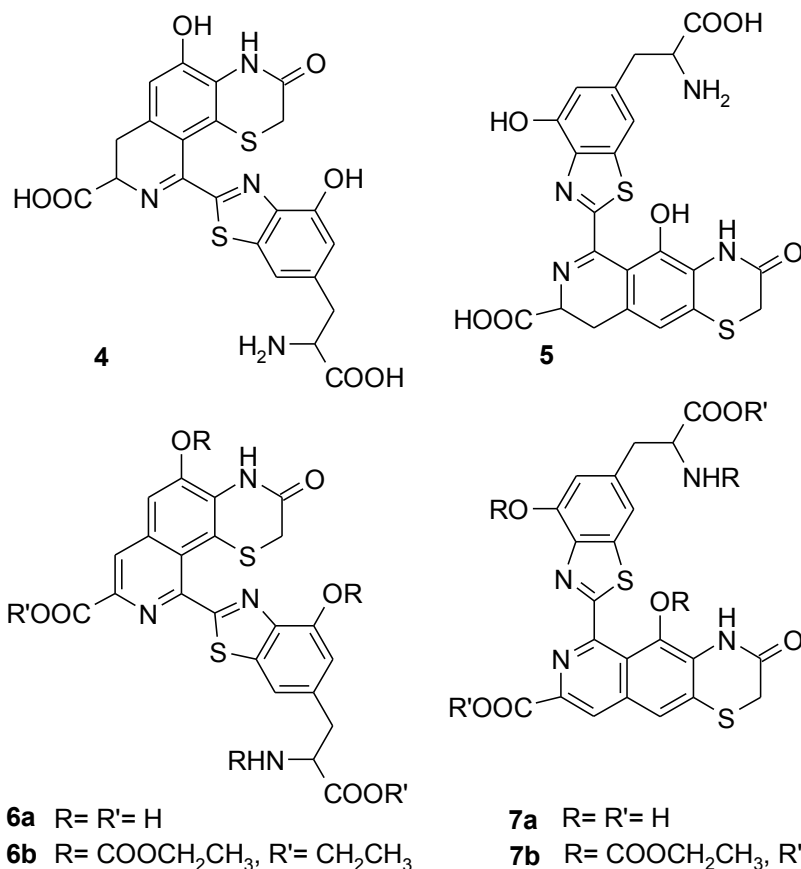


Fig. 45. HPLC (detection at 280 nm) traces and UV-vis spectra (HCl 0.1 M) of compound **A** as such and after reduction with NaBH_4 .

The ^1H NMR spectra of the latter compounds featured four aromatic singlets and the lack of one of the alanyl chains suggesting formation of an isoquinoline ring system as shown in structures **6a** and **7a**. However, also these compounds proved not definitely stable and a derivatization procedure was then considered to allow for a complete structural analysis. After several trials it was found that reaction of the products with ethyl chloroformate in ethanol/pyridine¹⁸¹ by an optimized procedure was the most useful strategy for the purposes of this study, converting **6a** and **7a** into stable derivatives fairly soluble in organic solvents. These latter were purified and subjected to extensive spectral analysis.

The product obtained by oxidation and derivatization of **A** exhibited a pseudomolecular ion peak $[\text{M}+\text{Na}]^+$ at m/z 807 (HR ESI (+)/MS found 807.1629 calcd. for $\text{C}_{35}\text{H}_{36}\text{N}_4\text{O}_{13}\text{S}_2\text{Na}$ 807.1613), indicating a pentasubstituted derivative. Noticeable features of the ^1H NMR spectrum were: a) a 1H singlet resonating at δ 8.54 and showing a one-bond correlation with a carbon signal at δ 125.1 and a ROESY contact with a singlet at δ 7.98, correlating in turn with a carbon at δ 117.1; b) two 1H singlets at δ 7.19 and 7.71, showing cross peaks in the HSQC spectrum with carbon resonances at δ 120.7 and 120.2, respectively. Close scrutiny of the 2D spectra of the compound and comparison of the data with those of compound ODHB following analogous

derivatization with ethyl chloroformate led eventually to formulate the compound as the *N,O*-ethoxycarbonyl-ethyl ester of 10-[6-(2-amino-2-carboxyethyl)-4-hydroxybenzothiazol-2-yl]-8-carboxy-5-hydroxy-3-oxo-3,4-dihydro-2*H*-[1,4]thiazino[5,6-*h*]isoquinoline (**6b**).



The product obtained from oxidation and derivatization of B displayed relatively similar NMR spectra which, in combination with ESI-MS and UV data, allowed straightforward identification as the isomeric *N,O*-ethoxycarbonyl-ethyl ester of 6-[6-(2-amino-2-carboxyethyl)-4-hydroxybenzothiazol-2-yl]-8-carboxy-5-hydroxy-3-oxo-3,4-dihydro-2*H*-[1,4]thiazino[6,5-*g*]isoquinoline (**7b**).

2.6.3. Chemical degradation behavior of isoquinoline derivatives

To assess whether and to what extent isoquinoline derivatives **4** and **5** are representative of structural components in human red hair pheomelanin, and whether they are precursors to TPCA, further experiments were aimed at determining the fragmentation products formed by chemical degradation of these compounds in comparison with BTZCA-dimers, the 3-oxobenzothiazine ODHB, human pheomelanin and synthetic pigment from dopa and cysteine currently used as a standard pheomelanin.¹³⁶ Degradation methodologies included oxidation with KMnO_4 ⁴² or alkaline H_2O_2 ³⁹ and HI treatment,⁷⁶ and the results are summarized in **Table 10**.

Table 10. Yields of degradation products from pheomelanins and related compounds.

Sample	Yield (ng/mg) ^a		
	TPCA	BTCA	4-AHP
Red hair	690	1210	1371
Synthetic			
dopa/cysteine	25950	285500	205000
pheomelanin			
Compound 4	21260	203000	75400

^a Shown are the mean values for three separate experiments with SD \leq 10%

In view of the lower stability and unfavorable solubility properties of **5** most of the degradation reactions were carried out on **4** which was available in sufficient amounts to allow for reliable quantitative analysis. The most relevant finding was that KMnO_4 degradation of **4** leads to a significant yield of TPCA, supporting the conclusion that **4** or related units are the missing precursors of this “orphan” pheomelanin degradation product. TPCA was also obtained by degradation of **5**. A possible artifactual formation of TPCA was ruled out by control experiments in which no trace of the marker was detected from other precursors, including 5SCD, ODHB, or BTZCA-dimers (data not shown). Interestingly, compound **4** gave on degradation all of the pheomelanin markers analyzed in this study, i.e. it could account for the entire pigment degradation profile (**Fig. 46**). Further analysis of data in **Table 10** indicated moreover a higher ratio of formation yield (on a weight basis) of TPCA relative to 4-AHP (an index of

benzothiazine units and a quantitative pigment marker)^{34,76} in the case of human pheomelanin with respect to compound **4** or synthetic pheomelanin. The main conclusion would therefore be that the red hair pigment contains a remarkably high level of isoquinoline units, exceeding that expected if it was made up mainly or exclusively of dimeric constituents related to **4**. It should be noted, in this connection, that formation of 4-AHP from **4** is intriguing since AHP markers are known to arise from benzothiazine but not benzothiazole units.³⁴ It is possible that 4-AHP derives in part from the pyridobenzothiazinone system via a reductive carbon-carbon bond fission as shown in the case of 3-oxobenzothiazine ODHB,³⁴ but this requires verification.

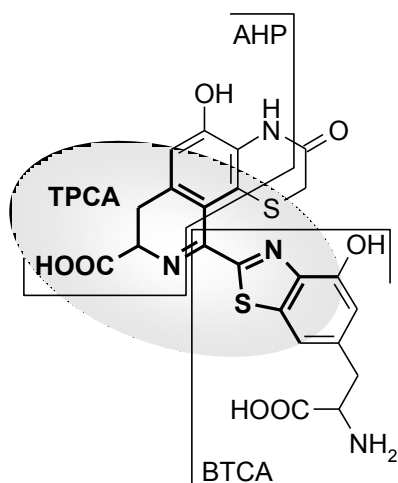


Figure 46. Origin of the main pheomelanin degradation products from fission of the skeleton of compound **4**: shadowed area indicates the structural moiety responsible for TPCA formation.

2.6.4. Absorption properties

Studies of the photochemical and photobiological properties of pheomelanins demonstrated that different molecular components may be involved in the transient absorption, emission and oxygen photoconsumption responses.^{63,64,182} To determine whether dihydroisoquinoline-containing structures may play a role in the photoactivity

of pheomelanin pigments, the absorption properties of purified **4** were briefly investigated in comparison with those of human hair pheomelanin.

The absorption spectrum of **4** (**Fig. 47**) showed a broad band with a shoulder around 310 and 360 nm in neutral buffer, and displayed reversible shifts in acids to 290, 340 and 400 nm, reflecting the superimposition of different chromophores.

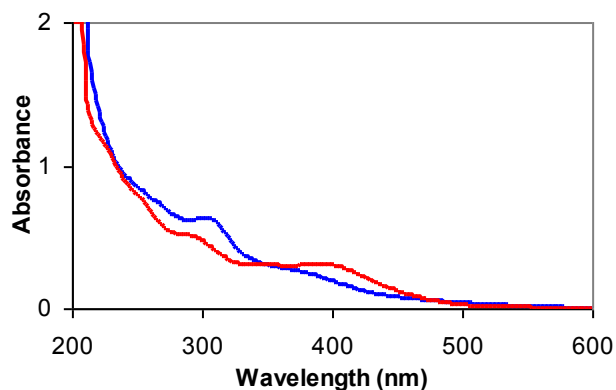


Figure 47. *UV-visible absorption spectra of compound 4 in 0.1 M phosphate buffer, pH 7.4 (blue trace) and 0.1 M HCl (red trace).*

However, the acid-induced band at 400 nm could not be accounted for by either of the benzothiazole moiety (ca. 300 nm with shoulders at 320 nm) (**Fig. 38**) or the 3-oxo-2H-1,4-benzothiazine system (300 nm) alone. Since the spectrum of **4** completely lost the feature at 400 nm upon reduction to the corresponding tetrahydroisoquinoline ($[M+H]^+$, m/z 517.0) with NaBH_4 (**Fig. 45**), it was argued that this band was due to the dihydroisoquinolinethiazinone chromophore.

Interestingly, a similar spectrophotometric behavior was exhibited by red hair pheomelanin, which showed in acids a distinct band around 400 nm (**Fig. 48**, black trace). Considering that this feature does not match with those of any of the known pheomelanin intermediates, including BTZCA, ODHB, BTZCA-dimers and the trichochromes,⁶² it could be speculated that the absorption band at 400 nm in the human pheomelanin spectrum is due at least in part to the contribution of structural units related to **4**.

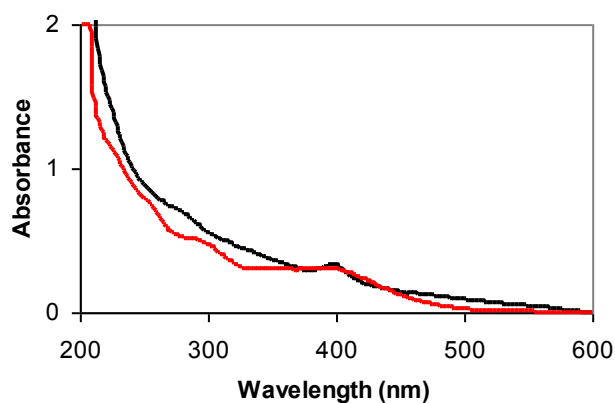


Figure 48. *UV-visible absorption spectra of human red hair pheomelanin (black line) and compound 4 (red line) in 0.1 M HCl.*

2.6.5. Mechanistic issues

The isolation of **4** and **5** raised a number of issues concerning the mechanism of formation of the isoquinoline moiety. In principle, diverse reaction pathways can be envisaged that could lead to the benzothiazole-linked pyridine substructure. For example Minale et al.⁴¹ suggested that TPCA arises from breakdown of partial structure **8** (Fig. 49) which features a tetrahydroisoquinoline moiety, and went on to propose that partial structure **8** is generated via benzothiazine ring contraction causing the C2 carbon to become exocyclic thus providing the necessary requisite for isoquinoline ring closure.

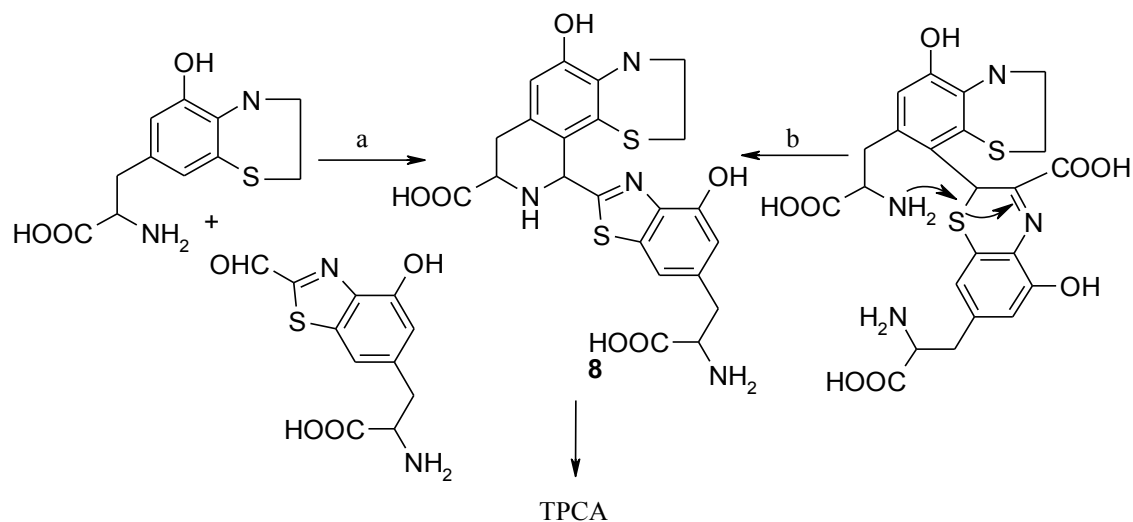


Figure 49. Suggested mechanisms of generation of TPCA from tetrahydroisoquinoline precursor units according to Minale et al.⁴¹

The details of the benzothiazole-forming step are unknown and remain one of the open issues in pheomelanin biosynthesis. According to a classical view, benzothiazine ring contraction results in the generation of an aldehyde group that is then engaged in Pictet-Spengler chemistry with another benzothiazine intermediate (**Fig. 49**, path a). Alternatively, two benzothiazine precursor units could couple at the 2- and 8-positions and then may undergo a transformation by which the benzothiazole and tetrahydroisoquinoline components are formed simultaneously (**Fig. 49**, path b).^{38,41}

Although both options are reasonable, they have never been supported by direct experimental evidence. Moreover, the biomimetic experiments reported in the present study indicated the formation of dihydroisoquinoline compounds, whereas previously suggested mechanisms led to tetrahydroisoquinoline derivatives. Since it is known that oxidation of tetrahydroisoquinoline compounds would not stop at the dihydroisoquinoline stage without further conversion to the fully aromatic derivatives,¹⁸³ the origin of this discrepancy was addressed by studying the reaction of 3-oxobenzothiazine ODHB with commercially available 2-formylbenzothiazole as a model aldehyde compound for Pictet-Spengler chemistry. Under neutral conditions, two main products were formed, that could be isolated and identified as the regioisomeric tetrahydroisoquinoline derivatives **9** and **10** (**Fig. 50**).

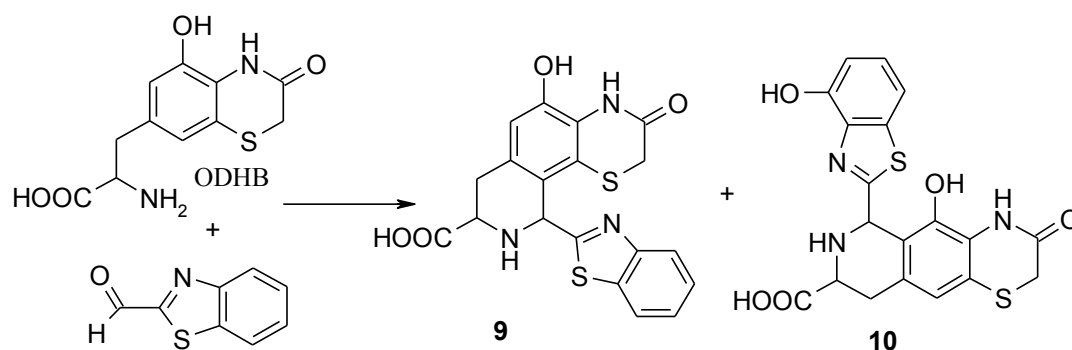


Figure 50. Pictet-Spengler reaction of 3-oxobenzothiazine ODHB with 2-formylbenzothiazole.

Notably, no dihydroisoquinoline or higher oxidation product could be detected. Moreover, attempts to oxidize **9** and **10** by peroxidase/H₂O₂ were defeated, the compounds being remarkably stable. On this basis, it was concluded that **4/5** are unlikely to arise by oxidation of tetrahydroisoquinoline precursors, as suggested by the previous authors.⁴¹ An alternate scheme accounting for the generation of dihydroisoquinoline derivatives was therefore worked out, which is shown in **Figure 51**. In this figure, which illustrates formation of **4**, initial attack of the enamine tautomer of benzothiazine BTZCA to the corresponding quinoneimine would generate a dimer intermediate. Oxidation of the latter would lead to a spirocyclic intermediate which would evolve via a ring-contracting rearrangement to give the dihydroisoquinoline derivative. Formation of the 3-oxobenzothiazine moiety would follow from a water addition-oxidation-decarboxylation sequence occurring during or after the coupling process.

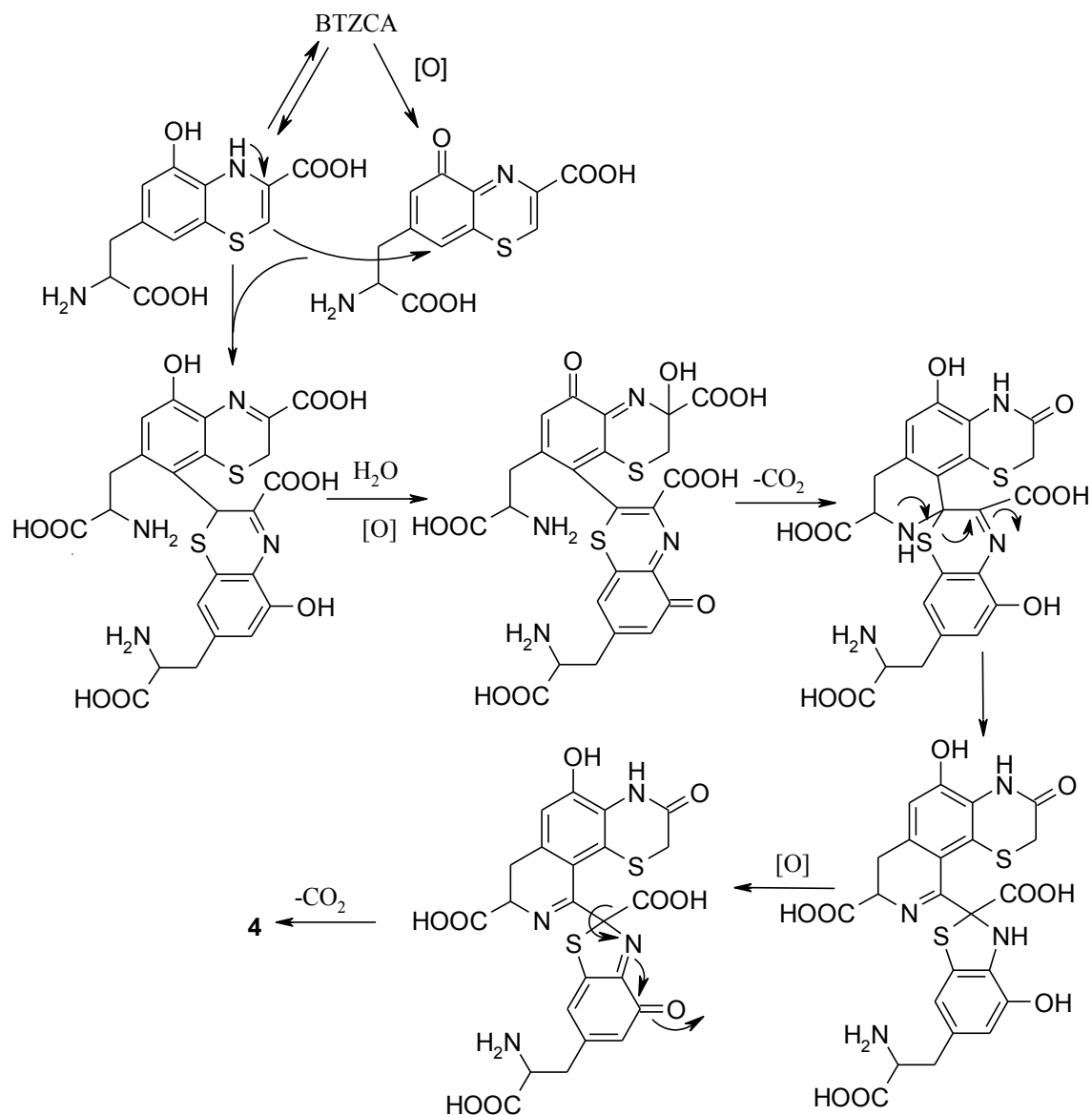


Figure 51. Suggested mechanism of formation of 4.

The reaction sequence in **Figure 51**, though basically similar to the mechanism proposed by the early authors^{38,41} envisages an additional oxidation step preceding the intramolecular attack of the amino group to give the spirocyclic intermediate. This oxidation step is pivotal for production of 4/5 since it would not only facilitate nucleophilic attack by the amino group in the intramolecular cyclization process but would also convincingly explain generation of the isoquinoline system at the dihydro level. Besides providing an explanation to dihydroisoquinoline formation, the proposed scheme is of considerable importance as it offers a most viable mechanism for the origin

of benzothiazole rings during pheomelanin synthesis, and may well account for the consistent proportion of benzothiazole units evidenced in natural pheomelanins, particularly red hair and chicken feathers by degradative analysis.³⁴ This specific issue was recently addressed in detail,^{5,34} but while the formation of benzothiazole moieties was demonstrated as a late event in the process, the possibility that this process is at least in part the outcome of a benzothiazine-coupling step has been so far overlooked and opens entirely new vistas into the process of pheomelanin synthesis *in vivo*. To stretch this speculation further, it may be guessed that similar coupling mechanisms may be extended beyond the dimer level, as previously suggested,⁴¹ thus pointing to dihydroisoquinoline ring closure as a chief benzothiazole-forming mechanism of pigment chain elongation. Moreover the mechanism of coupling of BTZCA as the enamine tautomer to the corresponding quinonimine may actually offer a unifying pathway accounting also for the formation of 2,2'-bibenzothiazine BTZCA-dimers and on further oxidation of trichochromes,³⁷ significant components of pheomelanin tissues.

2.7. Reaction of dihydrolipoic acid with juglone and related naphthoquinones: unmasking of a spirocyclic 1,3-dithiane intermediate en route to naphtho[1,4]dithiepin

As part of this PhD studies on thiol-quinone coupling as a viable biomimetic access to novel bioactive compounds for practical applications in medicinal and food chemistry, the attention was focused on the reaction of dihydrolipoic acid ((*R*)-6,8-dithiooctanoic acid, DHLA) with juglone (5-hydroxy-1,4-naphthoquinone), a characteristic constituent of walnut husks which has received considerable attention as a useful scaffold for the synthesis of bioactive compounds, e.g. antioxidants,¹⁸⁴ cysteine protease inhibitors,¹⁸⁵ and antitubercular¹⁸⁶ and antimelanoma agents.¹⁸⁷ Studies of this chemistry were further prompted by the growing interest in sulfur-substituted naphthoquinones as bioactive compounds.¹⁸⁸⁻¹⁹¹ During this study unexpected mechanistic features of this reaction led to the discovery of a novel class of spirocyclic DHLA derivatives of potential chemical and practical interest. Main outcomes of this investigation were 1) the characterization of the novel reaction products of DHLA with juglone and other naphthoquinones, 2) the expedient isolation of the spirocyclic juglone-DHLA adduct, and 3) the extension of the study to the spirocyclic adduct formed by reaction with a representative 2-substituted naphthoquinone.

2.7.1. Reaction of dihydrolipoic acid with juglone

α -Lipoic acid (LA) possesses a stereocenter at C-6 and the *R*-isomer, which is synthesized naturally, was used in this study. DHLA was prepared fresh before, accordingly a reported procedure.¹⁹² Briefly, to an aqueous solution of LA (0.25 M) in 0.25 M NaHCO₃, NaBH₄ (1.0 M) at -25°C was added. After 2h the mixture was acidified to pH 1 and extracted with toluene. The organic layer was analyzed by NMR. The ¹H NMR spectrum of the extract showed signals only in the region between δ 1.4-

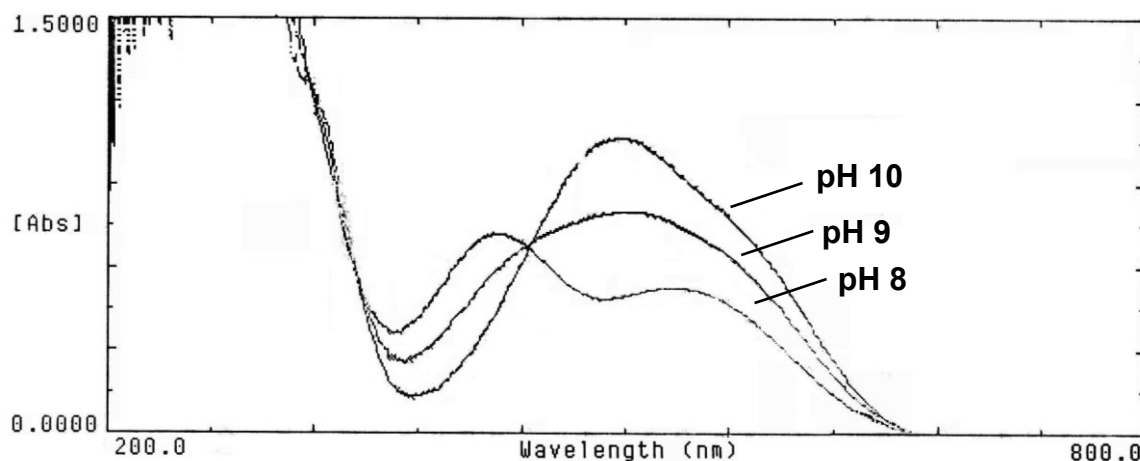


Figure 53. UV-vis spectra of **11a,b** (160 μ M) in 0.1 M phosphate buffer at different pHs.

Upon reduction with NaBH₄ it was changed into a finely structured chromophore (**Fig. 54**), which rapidly recovered the original features by reoxidation in air.

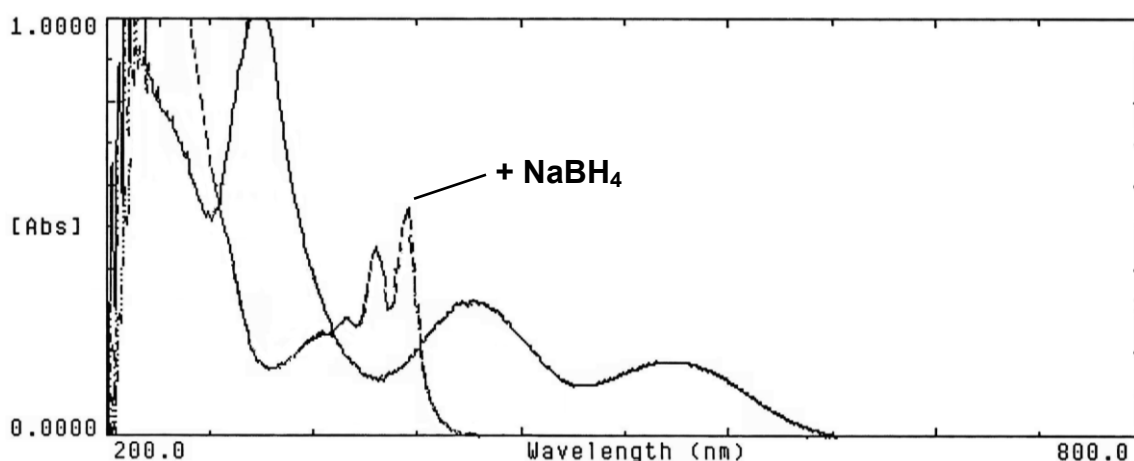


Figure 54. A solution of **11a,b** (6 mg, 15 μ mol) in chloroform (1 mL) was treated with a saturated solution of NaBH₄ in water. After color discharge, the mixture was acidified to pH 1 with HCl 6 M. UV-vis spectra of the organic layer, before and after reduction, were recorded after a 100-fold dilution in EtOH. The chromophore of the reduced species was stable over 15 min.

Formation of regioisomeric **11a,b** by the reaction of DHLA with juglone was of mechanistic interest. Previous studies of the reactions of juglone with thiols (e.g. thioglycolic acid, arylthiols) indicated the 3-position as the most reactive site.¹⁹³⁻¹⁹⁴ This was attributed to electron delocalization from the OH group to the carbonyl group at position 4, decreasing the electrophilic character of the corresponding β position at C-2 and, hence, favoring attack at C-3. On this basis, and assuming a preferential reactivity of DHLA via the less hindered SH group at C-8,^{134,195} isomer **11a** was predicted to be the main product via an initial chemo- and regioselective coupling. Though somewhat disappointing from a synthetic perspective, the unexpected lack of selectivity raised mechanistic issues that prompted further insights into this reaction. An explanation for this inconsistent result came eventually from careful HPLC analysis of the reaction course under higher dilution conditions. Kinetic monitoring showed the initial formation of a species (λ_{max} 356 nm) that gradually decayed concomitant to formation of the purple adducts. Initial attempts to isolate this unstable intermediate were unsuccessful. However after several trials it was found that conversion of this intermediate to products was blocked by acidification of the reaction mixture. Thus, acid quenching of a preparative scale mixture allowed the isolation of the labile intermediate. NMR spectroscopic analysis of this latter indicated a significant structural difference in the naphthoquinone moiety relative to **11a,b**. In particular, the resonances due to the C-2 and C-3 carbons (δ 145 and 143 in **11a,b**) were apparently replaced by a quaternary carbon signal at δ 53.1, suggestive of a dithioacetal function, and a methylene resonance at δ 50.0 (HSQC cross peak with protons at δ 3.33). A down-field shift of the carbonyl resonances by ca. 10 ppm was also apparent, indicating loss of the conjugated double bond. Moreover, the proton signals at δ 3.33 showed long-range correlations with the quaternary carbon resonances at δ 133.6 and 53.1, as well as with the carbonyl signals (δ 191 and 196). Likewise, correlations were apparent between one of the C-8 protons of the lipoic acid unit (δ 2.8) and the carbon signal at δ 53.1.

Based on these extensive 2D-NMR data, the compound was identified as the spirocyclic 1,3-dithiane derivative **11c**. Inspection of the proton and carbon spectrum revealed that most signals were present as a close pair, indicating that the compound was in fact a mixture of two diastereoisomers that differed in the configuration of the spirocenter, and could not be separated under a variety of chromatographic conditions. Exposure of **11c**

to TEA in ethanol or to phosphate buffer, pH 7.4, resulted in quantitative conversion to an equimolar mixture of **11a,b**, confirming its intermediacy in the route to naphthodithiepines.

On this basis, a plausible reaction mechanism for the reaction of DHLA with juglone can be proposed (**Fig. 55**).

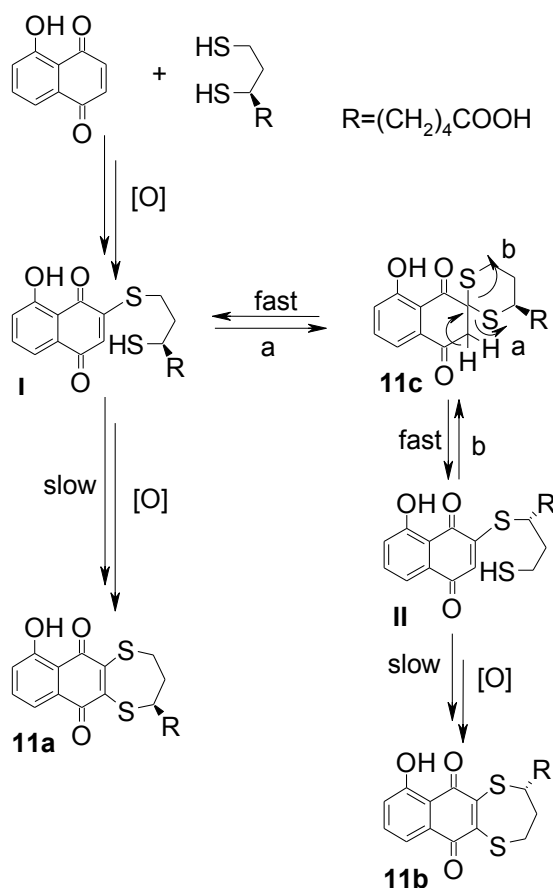


Figure 55. Proposed mechanism of reaction of juglone with DHLA.

In this figure, selective addition of DHLA via the SH group at C-8 to the 3-position of juglone leads to adduct **I** which then evolves via a fast intramolecular cyclization to give the spirocyclic 1,3-dithiane **11c**. This latter would be engaged in fast equilibria with the starting adduct **I** and the isomer **II**. Generation of products **11a,b** would then be the final outcome of slow, irreversible cyclization/oxidation processes from the ring-opened adducts **I** and **II**. The equimolar formation of **11a,b** is therefore the signature of the spirocyclic compound **11c** which partitions equally between the ring opening routes *a*

and *b*. Kinetic analysis of the reaction course (**Fig. 56**) demonstrates indeed the fast accumulation of **1c** and its slow decay concomitant to product formation.

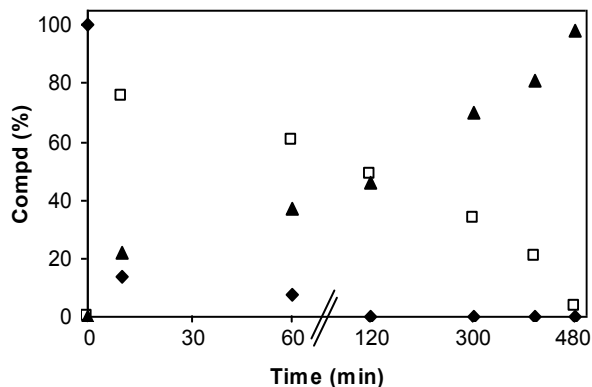
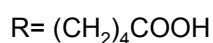
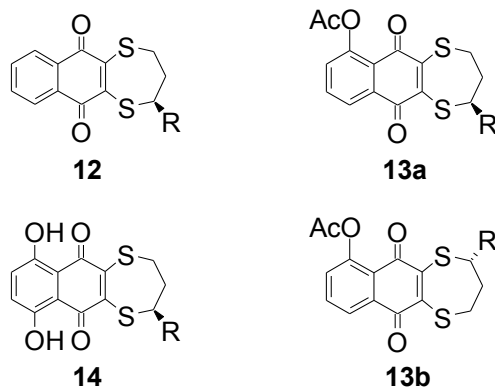


Figure 56. Kinetic profile of juglone decay (starting concn 0.5 mM) and product formation with DHLA; \blacklozenge : juglone, \square : **11c**, \blacktriangle : **11a,b**.

The reversible formation of the spirocyclic adduct raised the issue of what factors orient the initial ring closing attack of SH toward the *S*-substituted 3-position instead of the adjacent unsubstituted 2-position of **I**.

2.7.2. Reaction of dihydrolipoic acid with 1,4-naphthoquinones

To address the last issue, the reactions of DHLA with the parent 1,4-naphthoquinone, acetylated juglone and naphthazarin (5,8-dihydroxy-1,4-naphthoquinone) were investigated. In all cases the corresponding naphtho[1,4]dithiepinines **12-14** were obtained in 25-44% isolated yields.



For these reactions, the mass balance was accounted for by side products, possibly ring-opened diadducts and polymeric species that were not investigated further. Notably, all attempts to identify or isolate the first formed adducts of the type **I** met with failure, on account of their marked tendency to cyclize or react further via the free SH group.

The generation of an equimolar mixture of regioisomers from acetylated juglone supported operation of the spirocyclic mechanism which, however, could not be demonstrated despite several efforts. Nonetheless, the failure to isolate spirocyclic dithiane precursors to **12-14** under various concentration, pH and temperature conditions does not rule out their transient generation in the mixtures. On this basis, it can be argued that the observed accumulation of the spirocyclic intermediate in the case of juglone reflects specifically remote electronic control exerted by the OH substituent disfavoring fast attack at C-2.

To address in more detail the generation and fate of spirocyclic dithianes, subsequent experiments were directed to investigate the reaction of DHLA with menadione (2-methyl-1,4-naphthoquinone). Product analysis showed the formation of the *S,S'*-bisnaphthoquinone adduct **15a** (16%) and of a spirocyclic 1,3-dithiane intermediate which was isolated and identified as **15b**. For this latter product the presence of the spirodithiane ring at the 3-position of the menadione unit was deduced from distinct correlations of both the methyl protons at δ 1.5 and one of the C-8 protons of the lipoic acid unit (δ 2.77) with the dithioketal carbon resonating at δ 60 in the HMBC spectrum. Also in this case, most of the proton and carbon signals appeared as a couple, suggesting that this product, too, was a mixture of diastereoisomers. Thus, the presence of the methyl group on the 2-position inhibits formation of stable seven-membered

intramolecular cyclization products, by preventing the irreversible oxidation step leading to the thermodynamic stable 1,4-naphthoquinone system. The ring-opened isomeric adducts deriving from the spiro compound can then evolve only by coupling of the SH group with a second molecule of quinone to give **15a** (Fig. 57).

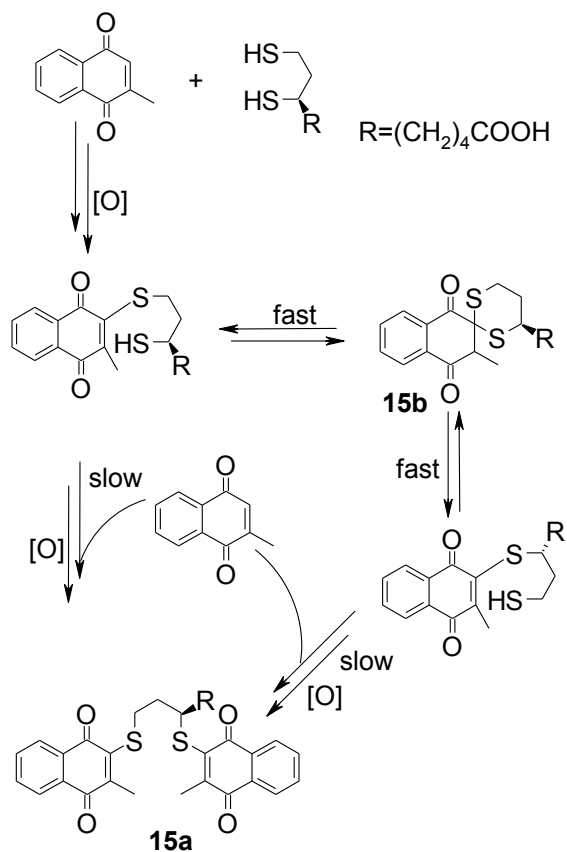


Figure 57. Proposed mechanism of reaction of menadione with DHLA.

The reaction behavior of the spirocyclic intermediates described herein is worthy of further attention. 1,3-Dithianes are valuable synthetic tools and have been employed in rearrangement reactions leading to ring expanded derivatives, but these reactions proceed usually in poor yields under conditions of acid or metal catalysis.¹⁹⁶⁻¹⁹⁹ No report is available of fast, efficient and mild, base-induced conversion of 1,3-dithianes to 1,4-dithiepinines.

2.8. Synthesis and antioxidant activity of new conjugates of dietary polyphenols of plant origin with dihydrolipoic acid

In the field of antioxidants research, recent efforts are direct to the preparation and properties evaluation of thioconjugates of polyphenols from natural sources.

Herein, it is described the set up of an efficient one pot strategy to prepare conjugates of hydroxytyrosol (HTYR), caffeic acid (CA) and piceatannol (PIC) with dihydrolipoic acid (DHLA) from the commercially available parent phenols.

The antioxidant properties of the conjugates were also examined and compared with those of the parent *o*-diphenols. For this purpose it was assessed the ability of the conjugated compounds to act as hydrogen donors by the 2,2-diphenyl-1-picrilidrazile (DPPH)¹¹⁰ assay and their tendency to oxidation, also in comparison with the related *o*-diphenols.

2.8.1. Synthesis of 5-*S*-lipoylhydroxytyrosol

To synthesize the conjugate of HTYR with DHLA, prepared as described (paragraph 2.7.1), a strategy was adopted, that involved the generation of the *ortho*-quinone of HTYR from the related phenol, tyrosol, followed by in situ addition of DHLA. Regioselective hydroxylation of tyrosol was achieved by use of 2-iodoxybenzoic acid (IBX)²⁰⁰ affording the *ortho*-quinone of HTYR. The reaction mechanism, shown in **Figure 58**, envisages the initial reaction of the phenol with IBX with elimination of a molecule of water to form the intermediate *A*, which subsequently rearranges leading to the specie *B*, with oxygenation of the *ortho*-position of the phenolic group. During this process the iodine (V) is reduced to iodine (III). Tautomerization of *B* leads to the intermediate *C*, from which the *o*-quinone and 2-iodobenzoic acid derive, with reduction of iodine (III) to iodine (I).²⁰¹

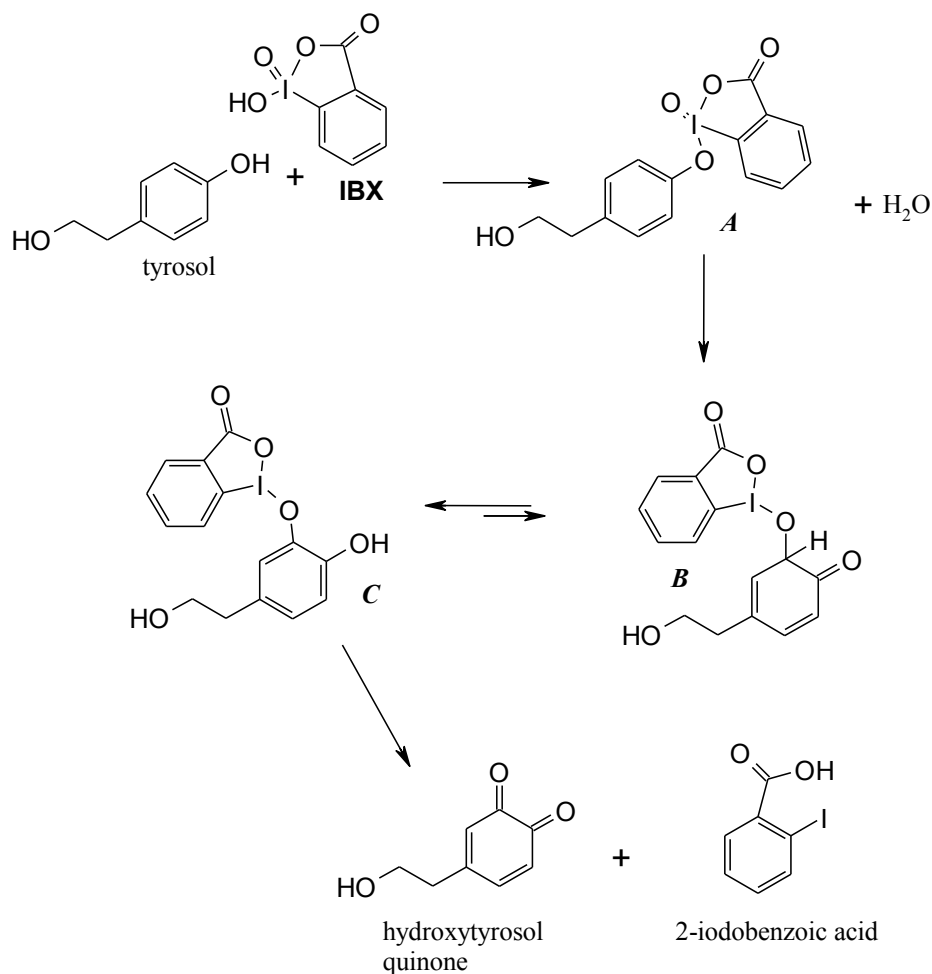


Figure 58. Reaction mechanism of tyrosol oxidation to *o*-quinone by IBX.

In detail, solid IBX (1.5 eq.) was added to a solution of tyrosol (75 mM) in methanol at -25°C , due the high instability of quinones at room temperature. After 1h DHLA (4 eq.) was added, and after 15 min the reaction mixture was treated with an aqueous solution of $\text{Na}_2\text{S}_2\text{O}_5$ and acidified until pH 1.

HPLC/UV analysis of reaction mixture (**Fig. 59**) showed the presence of 2-iodobenzoic acid formed as a by-product of the reaction from IBX (**Fig. 58**) and of a partially resolved component eluting at t_R 20.5 min. The peak at t_R 8.2 min was identified as the HTYR, product of a redox exchange between the *o*-quinone and DHLA, a reaction which competes with the nucleophilic addition of the thiol to the *o*-quinone.

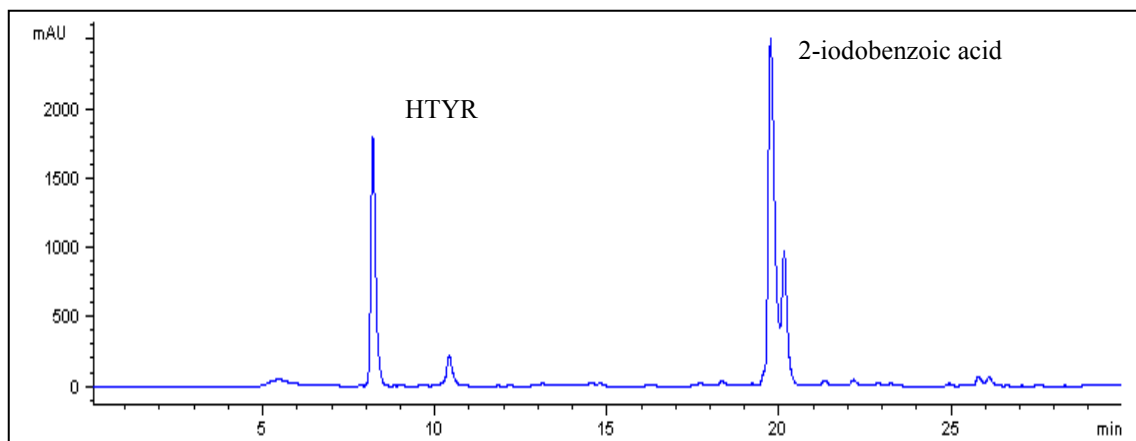


Figure 59. HPLC-UV trace of the reaction mixture of tyrosol with IBX and DHLA.

For product isolation the mixture was extracted with solvents of increasing polarity, toluene, chloroform and ethyl acetate. In particular with toluene 2-iodobenzoic acid and possible traces of unreacted DHLA and lipoic acid were removed, as confirmed by HPLC analysis of the aqueous layer. The product at 20.5 min was extracted with chloroform, while the more polar HTYR remained in solution and could be recovered by ethyl acetate extraction.

The ESI+/MS spectrum of the product exhibited a pseudomolecular ion peak $[M+H]^+$ at m/z 361.1, indicative of the addition of one DHLA unit to one moiety of HTYR. Consistent with this conclusion was the ^1H NMR spectrum in CH_3OD , showing in the aliphatic region resonances typical of DHLA and two triplets at δ 2.65 e 3.67 characteristic of the hydroxyethyl chain of HTYR. On the contrary the protons of the catechol displayed as two doublets at δ 6.63 and 6.72 with a J of 2.0 Hz typical of a meta relation. On this basis, the product was formulated as 5-*S*-lipoylhydroxytyrosol (lipoyl-HTYR) (**Fig. 60**).

The regiochemistry of the addition was similar to that of 4-alkyl *o*-quinones, as for example dopa and dopamine, with cysteine.^{29,136,169,202,203}

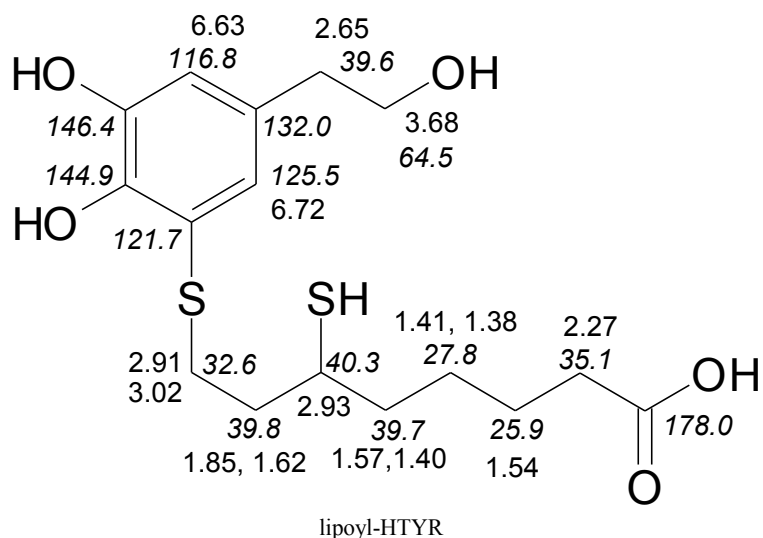


Figure 60. ^1H and ^{13}C NMR resonances of 5-*S*-lipoylhydroxytyrosol.

The product was isolated in 30% yield. The reaction scheme of lipoyl-HTYR preparation is shown in **Figure 61**.

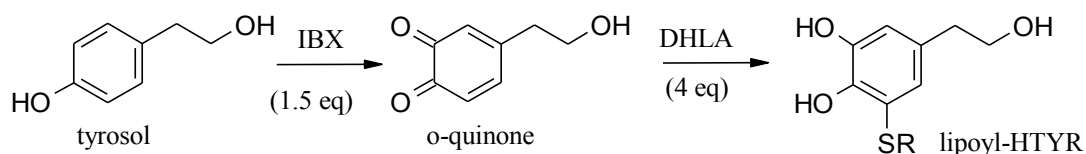


Figure 61. Reaction of tyrosol with IBX and DHLA.

2.8.2. Synthesis of 2-*S*-lipoylcaffeic acid

The conjugation reaction of CA with DHLA was carried out using the same strategy described in the synthesis of lipoyl-HTYR, but with coumaric acid as starting product.

In the early experiments the reaction with IBX was performed at -25°C , but HPLC/UV analysis of the reaction mixture showed a small consumption of the coumaric acid. The reaction was therefore carried out at room temperature. DHLA was added after 7 min, when all the coumaric acid had been converted to *o*-quinone of CA, as evidenced by periodical HPLC analysis.

The HPLC/UV profile of the final reaction mixture (**Fig. 62**) showed the presence of 2-iodobenzoic acid, of CA, resulting from a redox exchange between the *o*-quinone and DHLA, and of a component eluted at t_R 20.8 min.

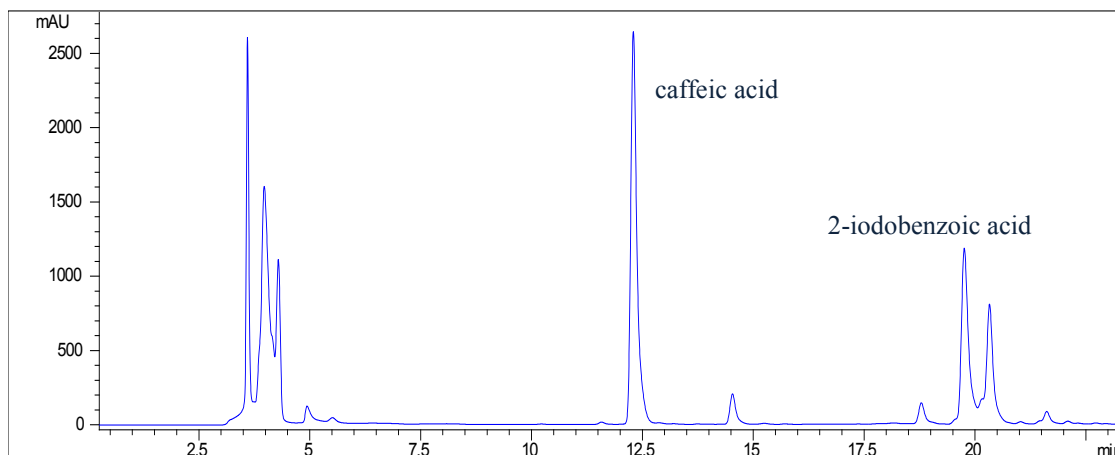


Figure 62. HPLC-UV trace of the reaction mixture of coumaric acid with IBX and DHLA.

To isolate this compound the mixture was extracted with solvent at increasing polarity, a mixture of hexane/ toluene (8:2, vol/vol), chloroform and ethyl acetate. Initially the pure toluene was used to remove 2-iodobenzoic acid and possible traces of unreacted DHLA and lipoic acid, but also the product at t_R 20.8 min was partially extracted, as confirmed by HPLC analysis of the aqueous layer. Consequently, a less polar solvent, as the mixture of hexane/toluene, was chosen. The product at 20.8 min was extracted with chloroform, while the more polar CA remained in solution and could be recovered with ethyl acetate extraction.

The ESI+/MS spectrum of product exhibited pseudomolecular ion peaks $[M+H]^+$ at m/z 387.1, indicative also in this case of the addition of one DHLA unit to one moiety of CA. By ^1H NMR and ^{13}C NMR analysis the product was identified as 2-*S*-lipoylcaffeic acid (lipoyl-CA) (**Fig. 63**).

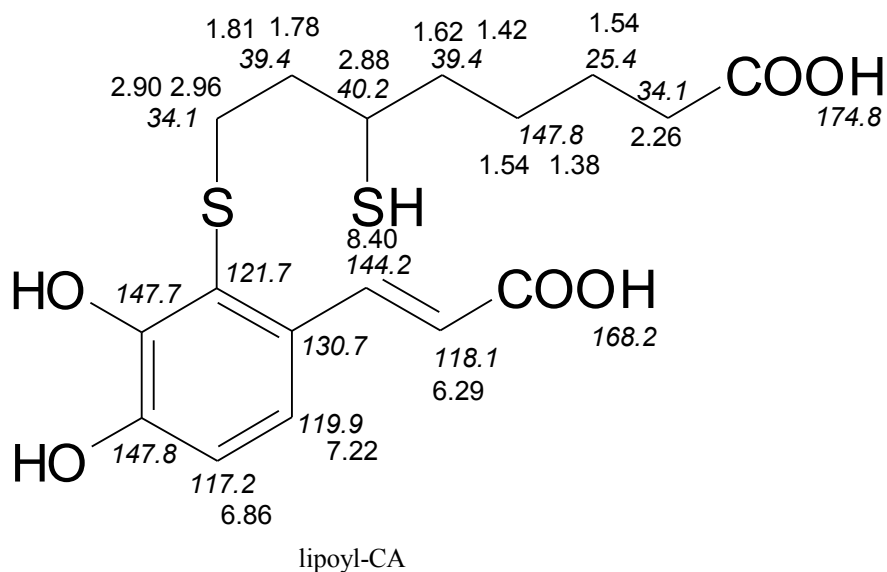


Figure 63. ^1H and ^{13}C NMR resonances of 2-S-lipoylcaffeic acid.

The regiochemistry of the addition was elucidated by ^1H NMR analysis of the catecholic nucleus, displaying two doublets at δ 6.86 and 7.22 with a J of 8.4 Hz typical of a ortho relation.

Indeed the cinnamic acids undergo nucleophilic addition at 2 position because of the conjugation of the propenoate chain with the acyl group.^{171,204-206}

The product was isolated in 44% yield. The reaction scheme of lipoyl-CA preparation is shown in **Figure 64**.

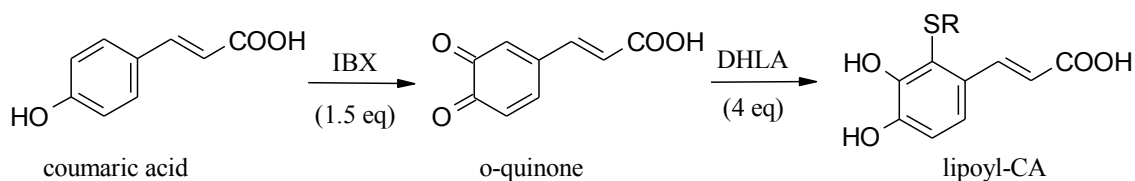


Figure 64. Reaction of coumaric acid with IBX and DHLA.

2.8.3. Synthesis of 5-*S*-lipoylpiceatannol

The conjugation reaction of piceatannol with DHLA was carried out using the same strategy described in the synthesis of lipoyl-HTYR, but with resveratrol as starting product.

The HPLC/UV profile of the final reaction mixture (**Fig. 65**) shown the presence of 2-iodobenzoic acid, of the piceatannol, product of a redox exchange between the *o*-quinone and DHLA, and of a peak at t_R 23.1 min.

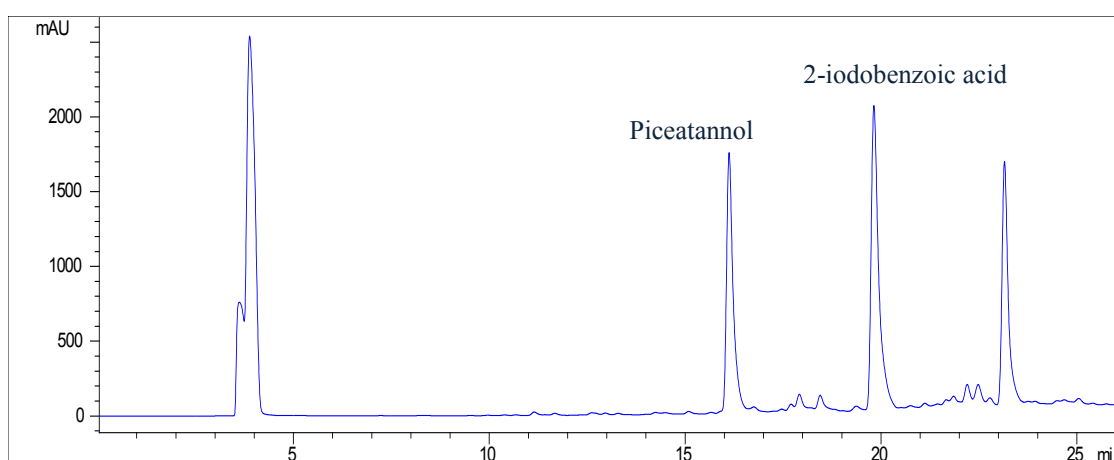


Figure 65. HPLC-UV trace of the reaction mixture of coumaric acid with IBX and DHLA.

The mixture was extracted with solvent at increasing polarity. In particular, 2-iodobenzoic acid and possible traces of unreacted DHLA and lipoic acid were extracted with a mixture of hexane/ toluene (7:3, vol/vol), the product at t_R 23.1 min was extracted with chloroform and, subsequently, the piceatannol with ethyl acetate, as confirmed by HPLC analysis of the aqueous layer, after each extraction.

The ESI+/MS spectrum of product at t_R 23.1 min exhibited a pseudomolecular ion peak $[M+H]^+$ at m/z 451.1, indicative also in this case of the addition of one DHLA unit to one moiety of piceatannol. By ^1H NMR and ^{13}C NMR analysis the product was identified as the 5-*S*-lipoylpiceatannol(lipoyl-PIC) (**Fig. 66**).

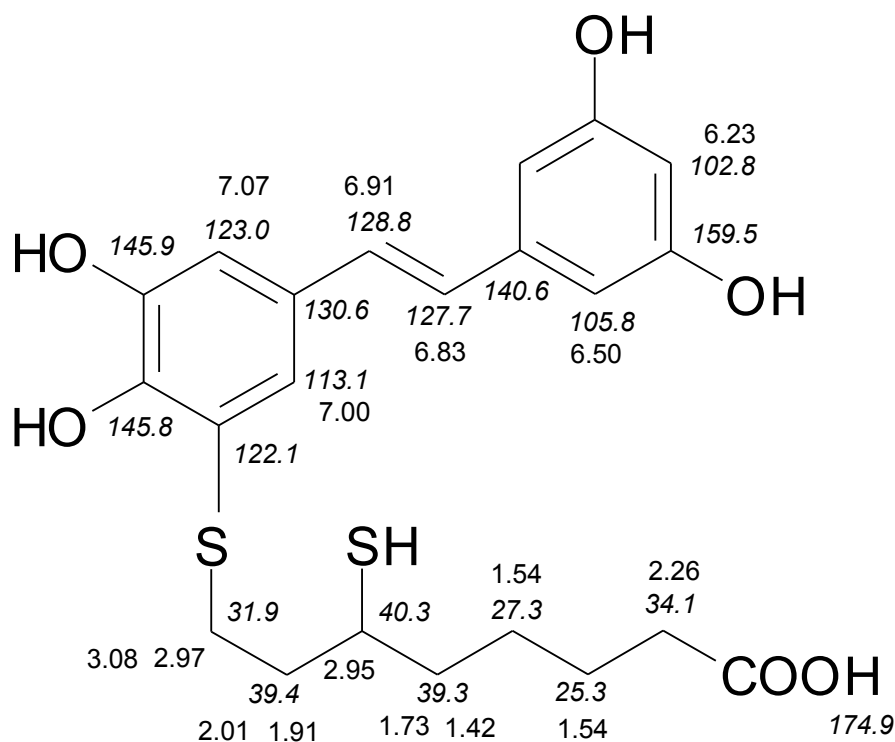


Figure 66. ^1H and ^{13}C NMR resonances of 5-S-lipoylpiceatannol.

Also in this case, the regiochemistry of the addition was elucidated by ^1H NMR analysis of the catechol unit, displaying two doublets at δ 7.00 and 7.07 with a J of 1.7 Hz typical of a meta relation.^{29,136,169,202,203}

The product was isolated in 33% yield. The reaction scheme of lipoyl-PIC preparation is shown in **Figure 67**.

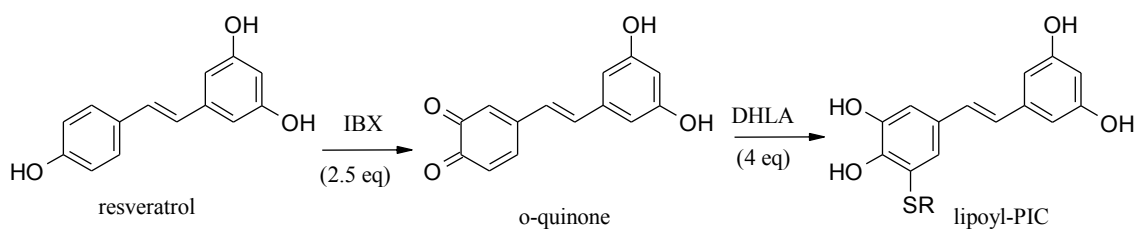


Figure 67. Reaction of resveratrol with IBX and DHLA.

2.8.4. Antioxidant properties of lipoylconjugates

In a further series of experiments the antioxidant properties of lipoyl-HTYR, lipoyl-CA and lipoyl-PIC were tested by the 2,2-diphenyl-1-picrilidrazole (DPPH) assay,¹¹⁰ also in comparison with the related catechols, HTYR, CA and PIC.

DPPH is a stable nitrogen-centered free radical. A quantitative analysis of the H-atom transfer reaction from a given phenol to DPPH provides a very simple and straightforward way to characterize the phenol by a set of parameters (*i.e.*, rate constants and stoichiometry) tightly related to its intrinsic antioxidant activity. The H-transfer reactions are monitored by UV/VIS spectroscopy by recording the decay of the DPPH visible absorption band ($\lambda_{\text{max}}=515$ nm in MeOH) that reflects the conversion of the DPPH radical into the corresponding colorless hydrazine by the antioxidant (**Fig. 68**).^{110,207}

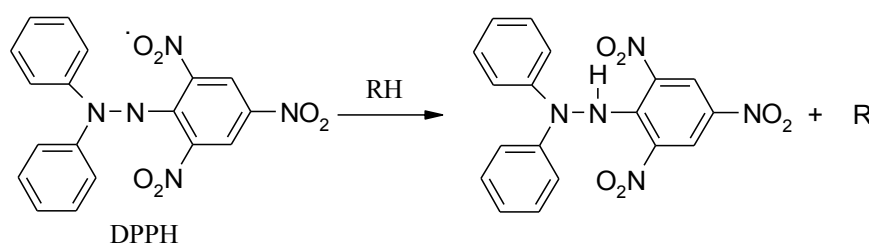


Figure 68. Reaction of DPPH with a generical H-transfer compound.

The experiments were run at a DPPH/antioxidant molar ratio of 4:1, in order to exhaust the H-donating ability of the antioxidant. With potent antioxidants, the visible absorbance quickly decays over 1–3 min as a result of the transfer of the most labile H-atoms of the antioxidant (fast step). This step may be followed by a much slower decrease of the visible absorbance featuring the residual H-donating ability of the antioxidant (slow step). All the experiment were extended over 20 min, monitoring the absorbance decay of DPPH every 5 sec.

The absorbance decays monitored for the three lipoyl-conjugates and related catechols are shown in **Figure 69**.

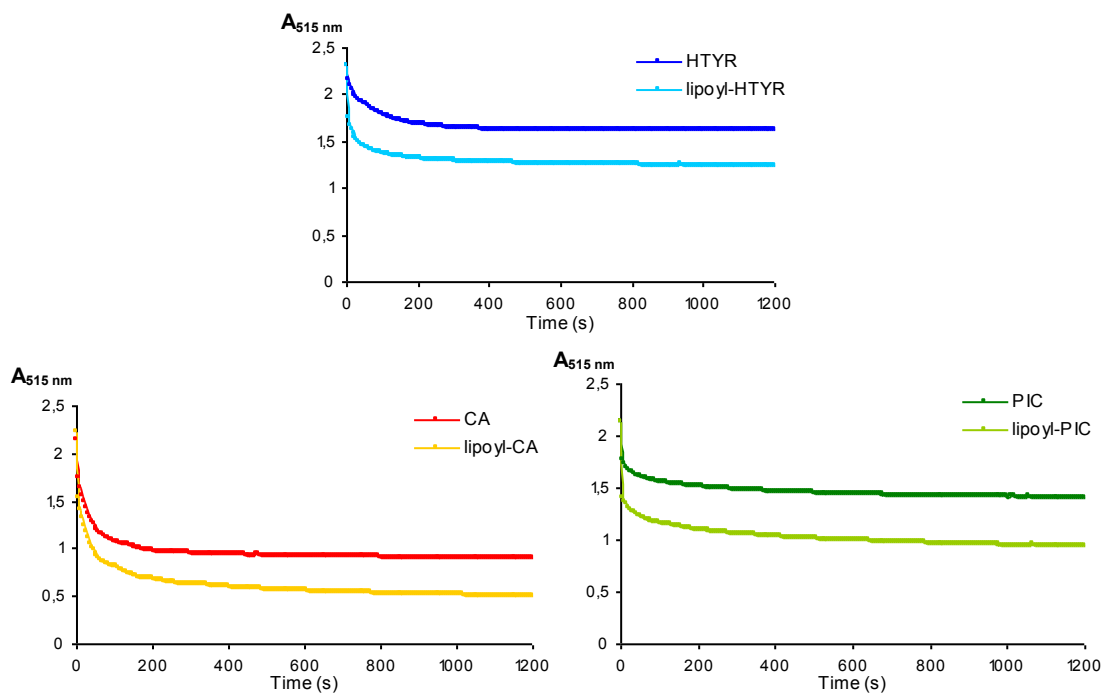


Figure 69. Decay of the visible absorbance (515 nm) of a DPPH solution in MeOH (0.2 mM) following addition of the antioxidant catechol (final concentration 50 μM).

In all the cases the lipoylconjugates produced a higher decay of DPPH absorbance (after 20 min) than the parent catechols.

Furthermore, each reaction was kinetically analyzed, accordingly a reported method.²⁰⁷

Experiments extending over 20 min were used for the determination of the total stoichiometry (n_{tot}) of the antioxidant using the equation 1 (A_f , final visible absorbance; A_0 , initial absorbance; c , initial antioxidant concentration; ϵ , DPPH molar absorption coefficient, $11240 \text{ M}^{-1}\text{cm}^{-1}$).

$$(1) \quad n_{\text{tot}} = A_0 - A_f / \epsilon c$$

The equation 2 gives the percentage of DPPH inhibition.

$$(2) \quad \text{DPPH inhibition (\%)} = A_f / A_0 \%$$

The kinetic model used for analyzing the H-atom-transfer reaction during the fast step does not afford hypothesis about the mechanism of antioxidant degradation.²⁰⁷ An antioxidant of stoichiometry n is simply regarded as n independent antioxidant subunits, AH, which all transfer a single H atom to DPPH with the same second-order rate constant k . The initial rate (R_0) of DPPH consumption may be written as (c_0 , initial DPPH concentration):

$$(3) \quad R_0 = kncc_0 = k_1cc_0$$

assuming that

$$(4) \quad k = k_1/n$$

where k_1 is the rate constant for the first H atom abstraction from the antioxidant.

The curve-fittings using this model were carried out with n and k_1 as the floating parameters, since k_1 allows a more straightforward comparison between antioxidants than k . The estimation of n and k_1 can be carried out simply: n can be estimated by using eq 1, with A_f now standing for the visible absorbance at the end of the fast step. On the other hand, eq 2 has to be integrated to yield eq 5.

$$(5) \quad \ln\{(1 - A_f/A)/(1 - A_f/A_0)\} = -\{k_1c/(A_0/A_f - 1)\}$$

Plotting eq 5 as function of time, a straight line with zero intercept is obtained over most of the duration of the fast step. The slope of the line with higher value of R^2 readily gives access to k_1 .

The results of the test obtained for the compounds under investigation are reported in **Table 11**.

Table 11. H-atom transfer reactions from catechols, lipoylconjugates and DHLA to DPPH.

	Δt (s)	k_1	n	k	n_{TOT}	DPPH inhibition % (50 s)
HTYR	40	266.10	0.67	400.12	1.20	17.3
Lipoyl-HTYR	30	746.24	1.43	520.77	1.88	37.0
CA	35	673.54	1.43	470.04	2.18	42.5
Lipoyl-CA	30	1024.30	1.82	562.93	2.90	55.6
PIC	50	492.30	0.93	526.34	1.29	24.7
Lipoyl-PIC	50	954.8	1.61	591.87	2.13	42.5
DHLA*	35	168.48	0.50	337.09	1.03	15.4

Shown are the mean values for three separate experiments with $SD \leq 5\%$

* DHLA concentration is $0.25 \mu M$.

It must be noted that the duration of the fast step, and consequently the n value, displays a somewhat arbitrary character since the visible absorbance typically keeps decaying over much longer periods, although much more slowly. Indeed, the duration of the fast step is determined by visual appreciation. Typically most of the H-donating activity of the tested compounds is dissipated within 50 s.

The reported $\Delta t(s)$ is the time when the H-atom transfer reaction relative to the fast step is completed, as evaluated by deviation from linearity of eq 5, and it is always less than 50 s. Consequently, DPPH inhibition % was calculated at 50 s. These data are independent on the number of H, that each compound can transfer and so allow a direct comparison among the tested compounds.

In each case the conjugation with DHLA enhanced the DPPH inhibition, in particular for HTYR. The lipoylconjugates showed also an higher value of k_1 , similarly for the three couple of compounds. Moreover, the lipoylconjugates displayed values of k, n_{tot} and n much higher than the parent catechols.

Overall, these data suggested that the conjugation with DHLA lead to an increase of the H-atom transfer tendency.

To assess the contribution to this increase provided by the SH group of the lipoyl-chain, the kinetic parameters of DHLA were also calculated. The experiments were

carried out with a concentration of DHLA ($0.25 \mu\text{M}$) half of that used for the other tested compound, to account for the two SH-groups.

Data in **Table 11** indicate that n and n_{tot} values are those expected on the basis of the stoichiometry of the DHLA. On the other hand, no indication can be derived from the simple sum of the rate of catechol and DHLA, since the relevant kinetic data and in particular k_1 do not refer to the total stoichiometry of H.

However, the conjugation with DHLA enhanced the H-donating activity of the catechols, not just for the presence of an additional H.

In a second series of experiments the antioxidant properties of the lipoylconjugates were tested by aerial oxidation of an equimolar mixture $500 \mu\text{M}$ of the couples lipoyl-HTYR/HTYR, lipoyl-CA/CA and lipoyl-PIC/PIC in phosphate buffer 0.1 M at pH 7.4 under vigorous stirring. The decay of the compounds was monitored by periodical HPLC/UV analysis.

In **Figure 70** the decay of each couple of compounds is reported at a reaction time of 30 min .

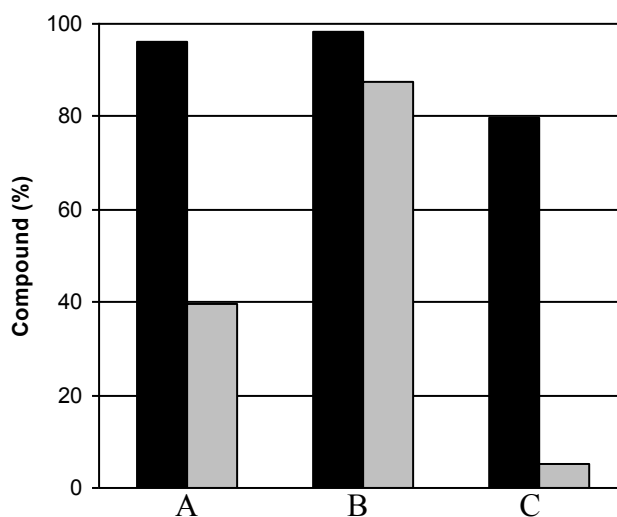


Figure 70. Lipoylconjugates (grey bars) and parent catechols (black bars) decay (starting concn 0.5 mM) in the aerial oxidation reaction after 30 min (A: HTYR/lipoyl-HTYR; B: CA/lipoyl-CA; C: PIC/lipoyl-PIC).

In all the three cases the lipoylconjugates decayed much faster than the parent catechols. Significant differences in the oxidation reaction were observed for lipoyl-HTYR and lipoyl-PIC, while lipoyl-CA decay was similar to CA. The conjugation with DHLA seemed to enhance the oxidability of PIC, more than in the case of CA. However, even in the latter case a decay of 50% for lipoyl-CA was observed after 3 h, when the decay of CA was not remarkable.

3. Conclusions

The unsolved questions in the studies of pheomelanins, the pigment of red hair, were recently summarized in a paper by Simon, et al. “*Current challenges in understanding melanogenesis: bridging chemistry, biological control, morphology, and function*”.⁵

Herein, a short excerpt is reported:

“...several important and challenging issues remain to be resolved. First consider the nature of postpolymerization modifications of eumelanin and pheomelanin. Two recent studies (Greco et al., 2009; Wakamatsu et al., 2009) have addressed the issue of post-polymerization modification of pheomelanin and have made much progress...

There are also important issues around the structure of pheomelanin itself and its post-polymerization modifications. It should be mentioned that we have not unambiguously established how the isoquinoline moiety is produced in the late stages of pheomelanogenesis. Pyridine-2,3,4,6-tetracarboxylic acid serves to indicate the participation of isoquinoline units in pheomelanin structure (Fattorusso et al., 1969). Unfortunately, this useful degradation product has not been studied since this original work. When we consider the possibility that the isoquinoline moiety may be of equal importance to the benzothiazine and benzothiazole species in defining the molecular structure of pheomelanin, the lack of information on the content (or even the presence) of isoquinoline moiety is a serious drawback.

Another issue that remains unsolved in the post-polymerization modifications is how the benzothiazine moiety is converted to the benzothiazole moiety... It is clear that the biological functions of melanin pigments are closely related to their structural features. In this review, we have shown how the process of mixed melanogenesis can be interpreted in terms of chemistry. However, several important issues remain to be solved through multi-disciplinary approaches. One of those important unsolved problems is the precise biochemical mechanism of switching between eumelanogenesis and pheomelanogenesis in vivo, which appears to depend not only on tyrosinase activity but also on the availability of cysteine (or cystine) in melanosomes... Finally, the assembly of the pigment within the intact melanosome remains unknown. Our insight into this important issue is likely to remain at a very qualitative level until there is a better understanding of the molecular structures of melanins.”

Most of these issues, underlined in the above text, have been addressed in this research work. Investigation on human red hair has shown that post-polymerization modification of pheomelanin do occur during hair growth probably as a consequence of oxidative processes related in part to sun exposure. Indeed the pigment derived from oxidative polymerization of cysteinyldopa isomers, namely 5SCD and 2SCD, suffers extensive

degradation during hair growth affecting mainly the 5SCD-derived components, whereas the 2SCD-derived units remain largely unaltered.

Moreover, a proof-of-concept investigation of a chemical mimic of the natural casing model of mixed melanogenesis has been disclosed. The new system relies on the hitherto unrecognized redox cycling properties of pheomelanin-like polymers, which can accelerate the aerial polymerization of catecholamines to give eumelanin-like deposits that encapsulate the pheomelanin core and gradually quench the redox centers. This model suggested that assembly of the pigments within the intact melanosomes is a process not dependent on external factor, as enzymes, but rather related to the intrinsic redox properties of the eumelanins and pheomelanins.

Related model studies carried out with synthetic pigments led to development of a pheomelanin casing model, according to which the pigment of red hair consists of a 2SCD-derived units core associated to a 5SCD-derived units surface, that turns out to be more exposed to air and sunlight and so more easily degradable, as observed during hair growth.

An improved analytical methodology of the oxidative degradation mixture of natural and synthetic pheomelanins led to identification of benzothiazole isomers BTCA and 2-BTCA which resulted predictive markers of skin cancer and melanoma. An efficient access to BTCA and 2-BTCA, as well as the decarboxy-derivates was developed. The proposed route is efficient, applicable up to hundreds milligram scale, environmentally benign (use of organic solvents or toxic reagents is avoided), and attractive for routine preparation of standard samples. The procedure which involves sequential oxidation and, where appropriate, decarboxylation steps in a single pot and including only a final purification step, avoids time-consuming isolation of intermediates, including labile benzothiazines, with significantly decreased operation costs

An extension of this study concerns the identification by ZIC-HILIC coupled with PDA detection of BTCA markers into urine in melanoma patients with diffuse melanosis but not in other melanoma patients or healthy subjects. This finding provides for the first time straightforward evidence that benzothiazoles are indeed intermediate pheomelanin metabolites. Formation of BTCA isomers seems to be associated with advanced stage of melanoma and might be the result of a chronic oxidative stress condition or due to an increased enzymatic process associated with melanocyte activity. Identification of free

BTCA isomers in urine provides a significant contribution in the field of urinary melanogens, with implications for biosynthetic activity of normal and pathologic melanocytes.

As part of studies aimed at defining the molecular bases of the photosensitizing and photocarcinogenesis properties of pheomelanins, the occurrence of isoquinoline moieties in human pheomelanin and their origin was demonstrated providing unambiguous experimental evidence to the long postulated isoquinoline cyclization pathway in cysteinyl-dopa oxidation. More specifically, the isolation of unprecedented dihydroisoquinoline-containing products from the biomimetic oxidation of 5SCD was achieved and a new mechanism for benzothiazole formation via benzothiazine ring contraction in the pigment pathway was proposed, also based on the results obtained with model compounds. Isoquinoline-derived pyridine fragments were identified by oxidative degradation of human red hair pheomelanin and synthetic pigments. In addition a remarkable matching of the chemical degradation products of the novel dihydroisoquinoline-containing intermediates with the entire pattern of diagnostic pheomelanin markers was observed.

The novel dihydroisoquinoline substructures showed absorption features closely similar to those of natural pheomelanin. Considering that this feature does not match with those of any of the known pheomelanin intermediates, it could be speculated that the characteristic absorption band at 400 nm in the human pheomelanin spectrum is due at least in part to the contribution of dihydroisoquinoline structural units.

Although caution should be exercised in applying the results from model reactions for interpreting the behavior of natural systems, the results presented would point to the diversity of structural motifs as emerging from the model synthetic studies as a basis to interpret the chemical and photobiological properties of natural pigments, supporting the value of the integrated approach described as a unique investigative tool.

Well framed in the general context of the PhD research work on conjugates of phenolic system with thiol compounds, the reaction of DHLA with representative 2,3-unsubstituted 1,4-naphthoquinones was explored uncovering an attractive, chemically robust novel heterocyclic system of potential practical interest. Besides the novel naphtho[1,4]dithiepine derivatives, a significant outcome of this study is the identification and chemical investigation of labile spirocyclic 1,3-dithiane derivatives of

DHLA. This is the first example of base-induced ring expansion of 1,3-dithianes to 1,4-dithiepies under mild conditions.

Furthermore, a straightforward synthetic access to new lipophilic antioxidants derived from conjugation of DHLA with naturally occurring polyphenols, such as hydroxytyrosol, caffeic acid and piceatannol, was developed. The synthetic route presented is based on one-pot hydroxylation and oxidation of the parent commercially available phenols to the *o*-quinones, followed by in situ coupling with DHLA. The lipoylconjugates were purified with simple extraction procedure in good yields (30-45%). They showed higher antioxidant power than the parent catechol, as evidenced by the higher H-donating ability and the tendency to oxidation at physiological pHs.

These conjugates are of potential interest as additives for preparation of functional foods.

4. Experimental Section

4.1. General methods

Materials. L-Dopa, L-cysteine, dopamine hydrochloride, L-epinephrine, hydrogen peroxide (30% v/v), zinc sulphate heptahydrate, potassium ferricyanide, potassium permanganate, sodium persulfate, sodium metabisulfite, 57% wt hydriodic acid, 30% wt hypophosphorous acid, sodium borohydride, ethyl chloroformate, benzothiazole-2-carboxaldehyde, 3-nitrotyrosine, 1,4-naphthoquinone, 5-hydroxy-1,4-naphthoquinone (juglone), 5,8-dihydroxy-1,4-naphthoquinone, 2-methyl-1,4-naphthoquinone (menadione), (*R*)-(+)-1,2-dithiolane-3-pentanoic acid (lipoic acid), sodium acetate, acetic anhydride, and triethylamine (TEA), 2-iodobenzoic acid, oxone®, resveratrol, tyrosol, coumaric acid, DPPH, horseradish peroxidase (EC 1.11.1.7), mushroom tyrosinase (EC 1.14.18.1), bovine erythrocytes superoxide dismutase (EC 1.15.1.1), bovine liver catalase (EC 1.11.1.6) were commercially available and were used as obtained.

5-*S*-cysteinyl-dopa (5SCD),¹⁶⁹ 2-*S*-cysteinyl-dopa (2SCD),¹⁷¹ 7-(2-amino-2-carboxyethyl)-5-hydroxy-3,4-dihydro-2*H*-1,4-benzothiazine-3-one (ODHB),²⁰⁸ 7-(2-amino-2-carboxyethyl)-3-carboxy-5-hydroxy-3,4-dihydro-2*H*-1,4-benzothiazine,²⁰⁹ 2,2'-bi[7-(2-amino-2-carboxyethyl)-3-carboxy-5-hydroxy-2*H*-1,4-benzothiazine] (BTZCA-dimers),³⁷ 6-(2-amino-2-carboxyethyl)-2-carboxy-4-hydroxybenzothiazole (BTCA),¹⁴¹ thiazole-2,4,5-tricarboxylic acid (TTCA),⁴⁰ thiazole-4,5-dicarboxylic acid (TDCA),²¹⁰ 4-amino-3-hydroxyphenylalanine (4-AHP)⁷⁶, 5,6-dihydroxyindole-2-carboxylic acid (DHICA),²¹¹ 5-*S*-cysteinyl-dopamine,²¹² pyrrole-2,3,5-tricarboxylic acid (PTCA)²¹³ were obtained as reported.

Synthetic pheomelanins from L-dopa and L-cysteine, 5SCD or 2SCD were prepared by tyrosinase oxidation as reported,¹³⁹ when not differently specified.

Biological samples. Lethal yellow (*A^y/a*) and recessive yellow (*Mcl^r^e/Mcl^r^e*) mice hair samples were those used previously.²¹⁴ Red feathers were obtained from New Hampshire chickens. Red and black hair locks were donated from healthy volunteers.

Informed consent was obtained from all subjects. Only hair samples that had not received dyeing or other chemical treatments were included in the present study.

Natural pheomelanin from red hair and natural eumelanin from black hair were isolated by enzymatic treatment as reported.²¹⁵

Urines from three patients who earlier had been operated for melanoma and had developed melanoma metastases and diffuse melanosis were analyzed. These patients had evidence of gray–blue discoloration of the skin at the time of investigation and their urines were dark colored.

Case 1 was a man who at the age of 25–30 years had several blue nevi surgically removed. At the age of 49 a local recurrence of malignant blue nevus was removed and a control computer tomography showed multiple metastases in the liver, adrenal gland, skeleton and several lymph node metastases in the abdomen. Laboratory investigation showed serum protein S100 to be 16 $\mu\text{g/l}$ (reference interval <0.12 $\mu\text{g/l}$) and lactate dehydrogenase 23 $\mu\text{katal/l}$ (reference interval <0.8 $\mu\text{cat/l}$). A carboplatin-DTIC course was given as well as X-ray treatment to the thoracic metastases. One month later a bluish melanotic coloration of his skin was noted, characteristic of melanosis. After the third carboplatin-DTIC course, the first urinary sample was taken. Three months later his clinical condition worsened. A new urinary sample was obtained, and he died a few days after the last urinary collection.

Case 2 was a man who at the age of 52 had a superficial spreading melanoma (Breslow thickness 0.82 mm, Clark III) removed from his back. Twelve years later the patient had a dark-bluish discoloration of the skin. Computer tomography showed multiple metastases of the liver, spleen and lungs. A liver biopsy confirmed malignant melanoma. Chemotherapy courses with carboplatin-DTIC were Fig. 1. protein was 9.4 $\mu\text{g/l}$ and lactate dehydrogenase was 10.4 $\mu\text{katal/l}$. The urine for pigment analysis was obtained after the third chemotherapy course. He died two months later because of brain metastases.

Case 3 was a patient with melanosis according to initial information obtained. Unfortunately the identity of this patient was obscure so the data from the medical record of the patient could not be reported. The urines obtained from the melanosis patients were very dark colored, melanuric, and had very high concentrations of 5SCD.

Urines from patients with melanoma sent routinely to the laboratory for analysis of 5SCD in urine were used as control samples. The control samples were selected to include 5SCD excretions over a wide range. Their color ranged from normal yellow to moderately colored. As a routine 5SCD concentration was determined for clinical purposes by a method previously described. These urine samples were thus also used for analysis of BTCAs. The clinics of the control samples were evaluated by review of their medical records. At the time urinary samples were sent to us they had metastatic disease from melanoma, which also was obvious from their S100 protein in serum and 5SCD in the urine. None of them had any notes of melanosis.

Urines from healthy persons of different skin phenotypes were collected on voluntary basis. Urine collection: 24-h specimens were collected in plastic bottles containing 35 ml concentrated acetic acid and were aliquoted and stored at $-20\text{ }^{\circ}\text{C}$.

Methods. UV-vis spectra were obtained on a diode array spectrophotometer equipped with a thermostated sample cell holder. ^1H NMR spectra were recorded at 200, 400, 500 or 600 MHz, ^{13}C NMR spectra at 50 or 100 MHz. ^1H , ^1H COSY, ^1H , ^{13}C (DEPT) HSQC, and ^1H , ^{13}C HMBC experiments were run at 400 or 600 MHz, on instruments equipped with a 5 mm ^1H /broadband gradient probe with inverse geometry using standard pulse programs. The HMBC experiments used a 100 ms long-range coupling delay. Chemical shifts are reported in δ values (ppm) downfield from TMS. Signals due to isomeric compounds are reported as δ/δ . IR spectra were obtained on a FT spectrophotometer. HR ESI+/MS spectra were obtained in 0.5% TFA-methanol 1:1 v/v; HR ESI-/MS spectra were obtained in methanol.

Analytical and preparative TLC were carried out on silica gel plates (0.25 and 0.50 mm, respectively) using chloroform/methanol/acetic acid (90:10:1) (eluant I) or cyclohexane/ethyl acetate/acetic acid (70:30:1) (eluant II) as eluants.

HPLC analysis of degradation mixtures. BTCA and 2-BTCA analyses were performed on an HPLC instrument equipped with UV-visible detector, set at 254 and 280 nm. A Synergi Hydro-RP80A column (250 \times 4.60 mm, 4 μm) was used, with 1% formic acid taken to pH 2.8 with sodium hydroxide/methanol 97:3 (v/v) as the eluant, at a flow rate of 0.7 ml/min.³⁹ AHP and AT analyses were performed on an HPLC instrument equipped with an EC detector set at + 500 mV vs an Hg/Hg₂Cl₂ reference electrode. A JASCO Catecholpak column (150 \times 4.60 mm, 7 μm) was used, with 0.1 M sodium

citrate buffer (pH 3.0) containing 1 mM sodium octanesulphonate and 0.1 mM Na₂EDTA/methanol 98:2 (v/v) as the eluant, at 50°C at a flow rate of 0.7 ml/min. TTCA analyses were performed on an HPLC instrument equipped with an UV detector set at 269 nm. A Shiseido Capcell Pak C18 (Type MG) column (250 × 4.60 mm, 5 μm) was used, with 0.1 M potassium phosphate buffer (pH 1.9)/methanol 99:1 (v/v) as the eluant, at 35 °C at a flow rate of 0.7 ml/min.

HILIC analysis with PDA detection. HILIC analysis was performed using an Ultimate 300 HPLC system (Dionex, Germering, Germany). Extracted urine samples were diluted threefold with the mobile phase and 5 μl was injected on a ZIC-HILIC column (length 150 mm, I.D. 2.1 mm particle size 3.5 μm) with a preceding matched guard column from SeQuant (Umeå, Sweden). The mobile phase was acetonitrile: 0.1 M ammonium acetate buffer, pH 5 (82:18, v/v). Chromatography was completed at a flow rate of 0.3 mL/min. Waters photo-diode array detector 996 (Waters, Milford, MA, USA) was set at 210, 250, 285 and 325 nm for acquiring chromatograms; UV spectra and 3D plots were recorded between 190 and 400 nm. Chromatographic evaluation and quantitation at 250 nm was performed with Chromeleon software (Dionex, Germering, Germany).

When it is not specified, the HPLC analysis was carried out on an apparatus equipped with a UV detector set at 254, 280 or 340 nm using a Sphèreclone ODS (5 micron, 4.6 × 250 mm) column, using the eluant in brackets.

Semipreparative HPLC was carried out on an instrument coupled with a UV detector set at 254 or 280 nm using an Econosil C18 (10 micron, 10 × 250 mm) column. Preparative HPLC was carried out on an instrument coupled with a UV detector set at 254 or 280 nm using an Econosil C18 (10 micron, 22 × 250 mm).

LC-MS analysis of pheomelanins. LC-MS analyses of the degradation mixtures of synthetic pheomelanins from 2SCD or 5SCD and pheomelanin isolated from red human hair were performed on an HPLC instrument with an electrospray ionization source in positive ion mode (ESI+) with single ion monitoring (SIM) detection at *m/z* 283. A Synergi Hydro-RP80A column (250 × 4.60 mm, 4 μm) was used, with 1% formic acid taken to pH 2.8 with ammonium hydroxide/methanol 97:3 (v/v) as the eluant, at a flow rate of 0.7 ml/min. (High resolution) mass spectra were registered in ESI+ mode with the cone and the fragmentator voltage set at 4 kV and 80 V, respectively.

SEM analysis of melanin polymers. Morphological analyses of DOPA-melanin, CD-melanin, polymer obtained by CD-melanin oxidation of DOPA (DOPA/CD-melanin 1:1 or 10:1, w/w) were performed using a FEI Quanta 200 FEG environmental scanning electron microscope (ESEM) (Eindhoven, The Netherlands) in low vacuum mode, using a large-field detector (LFD) and an accelerating voltage ranging between 15 and 20 kV. Before the analysis, samples were air-dried at 25°C and 50% relative humidity and mounted on aluminium stubs by means of carbon adhesive disks.

4.2. Isomeric cysteinyl dopas provide a (photo)degradable bulk component and a robust structural element in red human hair pheomelanin

Isolation of 2-BTCA

Synthetic pheomelanin from 2SCD (250 mg) was subjected to degradation in 1 M NaOH (50 ml) containing 1.5% H₂O₂.⁴⁰ After 24 h the mixture was treated with 5% Na₂S₂O₅ (10 ml), acidified to pH 3, and purified by preparative HPLC (eluant: 0.2% trifluoroacetic acid/methanol 8:2 (v/v); flow rate: 40 mL/min; UV: 280 nm) to give pure 2-BTCA (30 mg, > 98% purity estimated by ¹H NMR analysis). High resolution ESI+/MS found 283.0392, calcd for C₁₁H₁₁N₂O₅S 283.0389 [M+H]⁺, UV (0.5 M HCl) λ_{max} 252, 287, 346 nm (log ε 3.89, 3.63, 3.12). NMR spectral data are listed in **Table 1**.

Degradation procedure

Synthetic pheomelanins, finely minced human hair samples taken at various distances from the scalp, mice hairs and chicken feathers were degraded with 1 M NaOH containing 1.5% H₂O₂⁴⁰ or 57% HI/30% H₃PO₂⁷⁶ and were analyzed by HPLC after work up as above or as described, respectively.^{40,76} Hydrolytic treatments were carried out in a rubber cap sealed vial containing the minced hair samples to which a solution of 1 M NaOH that had been prior purged with a flux of argon for at least 20 min was added via a syringe. After 24 h the mixture was worked up as usual.⁴⁰

Oxidation of pheomelanin precursors

A solution of 5SCD or 2SCD or an equimolar mixture of the two isomers at 200 μM in 0.1 M phosphate buffer pH 9.0 was allowed to stand at room temperature under vigorous stirring. The mixtures were periodically analyzed by HPLC/UV (column: Synergi Hydro-RP80A (250 × 4.60 mm, 4 μm); eluant: 1% formic acid pH

2.8/methanol 97:3 (v/v); flow rate: 0.7 ml/min; UV: 254 and 280 nm) and UV spectrophotometry. The pigment was collected after 4, 24 and 72 h by centrifugation at 1300 g for 20 min at 4°C, lyophilized and subjected to degradation as above. Oxidation of L-dopa and L-cysteine by tyrosinase was performed as described¹³⁹ and the mixture was allowed to stand in air under vigorous stirring. Aliquots (750 μ L) of the reaction mixture were periodically withdrawn, subjected to degradation with 4 M NaOH (250 μ L) containing 1.5% H₂O₂ and then analyzed by HPLC.³⁹

Solar exposure experiments

Red hair locks were split in two parts, one of which was exposed to sunlight in June from 10:00 to 19:00, in the southwest of Italy (40°52' N; 14°5' E). The accumulated exposure time for each sample was 135 h. The other part of each lock was stored over the same timespan in the dark.

4.3. A melanin-inspired pro-oxidant system for aerial catechol(amine)-polymerization: implementing a non-enzymatic mimic of the natural casing model

Methods. Analytical HPLC was carried out on an apparatus equipped with a UV detector set at 254 or 280 using a Sphereclone ODS (5 micron, 4.6 × 250 mm) column, and as eluant a solution of 0.5% TFA/methanol (90:10, v/v) at flow rate of 0.8 mL/min. Analytical HPLC of the degradation mixtures was carried out as reported in general methods.

Synthetic pigment preparation. Eumelanin from L-DOPA was prepared by tyrosinase/O₂ oxidation as reported.²¹⁶ Pheomelanins from 5SCD were prepared by peroxidase/H₂O₂ oxidation as previously described.¹⁶³ The polymer from 5SCD-melanin induced oxidation of DOPA (DOPA/5SCD-melanin 10:1, w/w) was prepared according the following procedure. A solution of DOPA (35.0 mg, 0.17 mmol) in 0.1 M phosphate buffer (pH 7.4; 175 mL) in presence of 5SCD-melanin (3.5 mg) was allowed to stand at room temperature under vigorous stirring. After 24 h HPLC analysis of the mixture revealed that residual DOPA was up to 30%. The mixture was then acidified to pH 3, the melanin precipitated was collected by centrifugation (6793 g × min, 4°C, 30 min) and washed with 1% acetic acid (3 × 10 mL). The polymer from 5SCD-melanin induced oxidation of DOPA (DOPA/5SCD-melanin 1:1, w/w) was prepared according the same procedure described above. A solution of DOPA (20.0 mg, 0.10 mmol) in 0.1 M phosphate buffer (pH 7.4; 100 mL) in presence of 5SCD-melanin (20.0 mg) was allowed to stand at room temperature under vigorous stirring. After 24 h HPLC analysis of the mixture revealed no traces of residual DOPA. The mixture was then acidified to pH 3, the melanin precipitated collected as above.

The polymer from 5SCD-melanin induced oxidation of DOPA (DOPA/5SCD-melanin 5:1, w/w) was prepared according the same procedure described above. A solution of DOPA (5.0 mg, 0.025 mmol) in 0.1 M phosphate buffer (pH 7.4; 25 mL) in presence of 5SCD-melanin (1.0 mg) was allowed to stand at room temperature under vigorous stirring. After 24 h HPLC analysis of the mixture revealed no traces of residual DOPA.

The mixture was then acidified to pH 3, the melanin precipitated collected as above and lyophilized (3.0 mg).

5-*S*-cysteinyl-dopamine-melanin was obtained by oxidation of a solution of 5-*S*-cysteinyl-dopamine (27.0 mg, 0.1 mmol) in phosphate buffer (pH 6.8, 10 mL) with horseradish peroxidase (16.7 units/mL final concentration) and 30% v/v hydrogen peroxide (15 μ L). The mixture was allowed to stand at room temperature under vigorous stirring for 2 h and then acidified to pH 5. The melanin precipitated was collected by centrifugation (6793 g \times min, 4°C, 30 min), washed with water (3 \times 10 mL) and then lyophilized.

Catechol(amine) oxidation

A solution of DOPA (10.0 mg, 0.05 mmol) in phosphate buffer (pH 7.4, 50 mL) was allowed to stand at room temperature under vigorous stirring. When required this reaction was carried out in the presence of 5SCD-melanin (2.0 mg) or DOPA-eumelanin (2.0 mg). In other experiments the reaction was repeated in the presence of CD-melanin as above and i) superoxide dismutase (4 U/mL final concentration), or ii) catalase (25 U/mL final concentration), or iii) superoxide dismutase (4 U/mL final concentration) and catalase (25 U/mL final concentration) or iv) under an Ar atmosphere.

In other experiments a solution of DOPA (15.0 mg, 0.08 mmol) in phosphate buffer (pH 7.4, 75 mL) was allowed to stand at room temperature under vigorous stirring in the presence of variable amounts of 5SCD-melanin (1.0 mg, 3.0 mg or 15.0 mg).

A solution of DHICA, DA or EN (10.0 mg, 0.05 mmol) in phosphate buffer (pH 7.4, 50 mL) was allowed to stand at room temperature under vigorous stirring in the presence or in the absence of 5SCD-melanin (2.0 mg).

In other experiments a solution of DA (10.0 mg, 0.05 mmol) in phosphate buffer (pH 7.4, 50 mL) was allowed to stand at room temperature under vigorous stirring in the presence of 5-*S*-cysteinyl-dopamine-melanin (2.0 mg)

In all cases, aliquots of the reaction mixtures were periodically withdrawn and analyzed by HPLC/UV.

Oxidative degradation procedure

5SCD-melanin or the polymer from 5SCD-melanin induced oxidation of DOPA (DOPA/5SCD-melanin 5:1, w/w) (1.0 mg) was degraded with 1 M NaOH containing 1.5% H₂O₂ and was analyzed by HPLC after workup as reported.³⁹

In separate experiments each polymer (2.0 mg) was loaded on a nylon filter (Millex-GV, 0:22 mm) and treated with solutions at increasing pHs (4 × 200 μL phosphate buffer 0.1 M pH 8; 4 × 200 μL phosphate buffer 0.1 M pH 9; 4 × 200 μL 1 M NaOH). Each eluate was then treated with NaOH (100 μL) and 30% v/v H₂O₂ (15 μL) and allowed to stand at room temperature under vigorous stirring. After 24 h the reaction mixtures were treated with 5% Na₂S₂O₅ (40 μL), taken to pH 3 with 85% H₃PO₄ and analyzed by HPLC as reported.³⁹

The insoluble material was treated with NaOH (300 μL) and 30% v/v H₂O₂ (15 μL) and analyzed by HPLC after workup as reported.³⁹

4.4. Oxidative chemistry of cysteinyl dopas and properties of related synthetic pheomelanins

Synthetic pigment preparation. Synthetic pheomelanin from 5SCD or 2SCD was obtained by peroxidase/H₂O₂ oxidation as reported.¹⁶³

Oxidative chemistry of 2SCD

A solution of 2SCD (50 mg, 0.16 mmol) in phosphate buffer (pH 6.8, 50 mL) was allowed to stand at room temperature under vigorous stirring in the presence of L-DOPA (1.5 mg, 61 μmol) and tyrosinase (50 u/mL) under O₂ bubbling. Aliquots of the reaction mixtures were periodically withdrawn, treated with NaBH₄ and analyzed by HPLC/UV (eluant: 0.5% TFA (eluant A), methanol (eluant B); 0-15 min, from 10% to 15% eluant B; 15-55 min, from 15% to 60% eluant B; flow rate: 0.8 mL/min, UV: 254 nm). For preparative purpose, after 30 min of the reaction time the mixture was treated with NaBH₄ and purified by semipreparative HPLC/UV (eluant: 0.5% TFA (eluant A), methanol (eluant B); 0-5 min, 20% eluant B; 5-40 min, from 20% to 80% eluant B; flow rate: 3 mL/min, UV: 280 nm) to afford **1** (*t*_R 11.2 min, 10.2 mg, 27% yield), **2** (*t*_R 32.3 min, 4.9 mg, 11% yield), and **3** (*t*_R 36.6 min, 6.8 mg, 15% yield).

8-(2-amino-2-carboxyethyl)-5-hydroxy-3,4-dihydro-1,4-benzothiazine (1)

ESI(+)/MS: *m/z* 225 ([M+H]⁺)

¹H NMR (D₂O/DCI): δ 3.14 (1H, dd, *J*=8.6, 14.8 Hz, CH₂CH), 3.38 (1H, m, CH₂CH), 3.40 (2H, t, *J*=4.8 Hz, H-2), 3.81 (2H, t, *J*=4.8 Hz, H-3), 4.39 (1H, t, *J*=8.6 Hz, CH₂CH), 6.82 (1H, d, *J*=8.0 Hz, H-6), 7.19 (1H, d, *J*=8.0 Hz, H-7).

¹³C NMR (D₂O/DCI): δ 24.2 (C-2), 34.2 (CH₂CH), 43.1 (C-3), 53.5 (CH₂CH), 113.4 (C-6), 117.2 (C-4'), 124.1 (C-8), 130.4 (C-8'), 133.4 (C-7), 151.7 (C-5), 172.5 (COOH).

8-(2-amino-2-carboxyethyl)-3-carboxy-5-hydroxy-3,4-dihydro-1,4-benzothiazine (2)

ESI(+)/MS: *m/z* 269 ([M+H]⁺)

¹H NMR (D₂O/DCl): δ 3.00 (1H, dd, $J=9.6, 14.8$ Hz, H-2), 3.24 (1H, dd, $J=3.6, 13.2$ Hz, CH₂CH), 3.35 (1H, dd, $J=5.2, 14.8$ Hz, H-2), 3.41 (1H, dd, $J=4.4, 13.2$ Hz, CH₂CH), 4.22 (1H, dd, $J=5.2, 9.6$ Hz, H-3), 4.65 (1H, m, CH₂CH), 6.63 (1H, d, $J=8.0$ Hz, H-7), 6.68 (1H, d, $J=8.0$ Hz, H-6).

**8-(2-amino-2-carboxyethyl)-3-carboxy-5-hydroxy-3,4-dihydro-1,4-benzothiazine
(3)**

ESI(+)/MS: m/z 269 ([M+H]⁺)

¹H NMR (D₂O/DCl): δ 2.86 (1H, dd, $J=10.0, 14.8$ Hz, H-2), 3.22 (1H, dd, $J=4.0, 13.2$ Hz, CH₂CH), 3.29 (1H, dd, $J=4.8, 14.8$ Hz, H-2), 3.41 (1H, dd, $J=4.0, 13.2$ Hz, CH₂CH), 3.89 (1H, dd, $J=4.8, 10.0$, Hz, H-3), 4.68(1H, t, $J=4.0$, CH₂CH), 6.56 (1H, d, $J=8.0$, H-6 or H-7), 6.65 (d, $J=8.0$, H-7 or H-6).

Aerial oxidation of 5SCD and 2SCD

An equimolar solution of 2SCD (3 mg, 9.5 μ mol) and 5SCD (3 mg, 9.5 μ mol) in 0.1 M phosphate buffer (pH 7.4, 19 mL) was allowed to stand at room temperature under vigorous stirring. Aliquots of the reaction mixtures were periodically withdrawn and analyzed by HPLC/UV (0.5% TFA/methanol 90:10 (v/v); flow rate: 0.8 mL/min, UV: 254 nm).

Oxidation of 5SCD and 2SCD in the presence of synthetic and natural pheomelanins

A solution of 5SCD or 2SCD (5 mg, 15.8 μ mol) in 0.1 M phosphate buffer (pH 7.4, 16 mL) was allowed to stand at room temperature under vigorous stirring. When required this reaction was carried out in the presence of 2SCD-pheomelanin (1.0 mg), 5SCD-pheomelanin (1.0 mg or 10 mg), natural pheomelanin from red hair (10 mg), natural eumelanin from black hair (10 mg). Aliquots of the reaction mixtures were periodically

withdrawn and analyzed by HPLC/UV (0.5% TFA/methanol 90:10 (v/v); flow rate: 0.8 mL/min, UV: 254 nm).

Preparation of mixed pheomelanins

Mixed pheomelanin A. A solution of 5SCD (10 mg, 31.6 μmol) in 0.01 M phosphate buffer (pH 6.8, 2.5 mL) in the presence of 2SCD-pheomelanin (2.0 mg) was treated with horseradish peroxidase (16.7 units/mL final concentration) and 30% v/v hydrogen peroxide (4 μL). The mixture was allowed to stand at room temperature under vigorous stirring for 2h and then acidified at pH 3 with 2 M HCl. The pigment precipitated was collected by centrifugation (6793 $g \times \text{min}$, 4°C, 30 min) and washed with 1% acetic acid (3 \times 10 mL) and water (10 mL) and lyophilized (7.5 mg).

Mixed pheomelanin B. A solution of 2SCD (2 mg, 6.33 μmol) in 0.01 M phosphate buffer (pH 6.8, 2.5 mL) in the presence of 5SCD-pheomelanin (10.0 mg) was treated with horseradish peroxidase (16.7 units/mL final concentration) and 30% v/v hydrogen peroxide (4 μL). The mixture was allowed to stand at room temperature under vigorous stirring for 2h and then acidified at pH 3 with 2 M HCl. The pigment precipitated was collected as above and lyophilized (7.3 mg).

Oxidative degradation procedure

2SCD-melanin (2.0 mg), 5SCD-melanin (2.0 mg), a mixture of 2SCD-melanin (1.0 mg) and 5SCD-melanin (1.0 mg), mixed pheomelanin A (2.0 mg) or mixed pheomelanin B (2.0 mg) was degraded with 1 M NaOH containing 1.5% H_2O_2 and was analyzed by HPLC after workup as reported.³⁹

In separate experiments each polymer (2.0 mg) was loaded on a nylon filter (Millex-GV, 0:22 mm) and treated with solutions at increasing pHs (4 \times 200 μL H_2O ; 4 \times 200 μL phosphate buffer 0.1 M pH 8; 4 \times 200 μL phosphate buffer 0.1 M pH 9; 4 \times 200 μL 1 M NaOH). Each eluate was then treated with NaOH (100 μL) and 30% v/v H_2O_2 (15 μL) and allowed to stand at room temperature under vigorous stirring. After 24 h the

reaction mixtures were treated with 5% $\text{Na}_2\text{S}_2\text{O}_5$ (40 μL), taken to pH 3 with 85% H_3PO_4 and analyzed by HPLC as reported.³⁹

The insoluble material was treated with NaOH (300 μL) and 30% v/v H_2O_2 (15 μL) and analyzed by HPLC after workup as reported.³⁹

4.5. Biologically inspired one-pot access routes to 4-hydroxybenzothiazole aminoacids, red hair-specific markers of UV susceptibility and skin cancer risk

Preparation of BTCA from L-dopa

A solution of L-dopa (158 mg, 0.80 mmol) in 0.05 M phosphate buffer (pH 7.4) (34 mL) was sequentially treated with L-cysteine (194 mg, 1.60 mmol) and mushroom tyrosinase (77,800 units) and the mixture was taken under vigorous stirring at rt. After 2 h the mixture was treated with a solution of zinc sulfate heptahydrate (275 mg, 0.96 mmol) in water (4 mL) and a solution of potassium ferricyanide (260 mg, 0.80 mmol) in 0.05 M phosphate buffer (pH 7.4) (4 mL); after 20 min, sodium persulfate (570 mg, 2.40 mmol) and 12 M HCl (40 mL) was added to the oxidation mixture and, after additional 20 min, the reaction mixture was treated with sodium disulfite (305 mg, 1.60 mmol). The resulting mixture was fractionated by preparative HPLC/UV (eluant: 0.2% TFA/methanol 65:35 (v/v); flow rate: 20 mL/min; UV: 254 nm). After evaporation of the solvent the residue was dissolved in 0.1 M HCl and taken to dryness to afford BTCA⁴ as hydrochloride salt (145 mg, 57% yield, purity >98% as determined by ¹H NMR analysis).

Preparation of BT from L-dopa

The oxidation mixture obtained as above for BTCA preparation was heated at 90 °C for 1.5 h. The fraction obtained by preparative HPLC (eluant: 0.2% TFA/methanol 75:25 (v/v); flow rate: 20 mL/min; UV: 254 nm) was taken to dryness and treated with 0.1 M HCl to afford BT²¹⁷ as hydrochloride salt (120 mg, 55% yield, purity >98% as determined by ¹H NMR analysis).

Preparation of BTCA or 2-BTCA from 5SCD or 2SCD

The reaction of 5SCD or 2SCD (250 mg, 0.80 mmol) was carried out in 0.05 M phosphate buffer (pH 7.4) (34 mL) using zinc sulfate, potassium ferricyanide and sodium persulfate at the same reagent/substrate ratios indicated above followed by preparative HPLC as above. The residue was dissolved in 0.1 M HCl and taken to dryness to afford BTCA (152 mg, 60% yield, purity >98% as determined by ¹H NMR analysis) or 2-BTCA, (145 mg, 57% yield, purity >98% as determined by ¹H NMR analysis) respectively, as hydrochloride salt.

Preparation of BT or 2-BT from 5SCD or 2SCD

The mixture obtained by oxidation of 5SCD or 2SCD described above was heated at 90 °C for 1.5 h, and purified by preparative HPLC under the conditions described above for BT. Treatment of the residue with 0.1 M HCl afforded BT (125 mg, 57% yield, purity >98% as determined by ¹H NMR analysis) or 2-BT¹⁶⁷ (114 mg, 52% yield, purity >98% as determined by ¹H NMR analysis) respectively, as hydrochloride salt.

4.6. Pheomelanin-related benzothiazole isomers in the urine of patients with diffuse melanosis of melanoma

Urine sample preparation

The samples were used both for evaluation of methodology and for quantification of free BTCA isomers without oxidation procedure. The soluble and insoluble pigmented fractions of urine were subjected to oxidative degradation for determination of BTCAs. After thawing, urine samples were treated according to the following procedure.

Free BTCA. 10 mL urine was centrifuged at 3000 rpm for 10 min at 15 °C and 2 mL of the supernatant was taken to SPE.

Soluble and sedimented urinary pigment. 10 mL urine was centrifuged at 3000 rpm for 10 min at 15 °C. From the supernatant 5 mL was taken for oxidation and further processed. The urinary sediment was collected and 1 mL of 1 M NaOH was added. The sediment was then oxidized as described below.

Total urinary pigment. 5 mL of well-mixed urine was subjected to oxidation.

Oxidation procedure

The method was reported previously.³⁹ In short, 200 mg NaOH was added to 5 mL urine to give a concentration of 1 M. 1 mg pheomelanin and sediment from 10 mL urine was suspended in 1 M NaOH (1 mL). The samples were treated with 1.5% H₂O₂ (final concentration) at room temperature and under vigorous stirring. After 24 h the mixture was treated with 5% Na₂S₂O₅, and taken to pH 4 with 85% H₃PO₄.

Extraction of degradation products

The samples, 2 mL urine or oxidation mixtures, were adjusted to pH 1 and transferred to C18 cartridges (200 mg, 3 mL, Isolute SPE column, Sorbent, Sweden), previously

conditioned with 2 mL methanol, followed by 2 mL 0.1 M hydrochloric acid. After loading of the sample, the cartridge was dried out and washed with 1 mL 0.1 M hydrochloric acid. The components were eluted with 1 mL of acidified acetonitrile (600 μ L 0.1 M hydrochloric acid to 25 mL acetonitrile) and diluted 1:3 with mobile phase before injection into HPLC. Alternatively the eluates were evaporated under nitrogen to a volume of 200 μ L and the residue was diluted 1:3 with mobile phase before injection into HPLC.

4.7. Mapping structural diversity in red hair pheomelanin: key elusive benzothiazolyldihydroisoquinoline building blocks and their formation pathway uncovered

Synthetic pigment preparation

Pheomelanin from L-dopa and L-cysteine was prepared by tyrosinase/O₂ oxidation as reported.¹³⁹ Pheomelanins from 5SCD were prepared by tyrosinase/O₂ oxidation in the presence and in the absence of ZnSO₄ × 7H₂O (1.2 molar equivalents), as previously described.¹³⁹ Pheomelanins from 5SCD by peroxidase/H₂O₂ oxidation were prepared as reported, with slight modifications.¹⁶³ Briefly, to a solution of 5SCD (100 mg, 0.32 mmol) in 0.1 M phosphate buffer (pH 6.8; 25 mL) horseradish peroxidase (16.7 units/mL final concentration) and 30% v/v hydrogen peroxide (38 μL) were added. The mixture was allowed to stand at room temperature under vigorous stirring for 2 h and then acidified to pH 3. The melanin precipitated was collected by centrifugation (6793 g × min, 4°C, 30 min), washed with 1% acetic acid (3 × 10 mL), water (10 mL) and then lyophilized. When required, the reaction was run in the presence of ZnSO₄ × 7H₂O (111 mg, 1.2 molar equivalents). In other experiments, the reaction of 5SCD in the presence of ZnSO₄ × 7H₂O was run with 50 units/mL of peroxidase and 114 μL of 30% v/v hydrogen peroxide. The mixture was taken under stirring for 24 h, acidified to pH 3, and the melanin precipitate collected as above.

General degradation procedures

Alkaline permanganate degradation. 5 mg of the appropriate sample (*viz* synthetic pheomelanins, compound **4**, 5SCD, ODHB, BTZCA-dimers, 7-(2-amino-2-carboxyethyl)-3-carboxy-5-hydroxy-3,4-dihydro-2*H*-1,4-benzothiazine, pheomelanin isolated from red human hair) were dissolved in 2 M Na₂CO₃ (200 μL). Red or black human hair (5 mg) was pottered in 2 M Na₂CO₃ (200 μL). The mixture thus obtained was treated with a 3% solution of KMnO₄ (1 mL), added in ten portions at 10 min

intervals. Na₂S₂O₅ (72 mg) was then added to destroy residual oxidant, and the mixture was filtered through nylon membranes (13 mm, 0.45 μm; Alltech Associates, Deerfield, IL, USA) and washed with water (2 × 2 mL). The filtrate was acidified to pH 1, concentrated to a final volume of 200 μL and analyzed by HPLC/UV (Gradient A (0.5% TFA (eluant a)/methanol (eluant b): from 10 to 15% b, 0-15 min; from 15 to 60% b, 15-55 min; 60% b, 55-65 min; from 60 to 80% b, 65-80 min; 80% b, 80-90 min); flow rate 0.8 mL/min, UV: 254 nm).

Alkaline hydrogen peroxide degradation. Synthetic pheomelanins (5 mg), compound **4** (5 mg) or finely minced red human hair (10 mg) were degraded with 1 M NaOH containing 1.5% H₂O₂ and were analyzed by HPLC after workup as reported.³⁹

Hydriodic acid degradation. Synthetic pheomelanins (0.5 mg), compound **4** (0.5 mg) or finely minced red human hair (5 mg) homogenized in water were degraded with 57% HI/30% H₃PO₂ and were analyzed by HPLC after workup as reported.⁷⁶

Isolation of 2-[2'-(4',5'-dicarboxythiazolyl)]-3,4,6-pyridinetricarboxylic acid (TPCA).

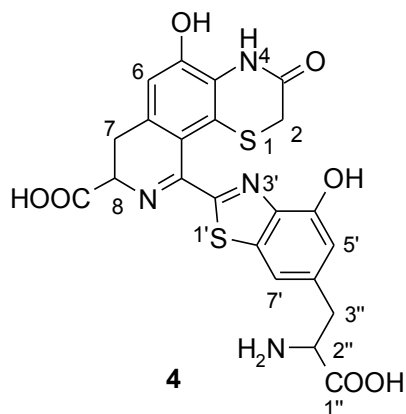
Pheomelanin (120 mg), obtained by oxidation of 5SCD (250 mg, 0.79 mmol) with 50 units/mL of peroxidase and 285 μL of 30% v/v hydrogen peroxide in the presence of ZnSO₄ × 7H₂O (273 mg, 1.2 molar equivalents) as described above, was dissolved in 2 M Na₂CO₃ (4.8 mL) and oxidized with 3% aqueous solution of KMnO₄ (16 mL), added in ten portions at 10 min intervals. The mixture was treated with Na₂S₂O₅ (1.15 g) to destroy residual oxidant, filtered through nylon membranes (47 mm, 0.45 μm; Alltech Associates, Deerfield, IL, USA) and washed with water (2 × 50 mL). The supernatant was acidified to pH 1, concentrated to a final volume of 20 mL and extracted with ethyl acetate (6 × 30 mL). The organic layer was taken to dryness, dissolved in 0.1 M HCl (1 mL) and purified by semipreparative HPLC (gradient A, flow rate 0.8 mL/min, UV: 254 nm) to give TPCA (yellowish oil, *t_R* 35.8 min, 2 mg, purity > 95%); UV (MeOH): λ_{max} 292, 318 nm; HR ESI(-)/MS: found *m/z* 380.9672 ([M-H]⁻), calcd for C₁₃H₅N₂O₁₀S *m/z* 380.9670; ¹H NMR (D₂O/DCI, 500 MHz): 8.56 (s).

Oxidation of 5SCD and isolation of 4 and 5.

To a solution of 5SCD (12 mM) in 0.1 M phosphate buffer (pH 6.8; 150 mL) $\text{ZnSO}_4 \times 7\text{H}_2\text{O}$ (1.2 molar equivalents), horseradish peroxidase (50 units/mL final concentration), and 30% v/v hydrogen peroxide up to a 38 mM final concentration were added. The mixture was allowed to stand at room temperature under vigorous stirring for 24 h. Aliquots of the reaction mixture were periodically withdrawn, reduced with NaBH_4 when required, and analyzed by HPLC (gradient A, flow rate: 0.8 mL/min; UV: 280 or 340 nm). For preparative purpose the reaction was carried out on 500 mg of 5SCD and after 5 h the mixture was cautiously acidified to pH 2 and the solid that separated was collected by centrifugation ($6793 \text{ g} \times \text{min}$, 4°C , 30 min) and purified by preparative HPLC (gradient A; flow rate 20 mL/min; UV: 280 nm) to afford **4** (orange-brown oil, t_R 39.8 min, 20 mg, 3% yield, purity >95%) and **5** (brown oil, t_R 63.7 min, 17 mg, 2% yield, purity >95% HPLC analysis).

10-[6-(2-Amino-2-carboxyethyl)-4-hydroxybenzothiazol-2-yl]-8-carboxy-5-hydroxy-3-oxo-3,4,7,8-tetrahydro-2H-[1,4]thiazino[5,6-*h*]isoquinoline (**4**).

UV (0.1 M HCl): λ_{max} 248, 282, 346, 392 nm; ESI(+)/MS: m/z 515.0 ($[\text{M}+\text{H}]^+$).



	δ_{H} (multiplicity, <i>J</i> , Hz) ^a
2	3.18 (s)
6	7.05 (s)
7	3.60 (dd, 6.0, 14.4)
8	3.64 (dd, 6.0, 14.4)
8	5.09 (t, 6.0)
5' ^b	7.09 (s)
7' ^b	7.65 (s)
2''	4.73 (t, 6.8)
3''	3.39 (dd, 6.8, 14.8)
3''	3.50 (dd, 6.8, 14.8)

^a NMR spectra recorded in $\text{D}_2\text{O}/\text{DCl}$.

^b Interchangeable.

6-[6-(2-Amino-2-carboxyethyl)-4-hydroxybenzothiazol-2-yl]-8-carboxy-5-hydroxy-3-oxo-3,4,8,9-tetrahydro-2H-[1,4]thiazino[6,5-*g*]isoquinoline (**5**).

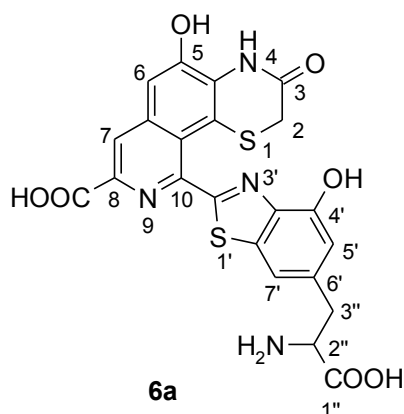
UV (0.1 M HCl): λ_{max} 245, 330, 394 nm; ESI(+)/MS: m/z 515.0 ($[\text{M}+\text{H}]^+$).

Preparation of 6a and 7a.

A solution of **4** or **5** (15 mg, 0.03 mmol) in 15 mL methanol/acetic acid (99:1 v/v) was allowed to stand at room temperature under vigorous stirring. Aliquots of the reaction mixture were periodically withdrawn and analyzed by HPLC (gradient A; flow rate 0.8 mL/min; UV: 340 nm). After 24 h the mixture was taken to dryness to afford, respectively, **6a** (brown oil, t_R 50.1 min, 15 mg, 99% yield, purity >95%) or **7a** (brown oil, t_R 80.6 min, 15 mg, 99% yield, purity >95%).

10-[6-(2-Amino-2-carboxyethyl)-4-hydroxybenzothiazol-2-yl]-8-carboxy-5-hydroxy-3-oxo-3,4-dihydro-2H-[1,4]thiazino[5,6-*h*]isoquinoline (**6a**).

UV (EtOH): λ_{max} 294, 355, 393 nm; HR ESI(-)/MS: found m/z 511.0400 ($[M-H]^-$), calcd for $C_{22}H_{15}N_4O_7S_2$ m/z 511.0388.



	δ_H (multiplicity, J, Hz) ^a	δ_C ^{a,b}
2	3.06 (s)	31.1
6	7.36 (s)	108.3
7	8.51 (s)	124.8
5' ^c	6.93 (s)	113.6
7' ^c	7.50 (s)	114.3
2''	4.29 (m)	55.1
3''	3.24 (m)	37.6
	3.44 (m)	

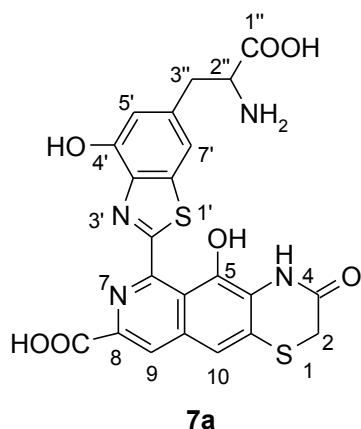
^a NMR spectra recorded in CD₃OD.

^b Assignments based on ¹H, ¹³C DEPT HSQC spectrum.

^c Interchangeable.

6-[6-(2-Amino-2-carboxyethyl)-4-hydroxybenzothiazol-2-yl]-8-carboxy-5-hydroxy-3-oxo-3,4-dihydro-2H-[1,4]thiazino[6,5-g]isoquinoline (7a).

UV (EtOH): λ_{\max} 273, 318, 397 nm; HR ESI(-)/MS: found m/z 511.0410 ($[M-H]^-$), calcd for $C_{22}H_{15}N_4O_7S_2$ m/z 511.0388; ^{13}C NMR (CD_3OD , 400 MHz): 28.5 (CH_2), 36.1 (CH_2), 53.8 (CH), 112.5 (CH), 112.8 (CH), 114.8 (C), 116.6 (CH), 125.2 (C), 125.8 (CH), 127.4 (C), 133.8 (C), 135.1 (C), 137.0 ($2 \times C$), 139.5 (C), 140.7 (C), 146.6 (C), 151.3 (C), 165.7 (C), 168.9 (C), 169.7 (C), 171.6 (C).



	δ_H (multiplicity, J, Hz) ^a	δ_C ^{a,b}
2	3.57 (s)	28.5
9	7.83 (s)	125.8
10 ^c	7.09 (s)	116.6
5' ^c	6.79 (s)	112.5
7' ^c	7.24 (s)	112.8
2''	4.35 (br s)	53.8
3''	3.22 (m)	36.1
	3.37 (m)	

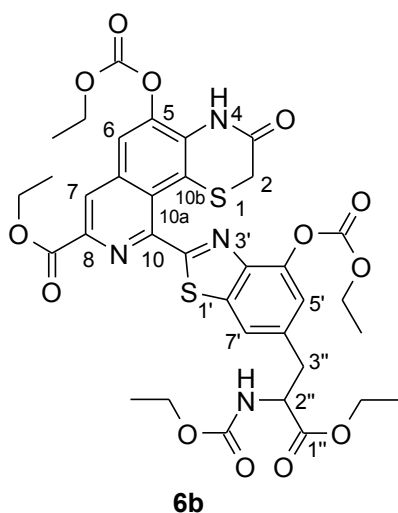
^a NMR spectra recorded in CD_3OD .

^b Assignments based on 1H , ^{13}C DEPT HSQC spectrum.

^c Interchangeable.

oil, t_R 31.2 min, 5 mg, 30% yield, purity >95%) or of **7a** (**7b**, yellow oil, t_R 31.6 min, 2 mg, 10% yield, purity >95%).

6b. UV (EtOH): λ_{max} 294, 350, 385 nm; HR ESI(+)/MS: found m/z 807.1629 ($[M+Na]^+$), calcd for $C_{35}H_{36}N_4O_{13}S_2Na$ m/z 807.1613.



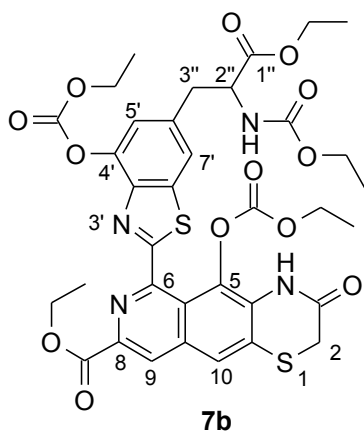
	δ_H (multiplicity, J, Hz) ^{a,b}	δ_C ^{a,b}
2	3.06 (s)	30.8
3		166.1
4	8.21 (s)	
4a		131.3
5		141.8
6	7.98 (s)	117.1
6a ^d		138.9
7	8.54 (s)	125.1
8		135.0
CO-C8		164.5
10		150.0
10a		125.1
10b		121.7
2'		170.0
3'a		145.3
4' ^d		144.9
5' ^c	7.19 (s)	120.7
6'		135.8
7' ^c	7.71 (s)	120.2
7'a ^d		140.3
1''		171.2
2''	5.26 (m)	54.7
3''	3.30 (m)	38.5

^a NMR spectra recorded in $CDCl_3$.

^b Resonances of ethoxy and ethoxycarbonyl groups: 1H NMR: δ 1.25 (3H \times 2), 1.34 (3H), 1.46 (3H), 1.48 (3H), 4.14 (2H), 4.20 (2H), 4.28 (2H), 4.43 (2H), 4.52 (2H); ^{13}C NMR: δ 14.1 ($CH_3 \times 3$), 14.4 (CH_3), 14.5 (CH_3), 61.4 (CH_2), 61.8 (CH_2), 62.1 (CH_2), 65.3 (CH_2), 66.4 (CH_2), 151.1 (CO), 153.3 (CO), 155.9 (CO).

^{c, d} Interchangeable

7b. UV (EtOH): λ_{max} 294, 341, 394 nm; HR ESI(+)/MS: found m/z 807.1630 ([M+Na]⁺), calcd for C₃₅H₃₆N₄O₁₃S₂Na m/z 807.1613.



	δ_{H} (multiplicity, J, Hz) ^{a,b}	δ_{C} ^{a,b,c}
2	3.49/3.59 (s)	33.7/28.8
4	8.05 (s)	
9	8.42/8.50 (s)	126.5/123.7
10	7.61/7.99 (s)	118.1/124.6
5' ^d	7.22/7.23 (s)	120/121
7' ^d	7.65/7.67 (s)	119.9/119.5
2''	5.21 (m)	54.6
3''	3.28/3.31 (m)	38.5

^a NMR spectra recorded in CDCl₃.

^b ¹H and ¹³C NMR resonances of ethoxy and ethoxycarbonyl groups were in the range 1.20-1.50 (CH₃), 3.80-4.60 (CH₂) and 14.0-15.0 (CCH₃), 61.4-66.3 (CCH₂) ppm, respectively.

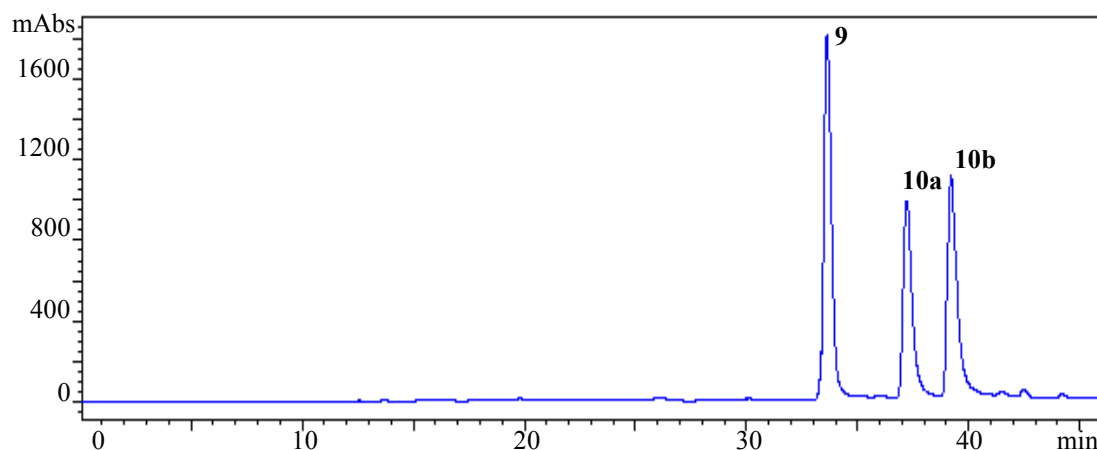
^c Assignments based on ¹H, ¹³C DEPT HSQC spectrum.

^d Interchangeable.

The two series of signals in the ¹H and ¹³C NMR spectrum were suggestive of two closely related species which could not be separated under a variety of conditions. It is possible that this reflects atropisomerism at the benzothiazole-isoquinoline bond due to the steric hindrance of the ethoxycarbonyl group at C-5, as would also be indicated by the lack of signal splitting in the underivatized compound. Yet, attempts to obtain experimental support to this hypothesis by analysis of the sample at higher temperature in different solvents failed because of the ease to decomposition exhibited by the compound.

Isolation of **9** and **10a/b**

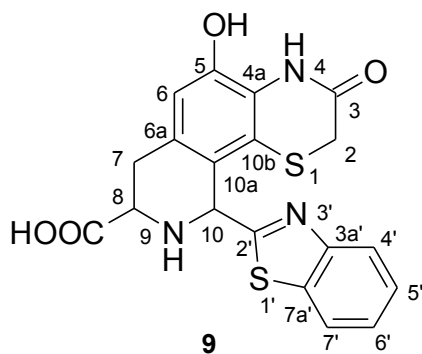
To a solution of ODHB (100 mg, 0.37 mmol) in 0.1 M phosphate buffer (pH 7.4; 25 mL) a solution of benzothiazole-2-carboxaldehyde (60 mg, 0.37 mmol) in acetonitrile was added and the mixture was allowed to stand at room temperature under vigorous stirring. After 7 h the reaction mixture was analyzed by HPLC (gradient B, UV: 254 nm, see profile below), acidified to pH 1 and extracted with ethyl acetate (10 × 30 mL).



The combined organic layers were taken to dryness, the residue was dissolved in water/methanol (2 mL, 1:1 v/v) and purified by preparative HPLC (0.3 % TFA/methanol 35/65 (v/v), flow rate 9 mL/min, UV: 254 nm). The eluates were concentrated to a final volume of 20 mL, extracted with ethyl acetate (10 × 30 mL) and the combined organic layers were dried over sodium sulfate to eventually afford **9** (yellow oil, t_R 12.9, 7 mg, 4% yield, purity >98%), **10a** (yellow oil, t_R 26.8, 6 mg, 4% yield, purity >98%) and **10b** (yellow oil, t_R 39.3, 13 mg, 8% yield, purity >98%). Based on NMR analysis and the relative abundance (HPLC trace) compounds **10a** and **10b** were formulated as diastereomers.

10-Benzothiazol-2-yl-8-carboxy-5-hydroxy-3-oxo-3,4,7,8,9,10-hexahydro-2H-[1,4]thiazino[5,6-*h*]isoquinoline (9).

UV (EtOH): λ_{\max} 236, 269, 299 nm; HR ESI(-)/MS: found m/z 412.0432 ($[M-H]^-$),
calcd for $C_{19}H_{14}N_3O_4S_2$ m/z 412.0431.



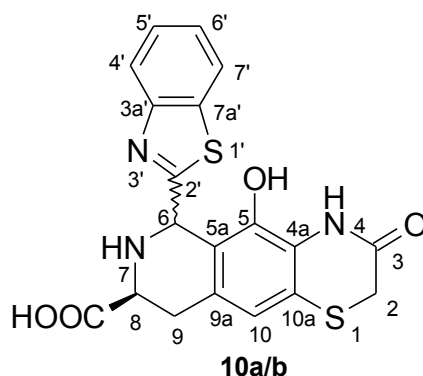
	δ_H (multiplicity, <i>J</i> , Hz) ^a	δ_C ^a
2	3.19 (d, 14.8)	29.4
	3.33 (d, 14.8)	
3		164.7
4	9.61 (s)	
4a		125.6
5		146.2
6	6.75 (s)	113.2
6a		127.0
7	3.04 (m)	28.5
	3.28 (m)	
8	4.36 (m)	51.0
COOH		170.4
10	6.11 (s)	53.8
10a		118.3
10b		120.4
2'		166.6
3'a		152.5
4'	7.98 (1H, d, 8.0)	123.6
5'	7.48 (m)	127.4
6'	7.45 (m)	126.4
7'	8.07 (d, 7.8)	122.8
7'a		135.8

^a NMR spectra recorded in DMSO- d_6 .

6(*R/S*),8(*S*)-6-Benzothiazol-2-yl-8-carboxy-5-hydroxy-3-oxo-3,4,6,7,8,9-hexahydro-2*H*-[1,4]thiazino[6,5-*g*]isoquinoline (10a/b).

10a: UV (EtOH): λ_{\max} 220, 244, 294 nm; HR ESI(-)/MS: found m/z 412.0436 ($[M-H]^-$), calcd for $C_{19}H_{14}N_3O_4S_2$ m/z 412.0431.

10b: UV (EtOH): λ_{\max} 220, 243, 294 nm; HR ESI(-)/MS: found m/z 412.0436 ($[M-H]^-$), calcd for $C_{19}H_{14}N_3O_4S_2$ m/z 412.0431.



10a	δ_H (multiplicity, <i>J</i> , Hz) ^a	δ_C ^a	10b	δ_H (multiplicity, <i>J</i> , Hz) ^a	δ_C ^a
2	3.41 (s)	29.4	2	3.40 (s)	29.4
3		165.1	3		165.1
4	9.53 (s)		4	9.48 (s)	
4a		125.6	4a		125.4
5		142.5	5		142.3
5a ^b		120.7	5a		122.2
6	6.00 (s)	53.9	6	5.76 (s)	53.0
COOH		167.3	COOH		174.0
8	4.11 (m)	54.1	8	3.82	51.6
9	2.85 (m)	30.0	9	2.80 (m)	30.5
	3.05 (m)			2.93 (m)	
9a		129.8	9a		129.3
10	6.88 (s)	119.0	10	6.78 (s)	119.2
10a ^b		120.9	10a		120.3
2'		172.0	2'		177.5
3'a		152.2	3'a		152.4
4'	7.93 (d, 7.0)	122.6	4'	7.90 (d, 8.0)	122.5
5'	7.50 (m)	126.6	5'	7.47 (t, 8.0)	126.4
6'	7.44 (m)	125.9	6'	7.40 (t, 8.0)	125.4
7'	8.05 (d, 8.0)	122.6	7'	8.03 (d, 8.0)	122.5
7'a		134.9	7'a		134.8

^a NMR spectra recorded in DMSO- d_6 .

^b Interchangeable.

4.8. Reaction of dihydrolipoic acid with juglone and related naphthoquinones: unmasking of a spirocyclic 1,3-dithiane intermediate en route to naphtho[1,4]dithiepin

Preparation of DHLA (6,8-dimercaptoottanoic acid)

To 1.0 g of lipoic acid, previously dissolved in 20.0 mL of an aqueous solution of NaHCO₃ (0.25 M), were added 740.0 mg of NaBH₄ and the mixture was taken under stirring at -25 °C. After 2 h the reaction mixture was acidified until pH 1 with HCl 6 M and extracted with toluene (5 x 20 mL). The residue was analysed by ¹H NMR to give DHLA in a pure form (920.0 mg, 91 % yield).

5-acetoxy-1,4-naphthoquinone

The title compound was prepared by acetylation of juglone according to a literature procedure with modifications.¹⁷¹ A solution of 5-hydroxy-1,4-naphthoquinone (100 mg, 0.58 mmol) and sodium acetate (590 mg, 7.2 mmol) in acetic anhydride (2 mL) was stirred at 120°C. After 30 min the mixture was diluted in 0.1 M phosphate buffer (pH 7.4) (5 mL) and extracted with chloroform (3 × 10 mL). The combined organic phases were dried over sodium sulfate, filtered and taken to dryness *in vacuo*. The compound was isolated as a brown powder (*R_f* 0.44 (eluant II), 110 mg, 88% yield, purity > 98%); UV (EtOH): λ_{max} 340 nm (log ε 3.41); IR(CHCl₃): ν_{max} 1766, 1671, 1613, 1596 cm⁻¹; HR ESI+/MS: found *m/z* 239.0332 ([M+Na]⁺), calcd for C₁₂H₈O₄Na *m/z* 239.0320; δ_H (200 MHz, CDCl₃) 2.43 (3H, s), 6.83 (1H, d, *J* = 10.6 Hz), 6.93 (1H, d, *J* = 10.6 Hz), 7.37 (1H, d, *J* = 7.8 Hz), 7.74 (1H, t, *J* = 7.8 Hz), 8.02 (1H, d, *J* = 7.8 Hz); δ_C (50 MHz, CDCl₃) 21.0 (CH₃), 123.2 (C), 124.9 (CH), 129.7 (CH), 133.5 (C), 134.8 (CH), 137.3 (CH), 139.8 (CH), 149.4 (C), 169.3 (C), 183.6 (C), 184.1 (C).

5-(2*H*-3,4-dihydro-7-hydroxy-6,11-dioxonaphtho[3,2-*b*][1,4]dithiepin-2-yl)pentanoic acid (11a) and 5-(2*H*-3,4-dihydro-7-hydroxy-6,11-dioxonaphtho[2,3-*b*][1,4]dithiepin-4-yl)pentanoic acid (11b)

To a solution of juglone (50 mg, 0.3 mmol) in absolute ethanol (6 mL) TEA (42 μ L, 0.3 mmol) and DHLA (62 mg, 0.3 mmol), previously dissolved in ethanol (600 μ L), were added under vigorous stirring. Aliquots of the mixture were periodically analyzed by TLC (eluant I) and HPLC (gradient C: 0.5% TFA (solvent a), acetonitrile (solvent b), 0-45 min from 5% to 90% solvent b, 45-50 min 90% solvent b, flow rate: 0.8 mL/min, UV: 254 nm). For preparative purpose after 10 min the reaction mixture was evaporated to dryness, and the residue obtained was dissolved in chloroform and fractionated by preparative TLC (eluant I) to afford **11a,b** as a purple red oil (R_f 0.59, 79 mg, 70% yield, purity > 98%); UV (EtOH): λ_{\max} 291, 416, 533 nm (log ϵ 3.92, 3.38, 3.15); IR(CHCl₃): ν_{\max} 3688, 3522, 1713, 1626, 1457 cm⁻¹; HR ESI+/MS: found m/z 379.0658 ([M+H]⁺), calcd for C₁₈H₁₉O₅S₂ m/z 379.0674; DHLA moiety δ_H (400 MHz, CDCl₃) 1.53 (1H, m, 4-H), 1.68 (5H, m, 3-H, 4-H and 5-H), 1.94 (1H, m, 7-H), 2.23 (1H, m, 7-H), 2.38 (2H, m, 2-H), 2.97/2.99 (1H, m, 8-H), 4.19 (1H, m, 8-H), 4.37 (1H, m, 6-H); juglone moiety δ_H 7.20 (1H, d, J = 8.0 Hz, 6-H), 7.55 (1H, t, J = 8.0 Hz, 7-H), 7.60 (1H, m, 8-H), 11.8 (1H, br s); DHLA moiety δ_C (100 MHz, CDCl₃) 24.3 (CH₂, C-3), 26.3 (CH₂, C-4), 29.8 (CH₂, C-8), 33.5 (2 \times CH₂, C-2 and C-7), 34.7/34.8 (CH₂, C-5), 45.3/45.5 (CH, C-6), 178.5 (C, C-1); juglone moiety δ_C 114.2 (C, C-4a), 119.7/119.8 (CH, C-8), 124.3 (CH, C-6), 131.7 (C, C-8a) 136.1 (CH, C-6), 143.0/143.2 (C, C-3), 145.7/145.9 (C, C-2), 161.4 (C, C-5), 179.5 (C, C-1), 185.1 (C, C-4).

5-(2',3'-dihydro-spiro[1,3-dithiane-2,3'-[5]hydroxy[1,4]naphthoquinone-4-yl)pentanoic acid (11c)

To a solution of juglone (50 mg, 0.3 mmol) in absolute ethanol (600 mL) TEA (42 μ L, 0.3 mmol) and DHLA (62 mg, 0.3 mmol), previously dissolved in ethanol (600 μ L), were added under vigorous stirring. Aliquots of the mixture were periodically analyzed by TLC (eluant I) and HPLC (gradient C, flow rate: 0.8 mL/min, UV: 254 nm). For

preparative purpose after 10 min the mixture was treated with TFA (6 mL) and concentrated *in vacuo*. The residue was purified by preparative HPLC (gradient C, flow rate: 3 mL/min, UV: 254 nm) to provide **11c** as a yellow oil (t_R 33.4 min, 50 mg, 44% yield, purity > 98%); UV (EtOH): λ_{max} 232, 356 nm; IR(CHCl₃): ν_{max} 3689, 3510, 1704, 1636, 1455 cm⁻¹; HR ESI+/MS: found m/z 381.0845 ([M+H]⁺), calcd for C₁₈H₂₁O₅S₂ m/z 381.0830; DHLA moiety δ_H (400 MHz, CDCl₃) 1.51 (4H, m, 3-H and 5-H), 1.54 (1H, m, 7-H), 1.58 (2H, m, 4-H), 2.24/2.26 (1H, m, 7-H), 2.36 (2H, t, J = 7.2 Hz, 2-H), 2.79/2.82 (1H, m, 8-H), 3.38 (1H, m, 8-H), 3.54 (m, 1H, 6-H); juglone moiety δ_H \square 3.33 (2H, s, 2-H), 7.28 (1H, d, J = 9.2 Hz, 6-H), 7.50 (1H, d, J = 7.2 Hz, 8-H), 7.60 (1H, m, 7-H), 11.95 (1H, s, OH); DHLA moiety δ_C (100 MHz, CDCl₃) 24.4 (CH₂, C-4), 25.4 (CH₂, C-3), 29.1 (CH₂, C-8), 31.0 (CH₂, C-7), 33.5 (CH₂, C-2), 35.5 (CH₂, C-5), 41.8 (CH, C-6), 178.2 (C, C-1); juglone moiety δ_C 50.0 (CH₂, C-2), 53.1 (C, C-3), 114.1 (C, C-4a), 117.7/117.8 (CH, C-8), 124.6/124.7 (CH, C-6), 133.6 (C, C-8a) 136.6/136.7 (CH, C-7), 162.8/163.1 (C, C-5), 191.4 (C, C-1), 196.3/196.4 (C, C-4).

General procedure for conjugation of 1,4-naphthoquinones with DHLA

The reaction was performed as described for **11a,b**. The reaction mixture was evaporated to dryness, and the residue obtained was dissolved in chloroform and fractionated by preparative TLC (eluant I) to afford **12-4** (reaction time: **12** and **14**, 10 min; **13**, 60 min).

5-(2H-3,4-dihydro-6,11-dioxonaphtho[2,3-b][1,4]dithiepin-2-yl)pentanoic acid (**12**)

Compound **12** was obtained as a purple red oil (R_f 0.62, 48 mg, 44% yield, purity > 98%); UV (EtOH): λ_{max} 236, 293, 514 nm (log ϵ 4.07, 4.25, 3.32); IR(CHCl₃): ν_{max} 3522, 1710, 1659, 1592 cm⁻¹; HR ESI+/MS: found m/z 363.0710 ([M+H]⁺), calcd for C₁₈H₁₉O₄S₂ m/z 363.0725; δ_H (400 MHz, CDCl₃) 1.51 (1H, m), 1.68 (5H, m), 1.91 (1H, m), 2.21 (1H, m), 2.36 (2H, t, J = 6.8 Hz), 2.95 (1H, m), 4.18 (1H, m), 4.34 (1H, m), 7.66 (2H, m), 8.03 (2H, m); δ_C (100 MHz, CDCl₃) 24.3 (CH₂), 26.3 (CH₂), 29.8 (CH₂), 33.6

(CH₂), 33.7 (CH₂), 34.7 (CH₂), 45.3 (CH), 126.8 (CH), 126.9 (CH), 131.7 (C), 131.8 (C), 133.7 (2 × CH), 144.2 (C), 144.4 (C), 178.8 (C), 180.2 (2 × C).

5-(7-acetoxy-2*H*-3,4-dihydro-6,11-dioxonaphtho[3,2-*b*][1,4]dithiepin-2-yl)pentanoic acid (13a) and 5-(7-acetoxy-2*H*-3,4-dihydro-6,11-dioxonaphtho[2,3-*b*][1,4]dithiepin-4-yl)pentanoic acid (13b)

Compound **3** was obtained as a purple red oil (*R_f* 0.79, 48 mg, 38% yield, purity > 95%); UV (EtOH): λ_{max} 296, 520 nm (log ε 3.92, 2.97); IR(CHCl₃): ν_{max} 3527, 1769, 1712, 1655, 1509 cm⁻¹; HR ESI+/MS: found *m/z* 421.0793 ([M+H]⁺), calcd for C₂₀H₂₁O₆S₂ *m/z* 421.0779; δ_H (400 MHz, CDCl₃) 1.49 (1H, m), 1.66 (5H, m), 1.89 (1H, m), 2.19 (1H, m), 2.35 (2H, m), 2.42/2.43 (3H, s), 2.93 (1H, m), 4.13 (1H, m), 4.31 (1H, m), 7.29 (1H, d, *J* = 8.0 Hz), 7.67 (1H, t, *J* = 8.0 Hz), 7.99/8.01 (1H, d, *J* = 8.0 Hz); δ_C (100 MHz, CDCl₃) 21.1 (CH₃), 24.3 (CH₂), 26.3 (CH₂), 29.7/29.8 (CH₂), 33.5 (2 × CH₂), 34.7 (CH₂), 45.2/45.3 (CH), 122.9/123.0 (C), 125.3/125.4 (CH), 129.5 (CH); 133.4/133.5 (C), 134.6 (CH), 143.1/143.3 (C), 145.4/145.6 (C), 149.6 (C), 169.4/169.5 (C), 178.5 (C), 178.6 (C), 179.4 (C).

5-(2*H*-3,4-dihydro-7,10-dihydroxy-6,11-dioxonaphtho[2,3-*b*][1,4]dithiepin-2-yl)pentanoic acid (14)

Compound **14** was obtained as a purple red oil (*R_f* 0.67, 48 mg, 25% yield, purity > 95%); UV (EtOH): λ_{max} 284, 507, 548 nm (log ε 4.14, 3.91, 3.74); IR(CHCl₃): ν_{max} 3690, 3601, 3503, 1713, 1597, 1456 cm⁻¹; HR ESI+/MS: found *m/z* 395.0606 ([M+H]⁺), calcd for C₁₈H₁₉O₆S₂ *m/z* 395.0623; δ_H (400 MHz, CDCl₃) 1.52 (1H, m), 1.68 (5H, m), 1.94 (1H, m), 2.21 (1H, m), 2.35 (2H, m), 2.97 (1H, m), 4.18 (1H, m), 4.37 (1H, m), 7.18 (2H, s), 12.17 (1H, br s); δ_C (100 MHz, CDCl₃) 24.2 (CH₂), 26.2 (CH₂), 29.7 (CH₂), 33.4 (CH₂), 33.6 (CH₂), 34.7 (CH₂), 45.4 (CH), 110.8 (2 × C), 129.1 (2 × CH), 144.5 (C), 144.8 (C), 157.5(C), 157.6 (C), 178.9 (C), 183.1 (2 × C).

Procedure for conjugation of menadione with DHLA

To a solution of menadione (52 mg, 0.3 mmol) in absolute ethanol (6 mL) TEA (42 μ L, 0.3 mmol) and DHLA (62 mg, 0.3 mmol), previously dissolved in ethanol (600 μ L), were added under vigorous stirring. After 2 h the mixture was evaporated to dryness, and the residue obtained was dissolved in CHCl_3 and fractionated by preparative TLC (eluant I) to afford **15a** (yellow oil, R_f 0.79, 26 mg, 16% yield, purity >98%) and **15b** (light yellow oil, R_f 0.70, 23 mg, 20% yield, purity >95%).

S,S'-bis(2-methyl-1,4-naphthoquinon-3-yl)-6,8-dithiooctanoic acid (**15a**)

UV (EtOH): λ_{max} 261, 319, 425 nm; IR(CHCl_3): ν_{max} 3522, 1702, 1663, 1593, 1465 cm^{-1} ; HR ESI+/MS: found m/z 549.1432 ($[\text{M}+\text{H}]^+$), calcd for $\text{C}_{30}\text{H}_{29}\text{O}_6\text{S}_2$ m/z 549.1425; δ_{H} (400 MHz, CDCl_3) 1.60 (2H, m), 1.63 (2H, m), 1.68 (2H, m), 1.92 (2H, m), 2.25 (3H, s), 2.33 (3H, s), 2.37 (2H, m), 3.38 (2H, m), 4.07 (1H, m), 7.64 (4H, m), 7.96 (4H, m); δ_{C} (100 MHz, CDCl_3) 15.1 (CH_3), 15.4 (CH_3), 24.3 (CH_2), 26.1 (CH_2), 31.4 (CH_2), 33.4 (CH_2), 35.2 (CH_2), 38.9 (CH_2), 47.1 (CH), 126.4 (CH), 126.5 (CH), 126.6 (CH), 126.7 (CH), 133.2 (CH), 133.3 (CH), 133.5 (CH), 133.7 (CH), 131.8 (C), 132.7 (C), 134.4 (2 \times C), 146.4 (2 \times C), 147.7 (2 \times C), 178.0 (C), 181.0 (C), 181.1 (C), 181.8 (C), 182.0 (C).

5-(2',3'-dihydro-spiro[1,3-dithiane-2,3'-[2]methyl[1,4]naphthoquinon-4-yl])pentanoic acid (15b**)**

UV (EtOH): λ_{max} 253, 301 nm; IR(CHCl_3): ν_{max} 3523, 1697, 1593, 1459 cm^{-1} ; HR ESI+/MS: found m/z 379.1022 ($[\text{M}+\text{H}]^+$), calcd for $\text{C}_{19}\text{H}_{23}\text{O}_4\text{S}_2$ m/z 379.1038; DHLA moiety δ_{H} (400 MHz, CDCl_3) 1.44 (2H, m, 3-H), 1.50 (2H, m, 5-H), 1.56 (1H, m, 7-H), 1.58 (2H, m, 4-H), 2.14/2.18 (1H, m, 7-H), 2.30/2.35 (2H, m, 2-H), 2.77 (1H, m, 8-H), 3.16/3.26 (1H, m, 8-H), 3.43 (1H, m, 6-H); menadione moiety δ_{H} 1.48/1.51 (3H, d, $J=7.0$ Hz, CH_3), 3.35 (1H, m, 2-H), 7.71 (1H, m, 6-H), 7.75 (1H, m, 7-H), 7.96 (1H, d, $J=$

7.2 Hz, 8-H), 8.12 (1H, d, $J=7.2$ Hz, 5-H); DHLA moiety δ_C (100 MHz, CDCl_3) 24.3 (CH₂, C-4), 25.4 (CH₂, C-3) 28.2/29.1 (CH₂, C-8), 31.5 (CH₂, C-7), 33.6 (CH₂, C-2), 35.5/35.7 (CH₂, C-5), 41.1/41.8 (CH, C-6), 178.7 (C, C-1); menadione moiety δ_C 12.8/13.4 (CH₃), 53.0/53.6 (CH, C-2), 60.4/60.7 (C, C-3), 126.3/126.4 (CH, C-8), 128.0/128.1 (CH, C-5), 132.2 (C, C-4a or C-8a), 132.4 (C, C-8a or C-4a), 134.0 (CH, C-7), 134.4 (CH, C-6), 189.1 (C, C-4), 195.6/195.9 (C, C-1).

4.9. Synthesis and antioxidant activity of new conjugates of dietary polyphenols of plant origin with dihydrolipoic acid

Preparation of *trans*-5-S-lipoylhydroxytyrosol

A solution of tyrosol (150.0 mg, 1.09 mmol) in methanol (15 mL) was treated with IBX (462 mg, 1.65 mmol) under vigorous stirring at -25°C. After 1h a solution of DHLA (920 mg, 4.42 mmol) in methanol (15 mL) was added. After additional 15 min the reaction mixture was treated with a solution of Na₂S₂O₅ (270 mL) and acidified with HCl 6 M to pH 1. Then the mixture was extracted with toluene (3 × 100 mL), chloroform (3 × 100 mL) and ethyl acetate (3×100 mL). Aqueous layer was periodically analyzed by HPLC (eluant: 0.5% TFA (solvent A), methanol (solvent B); 0-45 min from 5% to 90% solvent B; flow rate: 0.7 mL/min; UV: 280 nm). The combined chloroform layers were dried over sodium sulfate and taken to dryness to afford pure lipoyl-HTYR (117 mg, 30% yield) as an oily solid.

5-S-lipoylhydroxytyrosol (lipoyl-HTYR)

ESI+/MS: *m/z* 361 ([M+H]⁺), 383 ([M+Na]⁺);

UV: λ_{max} (CH₃OH) 256, 291 nm;

¹H NMR (CD₃OD) δ (ppm): 1.54 (m, 7H), 1.84 (m, 1H), 2.26 (t, *J*= 7.2 Hz, 2H), 2.65 (t, *J*= 7.2 Hz, 2H), 2.91 (m, 2H), 3.07 (m, 1H), 3.67 (t, *J*= 7.2 Hz, 2H), 6.62 (d, *J*=2.0 Hz, 1H), 6.71 (d, *J*= 2.0 Hz, 1H).

¹³C NMR (CD₃OD) δ (ppm): 25.9 (CH₂), 27.8 (CH₂), 32.6 (CH₂), 35.1 (CH₂), 39.6 (CH₂), 39.7 (CH₂), 39.8 (CH₂), 40.3 (CH), 64.5 (CH₂), 116.8 (CH), 121.7 (C), 125.5 (CH), 132.0 (C), 144.9 (C), 146.4 (C), 178.0 (C).

Preparation of 2-S-lipoylcaffeic acid

A solution of coumaric acid (177.0 mg, 1.08 mmol) in methanol (15 mL) was treated with IBX (462 mg, 1.65 mmol) under vigorous stirring at room temperature. After 7 min a solution of DHLA (920 mg, 4.42 mmol) in methanol (15 mL) was added. After

additional 15 min the reaction mixture was treated with a solution of Na₂S₂O₅ (270 mL) and acidified with HCl 6 M to pH 1. Then the mixture was extracted with hexane/toluene 8:2 (10 × 200 mL), chloroform (7 × 200 mL) and ethyl acetate (3×100 mL). Aqueous layer was periodically analyzed by HPLC (eluant: 0.5% TFA (solvent A), methanol (solvent B); 0-45 min from 5% to 90% solvent B; flow rate: 0.7 mL/min; UV: 280 nm). The combined chloroform layers were dried over sodium sulfate and taken to dryness to afford pure lipoyl-CA (182 mg, 44% yield) as an oily solid.

2-S-lipoylcaffeic acid (lipoyl-CA)

ESI+/MS: *m/z* 387 ([M+H]⁺), 409 ([M+Na]⁺);

UV: λ_{max} (CH₃OH) 252, 320 nm;

¹H NMR (CD₃OD) δ (ppm): 1.38 (m, 1H), 1.54 (m, 1H), 1.54 (m, 2H), 1.42(m, 1H), 1.62 (m, 1H), 1.78 (m, 1H),e 1.81(m, 1H), 2.26 (m, 2H), 2.88 (m,1H), 2.90 (m, 1H), 2.96 (m, 1H), 6.29 (d, J=16 Hz, 1H), 6.86 (d, J=8.4 Hz, 1H), 7.22 (d, 1H), 8.40 (d, J= 16 Hz, 1H).

¹³C NMR (CD₃OD) δ (ppm): 25.4 (CH₂), 27.3 (CH₂), 34.1 (CH₂), 34.1 (CH₂), 39.4 (CH₂), 39.4 (CH₂), 40.2 (CH), 117.2 (CH), 118.1 (CH), 119.9 (CH), 121.7 (C), 130.7 (C), 144.2 (CH), 147.7 (C), 147.8 (C), 168.2 (C), 174.8 (C).

Preparation of 5-S-lipoylpiceatannol

A solution of resveratrol (87.0 mg, 0.38 mmol) in methanol (5 mL) was treated with IBX (266 mg, 0.95 mmol) under vigorous stirring at -25°C. After 20 min a solution of DHLA (316 mg, 1.52 mmol) in methanol (5 mL) was added. After additional 15 min the reaction mixture was treated with a solution of Na₂S₂O₅ (90 mL) and acidified with HCl 6 M to pH 1. Then the mixture was extracted with hexane/toluene 7:3 (10 × 200 mL), chloroform (4 × 200 mL) and ethyl acetate (3×100 mL). Aqueous layer was periodically analyzed by HPLC (eluant: 0.5% TFA (solvent A), methanol (solvent B); 0-45 min from 5% to 90% solvent B; flow rate: 0.7 mL/min; UV: 280 nm). The combined chloroform layers were dried over sodium sulfate and taken to dryness to afford pure lipoyl-PIC (58.8 mg, 33% yield) as an oily solid.

5-S-lipoylpiceatannol (lipoyl-PIC)

ESI+/MS: m/z 451 ($[M+H]^+$), 473 ($[M+Na]^+$);

UV: λ_{max} (CH₃OH) 222, 268, 312, 325 nm;

¹H NMR (CD₃OD) δ (ppm): 1.42 (m, 1H), 1.73 (m, 1H), 1.54 (m, 2H), 1.54 (m, 2H), 1.91 (m, 1H), 2.01 (m, 1H), 2.26 (m, 2H), 2.95 (m, 1H), 2.97 (m, 1H), 3.08 (m, 1H), 6.23 (d, $J=1.6$ Hz, 1H), 6.50 (d, $J=1.6$ Hz, 2H), 6.83 (d, $J=16.3$ Hz, 1H), 6.91 (d, $J=16.3$ Hz, 1H), 7.00 (d, $J=1.7$ Hz, 1H), 7.07 (d, $J=1.7$ Hz, 1H).

¹³C NMR (CD₃OD) δ (ppm): 25.3 (CH₂), 27.3 (CH₂), 31.9 (CH₂), 34.1 (CH₂), 39.3 (CH₂), 39.4 (CH₂), 40.3 (CH), 102.8 (CH), 105.8 (CH), 113.1 (CH), 122.1 (C), 123 (CH), 127.7 (CH), 128.8 (CH), 130.6 (C), 140.6 (C), 145.8 (C), 145.9 (C), 159.5 (C), 174.9 (C).

DPPH assay

To a freshly prepared 0.2 mM solution of DPPH in methanol compounds under exam (50 μ M solution in methanol) were added separately. Spectra were recorded at 25°C every 0.5 s over 1-2 min for the determination of rate constants and stoichiometries. Kinetic runs over 20 min were used for the determination of total stoichiometries (see text for details). Tested compounds were HTYR, lipoyl-HTYR, CA, lipoyl-CA, PIC, lipoyl-PIC and DHLA (DHLA used at 25 μ M concentration). The reported values represent the media \pm SD obtained by three separate experiments.

Aerial oxidation of lipoylconjugates and parent catechols

A solution of HTYR (5 μ mol) and lipoyl-HTYR (5 μ mol) in phosphate buffer 0.1 M (pH 7.4, 10 mL) was allowed to stand at room temperature under vigorous stirring. Aliquots of the reaction mixture was periodically withdrawn and analyzed by HPLC-RP/UV (eluant: 0.5% TFA (solvent A), methanol (solvent B); 0-45 min from 5% to 90% solvent B; flow rate: 0.7 mL/min; UV: 280 nm)..

The experiment was repeated in the same conditions on the couple CA/lipoyl-CA and PIC/lipoyl-PIC.

5. References

1. Bliss, J. M.; Ford, D.; Swerdlow, A. J.; Armstrong, B. K.; Cristofolini, M.; Elwood, J. M.; Green, A.; Holly, E. A.; Mack, T.; Mackie, R. M.; Osterlind, A.; Walter, S. D.; Peto, J.; Easton, D. F. *Int. J. Cancer* **1995**, *62*, 367–376.
2. Elwood, J. M.; Whitehead, S. M.; Davison, J.; Stewart, M.; Galt, M. *Int. J. Epidemiol.* **1990**, *19*, 801–810.
3. Prota, G.; Nicolaus, R. A. On the biogenesis of pheomelanins. In: Montagna W, Hu F. *Advances in Biology of Skin*, vol 8. New York: Pergamon Press; **1967**. pp. 323–328.
4. Prota, G. *Melanins and Melanogenesis*. San Diego: Academic Press; **1992**. pp. 1–290.
5. Simon, J. D.; Peles, D.; Wakamatsu, K.; Ito, S. *Pigment Cell Melanoma Res.* **2009**, *22*, 563-579.
6. Hearing, V. J. The regulation of melanin production. In *Drug Discovery Approaches for Developing Cosmeceuticals, Advanced Skin Care and Cosmetic Products* (Hori, W., ed), IBC Library Series, Southborough, Massachusetts; **1997**, pp. 3.1.1–3.1.21.
7. Fitzpatrick, T. B.; Breathnach, A. S. *Dermatol. Wochenschr.* **1963**, *147*, 481–489.
8. Seiji, M.; Shima, K.; Birbeck, M. S.; Fitzpatrick, T. B. *Ann. N. Y. Acad. Sci.* **1963**, *100*, 497–533.
9. Kushimoto, T.; Basrur, V.; Valencia, J.; Matsunaga, J.; Vieira, W. D.; Ferrans, V. J.; Muller, J.; Appella, E.; Hearing, V. J. *Proc. Natl. Acad. Sci. U. S. A.* **98**, 10698–1070.
10. Berson, J. F.; Harper, D. C.; Tenza, D.; Raposo, G.; Marks, M. S. *Mol. Biol. Cell* **2001**, *12*, 3451–3464.
11. Toda, K.; Pathak, M. A.; Parrish, J. A.; Fitzpatrick, T. B.; Quevedo, W. C. Jr. *Nat. New Biol.* **1972**, *236*, 143–145.

12. Jimbow, K.; Quevedo, W. C. Jr.; Fitzpatrick, T. B.; Szabo, G. *J. Invest. Dermatol.* **1976**, *67*, 72–89.
13. Kobayashi, N.; Nakagawa, A.; Muramatsu, T.; Yamashina, Y.; Shirai, T.; Hashimoto, M. W.; Yshigaki, Y.; Ohnishi, T.; Mori, T. *J. Invest. Dermatol.* **1998**, *110*, 806–810.
14. Sturm, R. A.; Box, N. F.; Ramsay, M. *Bioessays* **1998**, *20*, 712–721.
15. Abdel-Malek, Z.; Scott, M. C.; Suzuki, I.; Tada, A.; Im, S.; Lamoreux, L.; Ito, S.; Barsh, G.; Hearing, V. J. *Pigment Cell Res.* **2000**, *13 Suppl. 8*, 156–162.
16. Healy, E. *Photodermatol. Photoimmunol. Photomed.* **2004**, *20*, 283–288.
17. Chakraborty, A. K.; Funasaka, Y.; Slominski, A.; Ermak, G.; Hwang, J.; Pawelek, J. M.; Ichihashi, M. *Biochim. Biophys. Acta* **1996**, *1313*, 130–138.
18. Funasaka, Y.; Chakraborty, A. K.; Hayashi, Y.; Komoto, M.; Ohashi, A.; Nagahama, M.; Inoue, Y.; Pawelek, J.; Ichihashi, M. *Br. J. Dermatol.* **1998**, *139*, 216–224.
19. Ozeki, H.; Ito, S.; Wakamatsu, K.; Hirobe, T. *J. Invest. Dermatol.* **1995**, *105*, 361–366.
20. Wilson, B. D.; Ollmann, M. M.; Kang, L.; Stoffel, M.; Bell, G. I.; Barsh, G. S. *Hum. Mol. Genet.* **1995**, *4*, 223–230.
21. Robbins, L. S. ; Nadeau, J. H. ; Johnson, K. R. ; et al. *Cell* **1993**, *72*, 827–834.
22. Flanagan, N.; Healy, E.; Ray, A.; et al. *Hum. Mol. Genet.* **2000**, *9*, 2531–2537.
23. Box, N. F.; Wyeth, J. R.; O’Gorman, L. E.; Martin, N. G.; Sturm, R. A. *Hum. Mol. Genet.* **1997**, *6*, 1891–1897.
24. Schioth, H. B.; Phillips, S.; Rudzish, R.; Birch-Machin, M.; Wikberg, J.; Rees, J. L. *Biochem. Biophys. Res. Commun.* **1999**, *260*, 488–491.
25. Smith, R.; Healy, E.; Siddiqui, S.; et al. *J. Invest. Dermatol.* **1998**, *111*, 119–122.
26. Naysmith, N.; Waterston, K.; Ha, T.; Flanagan, N.; Bisset, Y.; Ray, H.; Wakamatsu, K.; Ito, S.; Rees, J. L. *J. Invest. Dermatol.* **2004**, *122*, 423–428.
27. Beaumont, K. A.; Shekar, S. N.; Cook, A. L.; Duffy, D. L.; Sturm, R. A. *Hum. Mutat.* **2008**, *29*, 88–94.
28. Prota, G. *Fortsch. Chem. Org. Naturst.* Herz, W., Kirby, G. W., Moore, R. E., Steglich, W., Tamm, C. Eds., Springer-Verlag, Wien, **1995**, vol. 64, pp. 94–148.

29. Ito, S.; Prota, G. *Experientia* **1977**, *33*, 1118-1119.
30. Napolitano, A.; Di Donato, P.; Prota, G.; Land, E. J. *Free Radic. Biol. Med.* **1999**, *27*, 521-528.
31. Napolitano, A.; Costantini, C.; Crescenzi, O.; Prota, G. *Tetrahedron Lett.* **1994**, *35*, 6365-6368.
32. Napolitano, A.; Di Donato, P.; Prota, G. *Biochim. Biophys. Acta* **2000**, *1475*, 47-54.
33. Di Donato, P.; Napolitano, A. *Pigment Cell Res.* **2003**, *16*, 532-539.
34. Wakamatsu, K.; Ohtara, K.; Ito, S. *Pigment Cell Melanoma Res.* **2009**, *22*, 474-486.
35. Napolitano, A.; Memoli, S.; Crescenzi, O.; Prota, G. *J. Org. Chem.* **1996**, *61*, 598-604.
36. Palumbo, A.; Nardi, G.; d'Ischia, M.; Misuraca, G.; Prota G. *Gen. Pharmacol.* **1983**, *14*, 253-257.
37. Napolitano, A.; Di Donato, P.; Prota, G. *J. Org. Chem.* **2001**, *66*, 6958-6966.
38. Thomson, R. H. *Angew. Chem. Int.* **1974**, *13*, 305-312.
39. Panzella, L.; Manini, P.; Monfrecola, G.; d'Ischia, M.; Napolitano, A. *Pigment Cell Res.* **2007**, *20*, 128-133.
40. Napolitano, A.; Vincensi, M. R.; Di Donato, P.; Monfrecola, G.; Prota, G. J. *Invest. Dermatol.* **2000**, *114*, 1141-1147.
41. Minale, L.; Fattorusso, E.; Cimino, G.; De Stefano, S.; Nicolaus, R. A. *Gazz. Chim. Ital.* **1969**, *99*, 431-449.
42. Fattorusso, E.; Minale, L.; Cimino, G.; De Stefano, S.; Nicolaus, R. A. *Gazz. Chim. Ital.* **1969**, *99*, 29-45.
43. Ito, S.; Fujita, K. *Anal. Biochem.* **1985**, *144*, 527-536.
44. Ito, S.; Wakamatsu, K. *Pigment Cell Res.* **2003**, *16*, 523-531.
45. Thody, A. J.; Higgins, E. M.; Wakamatsu, K.; Ito, S.; Burchill, S. A.; Marks, J. M. *J. Invest. Dermatol.* **1991**, *97*, 340-344.
46. Bush, W. D.; Garguilo, J.; Zucca, F. A.; Albertini, A.; Zecca, L.; Edwards, G. S.; Nemanich, R. J.; Simon, J. D. *Proc. Natl. Acad. Sci. USA* **2006**, *103*, 14785-14789.

47. Samokhvalov, A.; Garguilo, J.; Yang, W. C.; Edwards, G. S.; Nemanich, R. J.; Simon, J. D. *J. Phys. Chem. B* **2006**, *108*, 16334–16338.
48. Ito, S. *Proc. Natl. Acad. Sci. USA* **2006**, *103*, 14647-14648.
49. Wakamatsu, K.; Hu, D. N.; McCormick, S. A.; Ito, S. *Pigment Cell Melanoma Res.* **2008**, *21*, 97–105.
50. Peles, D. N.; Hong, L.; Hu, D. N.; Ito, S.; Nemanich, R. J.; Simon, J. D. *J. Phys. Chem. B.* **2009**, *113*, 11346–11351.
51. Ito, S. *Pigment Cell Res.* **2003**, *16*, 230–236.
52. Ito, S.; Wakamatsu, K. *Photochem. Photobiol.* **2008**, *84*, 582–592.
53. Land, E. J.; Ito, S.; Wakamatsu, K.; Riley, P. A. *Pigment Cell Res.* **2003**, *16*, 487–493.
54. Wakamatsu, K.; Fujikawa, K.; Zucca, F.; Zecca, L.; Ito, S. *J. Neurochem.* **2003**, *86*, 1015–1023.
55. Zecca, L.; Bellei, C.; Costi, P. et al. *Proc. Natl Acad. Sci. USA* **2008**, *105*, 17567–17572.
56. Zucca, F. A.; Giaveri, G.; Gallorini, M. et al. *Pigment Cell Res.* **2004**, *17*, 610–617.
57. Chedekel, M. R.; Smith, S. K.; Post, P. W.; Pokora, A.; Vessell, D. L. *Proc. Natl. Acad. Sci. U.S.A.* **1978**, *75*, 5395-5399.
58. Brenner, M.; Hearing, V. J. *Photochem. Photobiol.* **2008**, *84*, 539-549.
59. Riesz, J.; Sarna, T.; Meredith, P. *J. Phys. Chem. B.* **2006**, *110*, 13985-13990.
60. Schmitz, S.; Thomas, P. D.; Allen, T. M.; Poznansky, M. J.; Jimbow, K. *Photochem. Photobiol.* **1995**, *61*, 650-655.
61. Takeuchi, S.; Zhang, W.; Wakamatsu, K.; Ito, S.; Hearing, V. J.; Kraemer, K. H.; Brash, D. E. *Proc. Natl. Acad. Sci. U.S.A.* **2004**, *101*, 15076-15081.
62. Simon, J. D.; Goldsmith, M. R.; Hong, L.; Kempf, V. R.; McGuckin, L. E. L.; Ye, T.; Zuber, G. *Photochem. Photobiol.* **2006**, *82*, 318-323.
63. Ye, T.; Pawlak, A.; Sarna, T.; Simon, J. D. *Photochem. Photobiol.* **2008**, *84*, 437-443.
64. Ye, T.; Simon, J. D. *Photochem. Photobiol.* **2003**, *77*, 41-45.
65. Ye, T.; Hong, L.; Garguilo, J.; Pawlak, A.; Edwards, G. S.; Nemanich, R. J.; Sarna, T.; Simon, J. D. *Photochem. Photobiol.* **2006**, *82*, 733-737.

66. Gambichler, T.; Stucker, M.; Kerner, K, et al. *Am. J. Clin. Dermatol.* **2008**, *9*, 267–270.
67. Böhm, M.; Schiller, M.; Nashan, D.; Stadler, R.; Luger, T. A.; Metze, D. *J. Am. Acad. Dermatol.* **2001**, *44*, 747–754.
68. Konrad, K.; Wolff, K. *Br. J. Dermatol.* **1974**, *91*, 635–655.
69. Steiner, A.; Rappersberger, K.; Groh, V.; Pehamberger, H. *J. Am. Acad. Dermatol.* **1991**, *24*, 625–628.
70. Tsukamoto, K.; Furue, M.; Sato, Y.; et al. *Dermatology* **1998**, *197*, 338–342.
71. Busam, K. J.; Wolchok, J.; Jungbluth, A. A.; Chapman, P. *J. Cutan. Pathol.* **2004**, *31*, 274–280.
72. Rorsman, H.; Agrup, G.; Hansson, C.; Rosengren, E. *Pigment Cell* **1983**, *6*, 93–115.
73. Kågedal, B.; Pettersson, A. *J. Chromatogr.* **1983**, *272*, 287–297.
74. Banfalvi, T.; Gilde, K.; Boldizsar, M.; et al. *Eur. J. Clin. Invest.* **2000**, *30*, 900–904.
75. Wakamatsu, K.; Kageshita, T.; Furue, M.; et al. *Melanoma Res.* **2002**, *12*, 245–253.
76. Wakamatsu, K.; Ito, S.; Rees, J. L. *Pigment Cell Res.* **2002**, *15*, 225–232.
77. Takasaki, A.; Nezirević, D.; Årstrand, K.; Wakamatsu, K.; Ito, S.; Kågedal, B. *Pigment Cell Res.* **2003**, *16*, 480–486.
78. Nezirević, D.; Årstrand, K.; Kågedal, B. *J. Chromatogr. A* **2007**, *1163*, 70–79.
79. Nezirević, D.; Rundström, A.; Kågedal, B. *J. Chromatogr. A* **2009**, *1216*, 5730–5739.
80. Agrup, G.; Lindbladh, C.; Prota, G.; Rorsman, H.; Rosengren, A. M.; Rosengren, E. *J. Invest. Dermatol.* **1978**, *70*, 90–91.
81. Rorsman, H.; Agrup, P.; Carlen, B.; et al. *Acta Derm. Venereol.* **1986**, *66*, 468–473.
82. Butterfield, D. A.; Castegna, A.; Pocernich, C. B.; Drake, J.; Scapagninib, G.; Calabrese, V. *J. Nutr. Biochem.* **2002**, *13*, 444–461.
83. Han, X.; Shen, T.; Lou, H. *Int. J. Mol. Sci.* **2007**, *8*, 950–988.
84. Gutteridge, J. M. *Free Radic. Res. Commun.* **1993**, *19*, 141–158.
85. Kehrer, J. P. *Crit. Rev. Toxicol.* **1993**, *23*, 21–48.

86. Becker, L. B. *Cardiovasc. Res.* **2004**, *61*, 461-470.
87. Valko, M.; Izakovic, M.; Mazur, M.; Rhodes, C. J.; Telser, J. *Mol. Cell. Biochem.* **2004**, *266*, 37-56.
88. Kovacic, P.; Jacintho, J. D. *Curr. Med. Chem.* **2001**, *8*, 773-796.
89. Ridnour, L. A.; Isenberg, J. S.; Espey, M. G.; Thomas, D. D.; Roberts, D. D.; Wink, D. A. *Proc. Natl. Acad. Sci. U.S.A.* **2005**, *102*, 13147-13152.
90. Valko, M.; Morris, H.; Cronin, M. T. D. *Curr. Med. Chem.* **2005**, *12*, 1161-1208.
91. Droge, W. *Physiol. Rev.* **2002**, *82*, 47-95.
92. Halliwell, B.; Gutteridge, J. M. C. (1999). *Free radical Biology and medicine* (3rd ed.). Oxford University Press.
93. Miller, D. M.; Buettner, G. R.; Aust, S. D. *Free Radic. Biol. Med.* **1990**, *8*, 95-108.
94. Pastor, N.; Weinstein, H.; Jamison, E.; Brenowitz, M. *J. Mol. Biol.* **2000**, *304*, 55-68.
95. Marnett, L. J. *Mut. Res.-Fund. Mol. Mech. Mutagen.* **1999**, *424*, 83-95.
96. Visioli, F.; Bellomo, G.; Galli, C. *Biochem. Biophys. Res. Commun.* **1998**, *247*, 60-64.
97. Owen, R. W.; Mier, W.; Giacosa, A.; Hull, W. E.; Spiegelhalder, B.; Bartsch, H. *Food Chem. Toxicol.* **2000**, *38*, 647-659.
98. Briante, R.; Febbraio, F.; Nucci, R. *J. Agric. Food Chem.* **2003**, *51*, 6975-6981.
99. Valvandis, A.; Nisiotou, C.; Papageorgiou, Y.; Kremli, I.; Satravelas, N.; Zinieris, N.; Zygalki, H. *J. Agric. Food Chem.* **2004**, *52*, 2358-2365.
100. Keys, A. *Am. J. Clin. Nutr.* **1995**, *61*, 1321S-1323S.
101. Owen, R. W.; Haubner, R.; Wurtele, G.; Hull, E.; Spiegelhalder, B.; Bartsch, H. *Eur. J. Cancer Prev.* **2004**, *13*, 319-326.
102. Tuck, K. L.; Hayball, P. J. *J. Nutr. Biochem.* **2002**, *13*, 636-644.
103. Monti, S. M.; Ritieni, A.; Sacchi, R.; Skog, K.; Borgen, E.; Fogliano, V. *J. Agric. Food Chem.* **2001**, *49*, 3969.
104. Rietjens, S. J.; Bast, A.; Haenen, G. R. M. M. *J. Agric. Food Chem.* **2007**, *55*, 7609-7614.

105. Visioli, F.; Bellomo, G.; Montedoro, G. F.; Galli, C. *Atherosclerosis* **1995**, *117*, 25-32.
106. Medina, I.; Tombo, I.; Satuè-Gracia, M. T.; German, J.B.; Frankel, E. N. *J. Agric. Food Chem.* **2002**, *50*, 2392-2399.
107. Pazos, M.; Lois, S.; Torres, J. L.; Medina, I. *J. Agric. Food Chem.* **2006**, *54*, 4417-4423.
108. Hashimoto, T.; Ibi, M.; Matsuno, K.; Nakashima, S.; Tanigawa, T.;Yoshikawa, T.; Yabe-Nishimura, C. *Free Radic. Biol. Med.* **2004**, *36*, 555-564.
109. Vissers, M. N.; Zock, P. L.; Katan, M. B. *Eur. J. Clin. Nutr.*, **2004**, *58*, 955.
110. Roche, M.; Dufour, C.; Mora, N.; Dangles, O. *Org. Biomol. Chem.* **2005**, *3*, 423-430.
111. Kono, Y.; Shibata, H.; Kodama, Y.; Sawa, Y. *Biochem. J.* **1995**, *312*, 947.
112. Higdon, J. V. et al. *Crit. Rev. Food Sci. Nutr.* **2006**, *46*, 101–123.
113. Kasai, H. et al. *Food Chem. Toxicol.* **2000**, *38*, 467–471.
114. Shibata, H. et al. *Biosci. Biotechnol. Biochem.* **1999**, *63*, 1295–1297.
115. Chung, T.; Moon, S.; Chang, Y.; et al. *FASEB J.* **2004**, *18*, 1670-1681.
116. Johnson, B. M.; van Breemen, R. B. *Chem. Res. Toxicol.* **2003**, *16*, 838-846.
117. Jeandet, P; Bessis, R.; Sbaghi, M.; Meunier, P.; Trollat, P. *J. Phytopathol.* **1995**, *143*, 135-139.
118. Cantos, E.; Espin, J. C.; Fernandez, M. J.; Oliva, J.; Tomas-Barberan, F.A. *J. Agric. Food Chem.* **2003**, *51*, 1208-1214.
119. Amorati, R.; Ferroni, F.; Pedulli, G. F.; Valgimigli, L. *J. Org. Chem.* **2003**, *68*, 9654-9658.
120. Caruso, F.; Tanski, J.; Villegas-Estrada, A.; Rossi, M. *J. Agric. Food Chem.* **2004**, *52*, 7279-7285.
121. Brinker, A. M.; Seigler, D. S. *Phytochemistry* **1991**, *30*, 3229-3232.
122. Renaud, S.; Gueguen, R.; Schenker, J.; d’Houtaud, A. *Epidemiology* **1998**, *9*, 184-188.
123. Constant, J. *Coron. Artery Dis.* **1997**, *8*, 645-649.
124. Roupe, K. A.; Remsberg, C. M.; Yanez, J. A. ; Davies, N. M. *Curr. Clin. Pharmacol.* **2006**, *1*, 81-101.

125. Piver, B.; Fer, M.; Vitrac, X.; Merillon, J. M.; Dreano, Y.; Berthou, F.; Lucas, D. *Biochem. Pharmacol.* **2004**, *68*, 773-782.
126. Torres, J. L.; Lozano, C.; Maher, P. *Phytochem.* **2005**, *66*, 2032-2037.
127. Amorati, R.; Fumo, M. G.; Menichetti, S.; Mugnaini, V.; Pedulli, G. F. *J. Org. Chem.* **2006**, *71*, 6325-6332.
128. Ley, J. P.; Bertram, H. J. *J. Agric. Food Chem.* **2003**, *51*, 4596-4602.
129. Jin, G.; Yoshioka, H. *Biosci. Biotechnol. Biochem.* **2005**, *69*, 440-447.
130. Gordon, M. H.; Paiva-Martins, F.; Almeida, M. *J. Agric. Food Chem.* **2001**, *49*, 2480-2485.
131. Reed, L. J.; DeBusk, B. G.; Gunsalus, I. C.; Hornber Jr., C.S. *Science* **1951**, *114*, 93-94.
132. Packer, L.; Witt, E. H. & Tritschler, H. *Free Radic. Biol. Med.* **1995**, *19*, 227-235.
133. Ono, K.; Hirohata, M.; Yamada, M. *Biochem. Biophys. Res. Commun.*, **2006**, *341*, 1046-1052.
134. Tsuji-Naito, K.; Hatani, T.; Okada, T.; Tehara, T. *Bioorg. Med. Chem.* **2007**, *15*, 1967-1975.
135. Borges, C. R.; Roberts, J. C.; Wilkins, D. G.; Rollins, D. E. *Anal. Biochem.* **2001**, *290*, 116-125.
136. Ito, S. *Pigment Cell Res.* **1989**, *2*, 53-56.
137. Porter, R. M. *J. Anat.* **2003**, *202*, 125-131.
138. Deibel, R. M. B.; Chedekel, M. R. *J. Am. Chem. Soc.* **1984**, *106*, 5884-5888.
139. Liu, Y.; Hong, L.; Wakamatsu, K.; Ito, S.; Adhyaru, B.; Cheng, C. Y.; Bowers, C. R.; Simon, J. D. *Photochem. Photobiol.* **2005**, *81*, 135-44.
140. Napolitano, A.; Memoli, S.; Nappi, A. J.; d'Ischia, M.; Prota, G. *Biochim. Biophys. Acta* **1996**, *1291*, 75-82.
141. Napolitano, A.; Vincensi, M. R.; d'Ischia, M.; Prota, G. *Tetrahedron Lett.* **1996**, *37*, 6799-6802.
142. Slominski, A.; Wortsman, J.; Plonka, P. M.; Schallreuter, K. U.; Paus, R.; Tobin, D. J. *Invest. Dermatol.* **2005**, *124*, 13-21.
143. Simon, J. D.; Hong, L.; Peles, D. N. *J. Phys. Chem. B* **2008**, *112*, 13201-13217.
144. Watt, A. A. R.; Bothma, J. P.; Meredith, P. *Soft Matter* **2009**, *5*, 3754-3760.

145. Meredith, P.; Sarna, T. *Pigment Cell Res.* **2006**, *19*, 572-594.
146. Bothma, J. P.; de Boor, J.; Divakar, U.; Schwenn, P. E.; Meredith, P. *Adv. Mat.* **2008**, *20*, 3539-3542.
147. Schweitzer, A. D.; Howell, R. C.; Jiang, Z.; Bryan, R. A.; Gerfen, G.; Chen, C.-C.; Mah, D.; Cahill, S.; Casadevall, A.; Dadachova, E. *PLoS One* **2009**, *4*, e7229.
148. Ambrico, M.; Cardone, A.; Ligonzo, T.; Augelli, V.; Ambrico, P. F.; Cicco, S.; Farinola, G. M.; Filannino, M.; Perna, G.; Capozzi, V. *Org. Electron.* **2010**, *11*, 1809-1814.
149. d'Ischia, M.; Napolitano, A.; Pezzella, A.; Meredith, P.; Sarna, T. *Angew. Chemie, Int. Ed. Engl.* **2009**, *48*, 3914-3921.
150. Gao, J.; Kim, Y. M.; Coe, H.; Zern, B.; Sheppard, B.; Wang, Y. *Proc. Natl. Acad. Sci. U.S.A.* **2006**, *103*, 16681-16686.
151. Postma, A.; Yan, Y.; Wang, Y.; Zelikin, A. N.; Tjipto, E.; Caruso, F. *Chem. Mater.* **2009**, *21*, 3042-3044.
152. Lee, H.; Dellatore, S. M.; Miller, W. M.; Messersmith, P. B. *Science* **2007**, *318*, 426-430.
153. Ryu, J.; Ku, S. H.; Lee, H.; Park, C. B. *Adv. Funct. Mater.* **2010**, *20*, 2132-2139.
154. Yu, B.; Wang, D. A.; Ye, Q.; Zhou, F.; Liu, W. *Chem. Commun.* **2009**, *44*, 6789-6791.
155. Cui, J.; Wang, Y.; Postma, A.; Hao, J.; Hosta-Rigau, L.; Caruso, F. *Adv. Funct. Mater.* **2010**, *20*, 1625-1631.
156. Kang, S. M.; Rho, J.; Choi, I. S.; Messersmith, P. B.; Lee, H. *J. Am. Chem. Soc.* **2009**, *131*, 13224-13225.
157. Zhu, L.-P.; Yu, J.-Z.; Xu, Y.-Y.; Xi, Z.-Y.; Zhu, B.-K. *Colloids Surf. B Biointerfaces* **2009**, *69*, 152-155.
158. Jaber, M.; Lambert, J.-F. *J. Phys. Chem. Lett.* **2010**, *1*, 85-88.
159. Bernsmann, F.; Ponche, A.; Ringwald, C.; Hemmerle, J.; Raya, J.; Bechinger, B.; Voegel, J.-C.; Schaaf, P.; Ball, V. *J. Phys. Chem. C* **2009**, *113*, 8234-8242.
160. Bernsmann, F.; Ersen, O.; Voegel, J.-C.; Jan, E.; Kotov, N. A.; Ball, V. *Chem. Phys. Chem.* **2010**, *11*, 3299-3305.

161. Samokhvalov, A.; Hong, L.; Liu, Y.; Garguilo, J.; Nemanich, R. J.; Edwards, G. S.; Simon, J. D. *Photochem. Photobiol.* **2005**, *81*, 145-148.
162. Wei, Q.; Zhang, F.; Li, J.; Li, B.; Zhao, C. *Polym. Chem.* **2010**, *1*, 1430-1433.
163. Napolitano, A.; De Lucia, M.; Panzella L.; d'Ischia, M. *Photochem. Photobiol.* **2008**, *84*, 593-599.
164. Panzella, L.; Szewczyk, G.; d'Ischia, M.; Napolitano, A.; Sarna, T. *Photochem. Photobiol.* **2010**, *86*, 757-764.
165. Ito, S.; Wakamatsu, K. In *The Pigmentary System. Physiology and Pathophysiology*; Nordlund, J. J., Boissy, R. E., Hearing, V. J., King, R. A., Oetting, W. S., Ortonne, J. P., Eds; Blackwell Publishing: New York, 2006; pp 282-310.
166. Feng, P. K.; Fernando, Q. *J. Am. Chem. Soc.* **1960**, *82*, 2115-2118.
167. Patil, D. P.; Chedekel, M. R. *J. Org. Chem.* **1984**, *49*, 997-1000.
168. Ismail, I. A.; Sharp, D. E.; Chedekel, M. R. *J. Org. Chem.* **1980**, *45*, 2243-2246.
169. Chioccaro, F.; Novellino, E. *Synth. Commun.* **1986**, *16*, 967-971.
170. Lowik, D. W. P. M.; Tisi, L. C.; Murray, J. A. H.; Lowe, C. R. *Synthesis* **2001**, *12*, 1780-1783.
171. Panzella, L.; De Lucia, M.; Napolitano, A.; d'Ischia, M. *Tetrahedron Lett.* **2007**, *48*, 7650-7652.
172. Kågedal, B.; Lenner, L.; Årstrand, K.; Hansson, C. *Pigment Cell Res.* **1992**, (Suppl 2), 304-307.
173. Agrup, G.; Agrup, P.; Hansson, C.; Rorsman, H.; Rosengren, E. *Acta Derm. Venereol.* **1979**, *59*, 456-457.
174. Tsukamoto, K.; Furue, M.; Sato, Y.; et al. *Dermatology* **1998**, *197*, 338-342.
175. Faraj, B. A.; Lawson, D. H.; Nixon, D. W.; et al. *Clin. Chem.* **1981**, *27*, 108-112.
176. Pavel, S.; van Nieuwpoort, F.; van der Meulen, H.; et al. *Eur. J. Cancer.* **2004**, *40*, 1423-1430.
177. Fitzpatrick, T. B.; Montgomery, H.; Lerner, A. B. *J. Invest. Dermatol.* **1954**, *22*, 163-172.
178. Duchon, J. *Sb. Lek.* **1994**, *95*, 297-307.

179. Nakamura, Y.; Nakamura, Y.; Hori, E.; et al. *Int. J. Dermatol.* **2009**, *48*, 763–767.
180. Tesema, T. J.; Pham, D. M.; Franz, K. J. *Inorg. Chem.* **2008**, *47*, 1087-1095.
181. Husek, P. *FEBS Lett.* **1991**, *280*, 354-356.
182. Piletic, I. R.; Matthews, T. E.; Warren, W. S. *J. Chem. Phys.* **2009**, *131*, 181106.
183. Bobbitt, J. M. In *Hetrocyclic Chemistry*; Katritzky, A. R., Boulton, A. J., Eds.; Academic Press: New York and London, 1973, vol. 15, p 117.
184. Foti, M. C.; Johnson, E. R.; Vinqvist, M. R.; Wright, J. S.; Barclay, L. R. C.; Ingold, K. U. *J. Org. Chem.* **2002**, *67*, 5190-5196.
185. Valente, C.; Moreira, R.; Guedes, R. C.; Iley, J.; Jaffar, M.; Douglas, K. T. *Bioorg. Med. Chem.* **2007**, *15*, 5340-5350.
186. Sharma, S.; Sharma, B. K.; Prabhakar, Y. S. *Eur. J. Med. Chem.* **2009**, *44*, 2847-2853.
187. Kiran Aithal, B.; Sunil Kumar, M. R.; Nageshwar Rao, B.; Udupa, N.; Satish Rao, B. S. *Cell Biol. Int.* **2009**, *33*,1039-1049.
188. Tandon, V. K.; Maurya, H. K.; Mishra, N. N.; Shukla, P. K. *Eur. J. Med. Chem.* **2009**, *44*, 3130-3137.
189. Tandon, V. K.; Maurya, H. K.; Yadav, D. B.; Tripathi, A.; Kumar, M.; Shukla, P. K. *Bioorg. Med. Chem. Lett.* **2006**, *16*, 5883-5887.
190. Mecklenburg, S.; Shaaban, S.; Ba, L. A.; Burkholz, T.; Schneider, T.; Diesel, B.; Kiemer, A. K.; Röseler, A.; Becker, K.; Reichrath, J.; Stark, A.; Tilgen, W.; Abbas, M.; Wessjohann, L. A.; Sasse, F.; Jacob, C. *Org. Biomol. Chem.* **2009**, *7*, 4753-4762.
191. Braud, E.; Goddard, M.; Kolb, S.; Brun, M.; Mondésert, O.; Quaranta, M.; Gresh, N.; Ducommun, B.; Garbay, C. *Bioorg. Med. Chem.* **2008**, *16*, 9040-9049.
192. Gunsalus, I. C.; Barton, L. S.; Gruber, W. *J. Am. Chem. Soc.* **1956**, *78*, 1763-1766.
193. Thomson, R. H. *J. Org. Chem.* **1951**, *16*, 1082-1090.
194. Ryu, C.-K.; Shim, J.-Y.; Chae, M. J.; Choi, I. H.; Han, J.-Y.; Jung, O.-J.; Lee, J. Y.; Jeong, S. K. *Eur. J. Med. Chem.* **2005**, *40*, 438-444.

195. Tsuji-Naito, K.; Hatani, T.; Okada, T.; Tehara, T. *Biochem. Biophys. Res. Commun.* **2006**, *343*, 15-20.
196. Ong, C. W.; Yu, C. Y. *Tetrahedron* **2003**, *59*, 9677-9682.
197. Waddell, S. T.; Blizzard, T. A.; Doss, G. A. *Heterocycles* **1993**, *36*, 1213-1215.
198. Saigo, K.; Hashimoto, Y.; Fang, L.; Hasegawa, M. *Heterocycles* **1989**, *29*, 2079-2082.
199. Zhao, X.; Zhong, Z.; Peng, L.; Zhang, W.; Wang, J. *Chem. Comm.* **2009**, 2535-2537.
200. Pezzella, A.; Lista, L.; Napolitano, A.; d'Ischia, M. *Tetrahedron Lett.* **2005**, *46*, 3541-3544.
201. Magdziak, D.; Rodriguez, A. A.; Van De Water, R. W.; Pettus, R. R. T. *Org. Lett.* **2002**, *4*, 285-288.
202. Zhang, F.; Dryhurst, G. *Bioorg. Chem.* **1995**, *23*, 193-216.
203. Ito, S.; Palumbo, A.; Prota, G. *Experientia* **1985**, *41*, 960-961.
204. Richard, F. C.; Goupy, P. M.; Nicolas, J. J.; Lacombe, J.; Pavia, A. A. *J. Agric. Food Chem.* **1991**, *39*, 841-847.
205. Ciliers, J. J. L.; Singleton, V. L. *J. Agric. Food Chem.* **1990**, *38*, 1789-1796.
206. Panzella, L.; Napolitano, A.; d'Ischia, M. *Bioorg. Med. Chem.* **2003**, *11*, 4797-4805.
207. Goupy, P.; Dufour, C.; Loonis, M.; Dangles, O. *J. Agric. Food Chem.* **2003**, *51*, 615-622.
208. Prota, G.; Scherillo, G.; Nicolaus, R. A. *Gazz. Chim. Ital.* **1968**, *98*, 495-510.
209. Prota, G.; Crescenzi, S.; Misuraca, G.; Nicolaus, R. A. *Experientia* **1970**, *26*, 1508-1509.
210. Erlenmayer, H.; Junod, J.; Guex, W.; Erne, M. *Helv. Chim. Acta* **1948**, *31*, 1342-1349.
211. Edge, R.; d'Ischia, M.; Land, E. J.; Napolitano, A.; Navaratnam, S.; Panzella, L.; Pezzella, A.; Ramsden, C. A.; Riley, P. A. *Pigment Cell Res.* **2006**, *19*, 443-450.
212. Ito, S.; Fujita, K. *J. Chromatogr.* **1986**, *375*, 134-140.
213. Napolitano, A.; Pezzella, A.; Vincensi, M. R.; Prota, G. *Tetrahedron*, **1995**, *51*, 5913-5920.
214. Lamoreux, M. L.; Wakamatsu, K.; Ito, S. *Pigment Cell Res.* **2001**, *14*, 23-31.

215. Liu, Y.; Kempf, V. R.; Nosfinger, J. B.; Weinert, E. E.; Rudnicki, M.; Wakamatsu, K.; Ito, S.; Simon, J. D. *Pigment Cell Res.* **2003**, *16*, 355-365.
216. Ito, S. *Biochim. Biophys. Acta* **1986**, *883*, 155-161.
217. Di Donato, P.; Napolitano, A.; Prota, G. *Biochim. Biophys. Acta* **2002**, *1571*, 157-166.

Publication List

- **Greco, G.**; Panzella, L.; Verotta, L.; Napolitano, A.; d'Ischia M. "Uncovering the Structure of Human Red Hair Pheomelanin: Benzothiazolylthiazinodihydroisoquinolines as Key Building Blocks" *J. Nat. Prod.* Manuscript ID: np-2010-00740n. Submitted.
- **Greco, G.**; Panzella, L.; Pezzella, A.; Napolitano, A.; d'Ischia M. "Reaction of dihydrolipoic acid with juglone and related naphthoquinones: unmasking of a spirocyclic 1,3-dithiane intermediate en route to naphtho[1,4]dithiepins" *Tetrahedron* **2010**, *66*, 3912-3916.
- Nezirević Dernroth, D.; Årstrand, K.; **Greco, G.**; Panzella, L.; Napolitano, A.; Kågedal, B. "Pheomelanin-related benzothiazole isomers in the urine of patients with diffuse melanosis of melanoma" *Clinica Chim. Acta* **2010**, *411*, 1195-1203.
- **Greco, G.**; Panzella, L.; Napolitano, A.; d'Ischia, M. "Biologically inspired one-pot access routes to 4-hydroxybenzothiazole amino acids, red hair-specific markers of UV susceptibility and skin cancer risk", *Tetrahedron Lett.* **2009**, *50*, 3095-3097.
- **Greco, G.**; Wakamatsu, K.; Panzella, L.; Ito, S.; Napolitano, A.; d'Ischia, M. "Isomeric cysteinyl dopas provide a (photo)degradable bulk component and a robust structural element in red human hair pheomelanin", *Pigment Cell Melanoma Res.* **2009**, *22*, 319-327.*

*Covered in: Simon, J. D. "Seeing red: pheomelanin synthesis uncovered", *Pigment Cell Melanoma Res.* **2009**, *22*, 382-383.

Acknowledgments

This work is the result of many brainstormings. This is the proof they were useful. No one more than my supervisor Prof. Alessandra Napolitano, Dr. Lucia Panzella and Prof. Marco d'Ischia knows what I mean, and I would like to express them all my frank gratitude.

Thanks to Luigia and Marianna, forever my PhD-labmates,
to all my undergraduate students, Sabrina first of all, open to my unusual teachings,
to Dr. Alessandro Pezzella, for his unusual teachings,
to Mary, Valentina and Luca, witnesses of a thousand trials and some results,
to my past Relatives and to my past Family,
to my next Relatives and to my next Family.